ΔΙΔΑΚΤΟΡΙΚΗ ΔΙΑΤΡΙΒΗ

Dendritic contributions to neuronal and synaptic memory allocation

ΚΑΣΤΕΛΛΑΚΗΣ ΓΕΩΡΓΙΟΣ

ΤΜΗΜΑ ΒΙΟΛΟΓΙΑΣ, ΠΑΝΕΠΙΣΤΗΜΙΟ ΚΡΗΤΗΣ

και

ΙΝΣΤΙΤΟΥΤΟ ΜΟΡΙΑΚΗΣ ΒΙΟΛΟΓΙΑΣ ΚΑΙ ΒΙΟΤΕΧΝΟΛΟΓΙΑΣ,

ΙΔΡΥΜΑ ΤΕΧΝΟΛΟΓΙΑΣ ΚΑΙ ΕΡΕΥΝΑΣ

2016

Dendritic contributions to neuronal and synaptic memory allocation

Georgios Kastellakis

Thesis presented in fulfillment of the requirements

for the Doctoral Degree to the

Department of Biology, School of Sciences, University of Crete

2016

Dedication

To my parents, Ioannis and Despina

Abstract

It is generally accepted that the brain stores memories in distributed neuronal representations. The long-term storage of memories is believed to take place through the strengthening and weakening of synaptic connections between neurons. Recent research has begun to probe the mechanisms that underlie these changes in synaptic connections and to identify the correlates of specific memories in the brain, which are known as memory engrams or traces. These studies have identified a number of different factors, which determine memory storage, from molecular processes to network electrophysiological phenomena. Despite this progress in identifying pieces of the puzzle of the mechanism of memory, we are still lacking a unified framework, which can explain the experimental findings with regards to memory, and can predict the structure of memory traces.

In this thesis we present a novel modeling approach to memory acquisition which combines multiple experimentally observed phenomena. We apply this model in specific well-studied memory-related experimental protocols and we use it to predict the structure of the resulting memory traces in multiple spatial scales, from the synaptic to the neuronal network level. In order to create a unifying framework for studying memory formation we incorporate mechanisms related to the consolidation of long-term memories in the brain. These include the mechanisms for plasticity-related protein capture according to the synaptic tagging and capture model, the localized modulation of excitability, as well as the effects of homeostasis and inhibition. Importantly, we study the effect of dendritic

compartmentalization, which is known to affect memory, by incorporating dendritic phenomena in the description of neurons.

Using this model, we show that the sub-cellular structure of memories, which consists of the distribution of synapses to specific neurons and specific dendritic branches is dependent on the ability of neurons to synthesize plasticity proteins in dendrites, and on the activation history of the neuron, which affects its excitability. In addition, we find that synapses tend to potentiate in groups, a phenomenon known as synapse clustering. We extend the model to the case of multiple memories in order to examine their possible interactions and find that the neuronal populations and the synapses that represent time-related memories are intertwined. Using the model, we predict the overlapping components of different memories as a function of time. Finally, we examine the role of dendritic spine reorganization, which occurs constantly in the brain, in the storage of memories.

Περίληψη

Είναι γενικά αποδεκτό ότι ο οι μνήμες αποθηκεύονται με διάσπαρτο τρόπο στον εγκέφαλο. Η μακρόχρονη αποθήκευση της μνήμης πιστεύεται ότι λαμβάνει χώρα μέσω της ενδυνάμωσης και αποδυνάμωσης των συναπτικών συνδέσεων μεταξύ νευρώνων.

Πρόσφατες έρευνες έχουν αρχίσει να εξερευνούν τους μηχανισμούς μέσω των οποίων γίνονται αυτές οι συνδέσεις, και να ταυτοποιούν το βιοφυσικό υπόστρωμα στο οποίο αποθηκεύονται συγκεκριμένες μνήμες, το ονομαζόμενο μνημονικό *έγγραμμα* ή ίχνος. Οι έρευνες αυτές έχουν ταυτοποιήσει ποικίλους διαφορετικούς μηχανισμούς, από το μοριακό ως το επίπεδο του νευρωνικού δικτύου, οι οποίοι καθορίζουν την μνημονική αποθήκευση. Παρ' όλη την πρόσφατη πρόοδο για την ανακάλυψη των μηχανισμών μνήμης, δεν υπάρχει ακόμα μια ολοκληρωμένη θεωρία που να μπορεί να εξηγήσει τα πειραματικά ευρήματα σχετικά με τη μνήμη και να μπορεί να προβλέψει τη δομή των μνημονικών εγγραμμάτων.

Σε αυτή την διατριβή παρουσιάζουμε μια πρότυπη προσέγγιση στην μοντελοποίηση της διαδικασίας της πρόσκτησης μνήμης που λαμβάνει υπόψιν της πολλαπλά πειραματικώς επιβεβαιωμένα φαινόμενα. Εφαρμόζουμε το μοντέλο αυτό σε συγκεκριμένα καλά μελετημένα πειραματικά πρωτόκολλα μνήμης και το χρησιμοποιούμε για να προβλέψουμε την εσωτερική δομή των εγγραμμάτων μνήμης σε πολλαπλές χωρικές κλίμακες, από την κλίμακα των συνάψεων ως την κλίμακα του νευρωνικού δικτύου. Προκειμένου να δημιουργήσουμε ένα ενοποιημένο υπόβαθρο για τη μελέτη της πρόσκτησης μνήμης, εισάγουμε

πολλαπλούς μηχανισμούς και κανόνες σχετικούς με την παγιοποίηση της μακρόχρονης μνήμης. Σε αυτούς τους μηχανισμούς συγκαταλέγονται οι μηχανισμοί για την δέσμευση πρωτεϊνών από συνάψεις σύμφωνα με το μοντέλο "συναπτικής σήμανσης και δέσμευσης", ο μηχανισμός δενδριτικής αλλαγής της διεγερσιμότητας των νευρώνων, καθώς και οι συνέπειες των ομοιοστατικών μηχανισμών και η επίδραση των κατασταλτικών νευρώνων. Ένα σημαντικό χαρακτηριστικό είναι ότι μελετάμε τις συνέπειες της δενδριτικής διαμερισματοποίησης των νευρώνων, που είναι γνωστό ότι επηρεάζει τις ιδιότητες της μνήμης, υλοποιώντας κανόνες που αντιστοιχούν σε δενδριτικά φαινόμενα στους νευρώνες του μοντέλου.

Αρχικά, χρησιμοποιώντας το μοντέλο, δείχνουμε ότι η υποκυτταρική δομή των εγγραμμάτων μνήμης, που αποτελείται από την κατανομή συνάψεων σε συγκεκριμένους νευρώνες και σε συγκεκριμένους δενδριτικούς κλάδους, εξαρτάται από την διαθεσιμότητα πρωτεϊνών στους δενδρίτες και από το ιστορικό ενεργοποίησης του νευρώνα, το οποίο επηρεάζει τη διεγερσιμότητά του. Επιπλέον, βρίσκουμε ότι οι συνάψεις τείνουν να ενδυναμώνονται κατά ομάδες δημιουργώντας συστάδες συνάψεων. Στη συνέχεια επεκτείνουμε το μοντέλο στη μελέτη περισσότερων από μία μνημών και βρίσκουμε ότι οι νευρωνικοί πληθυσμοί που αντιπροσωπεύουν τις διαφορετικές μνήμες είναι αλληλοεπικαλυπτόμενοι. Με χρήση του μοντέλου, προβλέπουμε την αλληλοεπικάλυψη ως συνάρτηση του χρόνου. Τέλος, εξετάζουμε το ρόλο της ανακατάταξης συναπτικών συνδέσεων (η οποία γίνεται συνεχώς στον εγκέφαλο) , στην μνημονική αποθήκευση.

Επταμελής Εξεταστική Επιτροπή

- **Παναγιώτα Ποϊραζη** (Επιβλέπουσα Ερευνήτρια), Διευθύντρια Ερευνών , Εργαστήριο Υπολογιστικής Βιολογίας, IMBB/Ιδρυμα Τεχνολογίας και Έρευνας
- **Κωνσταντία Λύκα** (Επιβλέπουσα Καθηγήτρια), Αναπληρώτρια Καθηγήτρια, Τμήμα Βιολογίας Πανεπιστημίου Κρήτης
- **Κυριακή Σιδηροπούλου** (Μέλος Τριμελούς), Επίκουρη Καθηγήτρια, Τμήμα Βιολογίας Πανεπιστημίου Κρήτης
- **Γεωργία Γρηγορίου**, Επίκουρη Καθηγήτρια Φυσιολογίας, Τμήμα Ιατρικής, Πανεπιστήμιο Κρήτης
- **Δόμνα Καραγωγέως**, Καθηγήτρια Μοριακής Βιολογίας-Αναπτυξιακής Νευροβιολογίας. Τμήμα Ιατρικής, Πανεπιστήμιο Κρήτης
- **Βασίλης Ράος**, Επίκουρος Καθηγητής Φυσιολογίας, Τμήμα Ιατρικής, Πανεπιστήμιο Κρήτης
- **Ιωάννης Χαραλαμπόπουλος**, Επίκουρος Καθηγητής Φαρμακολογίας, Τμήμα Ιατρικής, Πανεπιστήμιο Κρήτης

Acknowledgements

During the process of my PhD studies, many people have assisted and inspired the work presented here, and I would like to thank them. Primarily, I would like to thank Yiota Poirazi, who hosted me in her lab, undertook the task of supervising my PhD, and from whom I have learned a lot. She has been instrumental in helping me get on track with the process of computational neuroscience, provided guidance and criticism, and secured the computational equipment and funding of the lab. Yiota is an ambitious scientist with a critical eye for what is important and the ability to build a vibrant laboratory. Her door is always open (literally and figuratively) and we have spent many hours discussing every aspect of our work and beyond. She additionally gave me the opportunity to meet many neuroscientists from whom I learned a lot, through our collaborations with other labs, conference trips, and by organizing the hugely successful Dendrites conferences. For all those reasons, I wish to thank her. Prof. Alcino Silva is another person who has been instrumental in setting the goals for my PhD project. Through our meetings I had the opportunity to learn about new things and pick up new research directions which were unimaginable before. Denise Cai, (a member of the Silva lab) was the person who provided hugely helpful comments on my papers, helped me improve my (admittedly limited) knowledge of basic cellular neuroscience, and we had the pleasure to publish a review paper together. I would like to thank them both, as well as Justin Shobe, Adam Frank, and the other members of the Silva lab.

I would like to thank my Supervisor, Konstandia Lika for undertaking the official supervision of my PhD project on behalf of the Dept. of Biology. I would also like to thank my co-supervisor Kiki Sidiropoulou, who was the person who invited me to start the PhD project, and has always been available to help me. They both provided useful feedback to my PhD thesis, and helped me with administrative issues and I thank them for that. I would also like to thank the other members of my PhD committee, Georgia Gregoriou, Vassilis Raos, Ioannis Charalampopoulos

and Domna Karagogeos for their critical reading of the PhD text and useful discussions.

Through all these years I have had the opportunity to work with a number of wonderful collaborators and scientists in the Poirazi lab. I would first like to thank my co-worker and friend Athanasia Papoutsi for sharing an office with me all these years, and for having countless discussions and arguments for just about anything conceivable. She is a wonderful colleague and a bright young scientist. I would like to thank previous members of the lab that I had the opportunity to work with, Eleftheria Pissadaki, Eleftheria Tzamali, Xenia Konstantoudaki, Johannes Luthman, and Vassilis Cutsuridis from whom I have learned a lot. I would also like to thank the current members of the lab for their support, Panayiotis Petrantonakis, Stefanos Stefanou, Constantinos Melachrinos, Spyros Chavlis, Panayiotis Bozelos and Pavlos Pavlidis. They form a great team of scientists and make the lab a much more fun place to work in.

Finally, I would like to thank my parents Ioannis and Despina and my brother Manos for their continued support. They have always valued education and encouraged me to pursue my academic goals.

Declaration

I declare that this thesis was composed by myself, that the work contained herein is my own except where explicitly stated otherwise in the text, and that this work has not been submitted for any other degree or professional qualification except as specified.

Curriculum Vitæ

Georgios Kastellakis

Computational Biology Lab, IMBB/FORTH, Heraklion, Greece
Tel: +30 2810-391130
E-mail: gk@ignimedia.com

Education

2010 -	PhD Candidate, Dept. of Biology, University of Crete & Computational Biology Lab, IMBB-FORTH
2009	Master's Degree in the Brain and Mind sciences Faculty of Medicine, University of Crete
2004	Ptychion (Bsc) in Physics Department of Physics, University of Crete

Employment

2008 -	Ignimedia EE, Heraklion, Greece Co-Founder
2006 - 2008	Networking Center, University of Crete, Greece Software Engineer
2000 – 2005	Phaistos Networks SA, Heraklion, Greece Software Engineer

Table of Contents

List of Figures

List of Tables

Chapter 1.

Introduction

One of the long standing mysteries of neuroscience is the way in which the brain stores memories. It is generally believed that complex memories are stored in distributed representations throughout the brain (Josselyn 2010), however, the mechanisms underlying the formation of these representations are still under intense scrutiny. The most widely accepted theory for memory formation is the connectionist model, in which memories are stored through changes in the synaptic weights connecting neurons in the brain. The postulate about how this is achieved dates back to the 1940s and the synaptic potentiation hypothesis of Donald Hebb: *synapses between neurons are potentiated when the neurons are concurrently activated*. This hypothesis provides currently the most popular candidate for a physiological foundation of learning and memory (Hebb 1949). The long-term potentiation (Bliss & Lomo 1973) (LTP) of synaptic efficacies provides a putative biophysical implementation of the Hebbian rule, which is complemented by the respective long-term depression (Stent 1973) (LTD) of synaptic strengths. Inspired by Hebb's ideas, McCulloch & Pitts proposed the theoretical equivalent of a neuronal network, where neurons are represented as point processes, ignoring their elaborate dendritic morphology (McCulloch & Pitts 1943).

Although known to exist since the early 1900's, dendritic processes were either ignored in models of memory, or treated as passive summation devices, whose function is to provide the physical substrate for transferring incoming stimuli to the somatic region of the neuron. Thus, memory representations (i.e., engrams) were thought to be stored in the connections between populations of neurons exclusively through the modification of synaptic weights. Research over the past 20 years, however, suggests that dendritic segments can act as local processing devices and that they may contribute to memory storage and recall, not just by passively transferring electrical signals, but by actively and dynamically reshaping their local responses and, in turn, the output of the neuron (Poirazi et al. 2003b; Poirazi et al. 2003a; Polsky et al. 2004; Losonczy & Magee 2006; Spruston 2008; Branco et al. 2010; Pissadaki et al. 2010; Sidiropoulou & Poirazi 2012). In addition, local chemical signaling in dendrites can contribute to the memory encoding, consolidation and maintenance (Sutton & Schuman 2006; Winnubst et al. 2012). These facts have brought forward the theory that dendrites are to be considered fundamental units of function and plasticity (Poirazi & Mel 2001; Branco & Häusser 2010b; Govindarajan et al. 2006), a theory that has received substantial experimental support (Polsky et al. 2004; Govindarajan et al. 2010; Makara et al. 2009).

This thesis examines a computational approach to the implications of dendritic memory storage. It presents a novel neuronal network model that incorporates dendritic subunits and studies the process of engram formation in a number of different experimental paradigms.

1.1 Overview

Computational modeling of memory has been instrumental in the quest for understanding memory functions. Connectionist models of memory propose that memory is stored in changes in the synaptic connection weights between neurons. The advantages of such distributed memory representations, such as their ability to generalize and their adaptability are well studied (Rumelhart & MacClelland 1988). However, these models usually ignore dendrites and fail to benefit from the advantages provided by dendritic nonlinearities with respect to storage capacity and temporal/feature binding (Poirazi & Mel 2001; Poirazi et al. 2003b; Legenstein & Maass 2011; O'Donnell et al. 2014). Although it is known that dendritic events have a role in memory function, studies of memory storage have either completely ignored dendrites (Rumelhart & MacClelland 1988), or studied dendritic phenomena in isolation (Segev & Rall 1988; Mel 1993; Traub et al. 1994). When dendritic nonlinearities are taken into account, the pattern discrimination capacity of simplified model neurons and neural networks has been shown to expand by at least one order of magnitude (Poirazi & Mel 2001), raising the critical issue of how real neurons could exploit these advantages for memory storage. In addition, neuron models with nonlinear dendrites that implement realistic plasticity rules can help investigate phenomena like memory storage and make predictions about the role of plasticity mechanisms in memory consolidation (Legenstein & Maass 2011; O'Donnell et al. 2014).

Reliable modeling of dendritic function, however, requires that models are constrained by experimental data. Recent experiments have allowed the investigation

of memory functions with unprecedented detail and have provided insights into the process of memory formation. In Chapter 2 we review the mechanisms which are known to affect the synaptic modifications that underlie memory formation. In Chapter 3 we provide a detailed description of the simulation strategy we used and the justification for the approach taken. We present a model of memory formation that incorporates dendritic subunits and dendritic plasticity as an integral component. The network implements a number of plasticity and memory-related rules, which affect the process of memory formation. In Chapter 4 we use the model to study the process of memory formation and the properties of the resulting memory engram at the neuronal network level, at the cellular level and at the dendritic level. We find that the protein synthesis-dependent memory consolidation leads to memory engrams with realistic properties and that the location of protein synthesis can affect the properties of the memory engram. We show that synapse clustering is an essential characteristic of memory formation under different conditions.

In Chapter 5 we examine the properties of memory formation and consolidation under the behavioral tagging paradigm. Behavioral tagging is a mechanism via which a short term memory can be converted to long-term. We find the conditions under which this memory strengthening can occur and show that the location of protein synthesis can crucially affect this process.

We then proceed to study more generally the interactions between two memories in chapter 6. Our modeling studies show that certain characteristics of memory such as association and interference can be attributed to low-level binding of memories in the same dendrites and neurons. In chapter 7 we examine whether the same mechanism

can be used to bind together strings of memories. We argue that these mechanisms, which bind memories together can be used to create episodes of memories.

In chapter 8 we apply the model to a repetitive learning protocol, which is shown by a recent study (Fu et al. 2012) to lead to increased clustering of synapses. We examine the conditions under which this clustering arises through repeated learning. A summary of the findings and brief discussion is presented in Chapter 9. The model used throughout this thesis and a subset of the results have been published in (Kastellakis et al. 2016) and discussed theoretically in (Kastellakis et al. 2015).

Chapter 2.

Background on memory allocation and trace formation

In order to study the formation of memory engrams we need a model of the basic components of memory formation and consolidation. We thus sought to identify the most important processes, which enable memory storage in neurocircuits and to develop models for each of them that are simple enough to be both tractable computationally and amenable to investigation. We based our neuronal network model on recent empirical studies, which have identified a number of different players involved in memory storage.

The storage of memories in neuronal populations is believed to rely on structural and biophysical changes in the synapses between interconnected neurons. Ramon y Cajal was the first to suggest that synaptic contacts between neurons could play a role in memory storage (Ramón y Cajal & y Cajal 1893). The term *memory engram* was first coined by Richard Semon (Semon 1904; Schacter 2001), who advocated a physical theory of memory and defined the engram as the lasting modification produced by experience and stimulation. Early attempts to find the engram in the brain were pioneered by Karl Lashley, who performed lesion experiments in the cerebral cortex in an attempt to find associations between the lesions and the ability of animals to solve a maze task. While the lesions did cause memory impairments, Lashley's

studies found that this was irrespective of the location of the lesion, leading him to conclude that the memory engram is not localized, but it is spread broadly and indiscriminately throughout the brain (Lashley 1950). Later experiments, however, found that this conclusion was not true. Penfield and Rasmussen found that electrical stimulation in specific brain regions, which were applied to epileptic patients in order to identify the centers of seizures, could cause the vivid recall of random memories (Penfield & Rasmussen 1950). Several years later, the famous case of patient H.M., whose bilateral removal of the medial temporal cortex led to anterograde amnesia, bolstered the idea that episodic memories may be processed in the hippocampus (Scoville & Milner 1957). More recent studies have established the existence of a memory trace that is both causal and necessary for the expression of memory and the mechanisms underlying the formation of these representations remain under intense investigation (Tonegawa et al. 2015).

Novel experimental technologies, such as ligand- and light-driven neuronal activation systems, have been used to identify the biophysical correlate of memories in the brain (the *memory engram*). These studies have shown that memories are stored in populations of neurons through synaptic strength modifications, and that stimulation or suppression of these neurons leads to memory recall or suppression, respectively (Garner et al. 2012; Han et al. 2007; Josselyn 2010; Kim et al. 2014; Liu et al. 2012). These studies have shown that the allocation of a memory into a neuronal population is dependent on the excitability (specifically, spike adaptation properties) of neurons (Silva et al. 2009; Kida et al. 2002).

The mechanism that allows the formation of memory engrams is believed to be the plasticity of synaptic efficacies. These alterations in synaptic connectivity and strength take place mainly on the dendritic elaborations of neurons. Thus, synaptic plasticity is dependent on the biophysical and anatomical substrate that is provided by the dendrites. The complex branching morphology of dendrites can affect electrical signal propagation and constrain the movement of chemical substances (Cui-Wang et al. 2012; Vetter et al. 2001). For example, the high impedance of dendritic spine necks allows spines to act as compartments that enhance input cooperativity (Harnett et al. 2012). In addition, a large variety of voltage and ligand-dependent channels reside in dendrites and shape both the electrical integration as well as the biochemical signaling that determines plasticity phenomena. (Mainen & Sejnowski 1996; Häusser et al. 2000; Sjöström et al. 2008; Spruston 2008; Major et al. 2013). These enable dendrites to support the generation of dendritic spikes, singular electrical events, which can greatly amplify inputs and generate large local calcium transients in the dendrites (Schiller et al. 1997; Häusser et al. 2000; Wei et al. 2001; Nevian et al. 2007; Larkum et al. 2009). Lastly, through electrical and chemical compartmentalization, dendrites are able to support spatially restricted plasticity (Golding et al. 2002; Losonczy et al. 2008; Sjöström et al. 2008; Hardie & Spruston 2009). These properties furnish dendrites with the ability to regulate synapse modification in complex, nonlinear ways, which adds an additional level of computation that determines the response properties of neuronal populations. It is therefore important to include a description of dendritic events in models of memory, in order to study their role and their effects in memory phenomena.

The process of synapse reorganization, modification and consolidation has been known to be protein-dependent (Trifilieff et al. 2006; Maren et al. 2003; Lynch et al. 2014). This dependence creates an interesting problem for neurons, as the synthesis of these proteins may require nuclear transcription or somatic protein translation. The synaptic tagging and capture (STC) theory postulates that synapse activation generates a transient synaptic "tag", and that permanent changes in synaptic weight require the production and capture of plasticity-related proteins (PRPs) by the "tagged" synapses. This model has been supported by a number of experimental studies (Frey & Morris 1997; Moncada & Viola 2007; Martin et al. 1997) and is now a well described and widely accepted theory about the consolidation of the long-term potentiation of synapses.

Apart from the changes in connectivity of excitatory synapses, inhibition also plays a major role in determining the electrophysiological response of postsynaptic structures where synapses reside. Inhibitory connections have multiple roles, which allow them to tune the effect of excitatory synapses in the depolarization of the postsynaptic neuron (Müller et al. 2012).

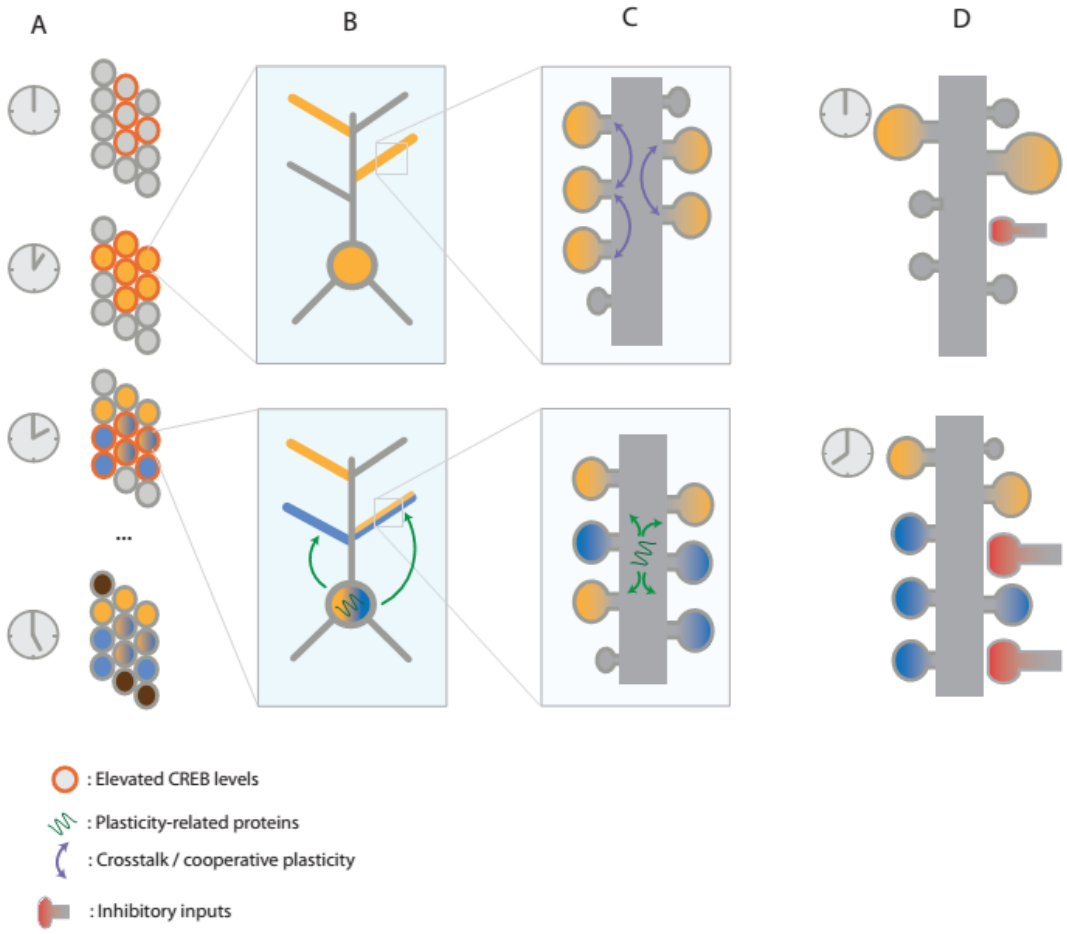

Figure 2.1 Multiple levels of plasticity determine memory storage. A) CREB-dependent excitability can determine the recruitment of neurons to form memory traces over time. Neurons with high excitability or CREB activation are more likely to participate in a memory storage (yellow). This new learning in itself results in increased excitability, which leads to a second memory (blue) being co-allocated in the same neurons. B) At the neuronal level, alterations in local excitability occur as a result of dendritic activation. Therefore, subsequent learning is more likely to activate these dendrites .C) At the dendritic level, crosstalk between synapses enables associative LTP, which leads to clustered potentiation of synapses. Synaptic tagging and capture also enables new memories to be co-clustered in

the same dendrites (blue synapses). D) Over long timescales, homeostatic mechanisms and the plasticity of inhibition balance the excitation received by dendrites in order to ensure normal neuronal activation levels.

Other major sources, which affect synaptic connectivity are homeostasis and the plasticity of intrinsic excitability. Homeostasis is a physiological process that maintains the firing rate of neurons within physiological ranges, and this is done through modifications of synaptic strengths. In addition, in response to dendritic or neuron-wide stimulation, neurons can change their electrophysiological behavior by changing the ionic channel content of their membrane, which, in turn, affects the impact of synapses (Zhang & Linden 2003).

The processes outlined above provide the basic components of a memory formation model. Figure 2.1 summarizes the various scales at which plasticity is organized. In the following subsections, we elaborate each of those components, and discuss the experimental findings regarding their role in memory formation.

2.1 Memory storage in neuronal populations

Recent studies using ligand- and light-driven neuronal activation systems have identified and explored the properties of the cellular populations engaged in the long-term storage of memories. Their findings suggest that memory representations are directed to region-specific neuronal ensembles that can be visualized by a variety of imaging techniques (Guzowski et al. 1999; Han et al. 2007; Reijmers et al. 2007).

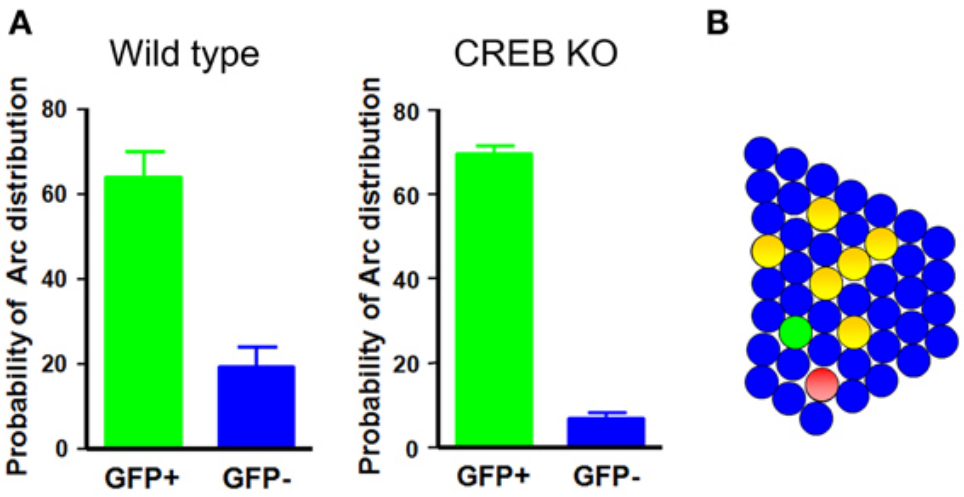

Figure 2.2 Neurons with increased CREB activation are preferentially recruited in a memory trace

A) Wild type and CREB -deficient mice are more likely to be recruited when virally injected with a constitutively active form of CREB. B) Schematic of memory trace Green: CREB+ neurons, red: Arc+ neurons which indicate neuronal activity. Yellow: overlap. Image from (Kim et al. 2013), reproduced under the Creative Commons license CC-BY.

Evidence for the existence of specific neuronal populations that constitute the memory engram comes from recent optogenetics studies. Using the c-fos immediate early gene promoter to selectively express fluorescent proteins and channel rhodopsin 2 channels (ChR2) in dentate gyrus neurons activated during contextual fear training, it became possible to identify the neurons participating in a memory (Liu et al. 2012). Light-activation of these ChR2 neurons triggered both neuronal spiking, and a fear response, suggesting that activation of neurons engaged in learning is sufficient to trigger recall of the stored memory. It is now possible to manipulate these memory engrams as well: By activating a preexisting memory engram while learning a fearful event, either pharmacologically (Garner et al. 2012) or optogenetically (Liu et al.

2014), it became possible to create a fearful response to a preexisting, innocuous memory. This created a "synthetic" memory that associated a not-conditioned stimulus with a fear response. Further studies have been able to use the identifiable memory traces and manipulate the valence of memories (i.e. whether they are rewarding or aversive), by optogenetically creating artificial associations (Redondo et al. 2014).

How these populations of neurons are selected to encode a memory and participate in a memory trace (a process termed memory allocation (Rogerson et al. 2014)) is not yet fully known. Mounting evidence indicates, however, that the activity of the transcription factor CREB (cAMP response element binding protein), a molecule with a known role in long-term memory storage (Dash et al. 1990; Silva et al. 1998) is crucial for the recruitment of neurons during memory formation. In particular, CREB phosphorylation seems to play a critical role in determining whether neurons will become engaged in storing a memory. Using viral vectors that artificially increase the levels of CREB activity in an identifiable sub-population of lateral amygdala neurons, it was shown that neurons with higher CREB levels are more likely to be involved in fear memory (Han et al. 2007) (Figure 2.2). Subsequent inactivation or ablation of cells with elevated CREB weakened the fear memory, indicating that these particular cells were critical for recall (Han et al. 2009; Silva et al. 2009). Electrophysiological studies showed that neurons with high CREB levels are more excitable compared to controls, having reduced afterhyperpolarization (AHP) current. Thus, cells with elevated CREB levels are more excitable, therefore more likely to be active while learning an event, and therefore are also more likely to undergo synaptic plasticity and become part of a memory engram (Silva et al. 2009).

These studies have established that specific cellular populations can encode basic forms of memories. However, synaptic plasticity, which is the mechanism via which memories are stored in these populations, acts mainly on the dendritic regions of cortical neurons. In order therefore to understand how memory engrams are formed, a deeper investigation of how dendrites contribute to the complex functions of memory encoding, storage and retrieval is needed.

2.2 Dendritic branches contribute to memory storage

In neocortical pyramidal neurons, dendritic branches (Figure 2.3) provide the physical substrate where synapses are formed and modified through plasticity operations. Dendrites are equipped with an array of biophysical mechanisms that determine their postsynaptic responses. This allows them to integrate the excitatory postsynaptic potentials (EPSPs) of the afferent synapses that impinge upon them in a linear or nonlinear way (Ariav et al. 2003; Häusser & Mel 2003; Poirazi et al. 2003a; Losonczy & Magee 2006; Silver 2010; Branco & Häusser 2011; Yuste 2011; Longordo et al. 2013). This distinction is important for computational reasons, since the mode of synaptic integration can allow dendrites to perform distinct arithmetic operations of their inputs (Silver 2010).

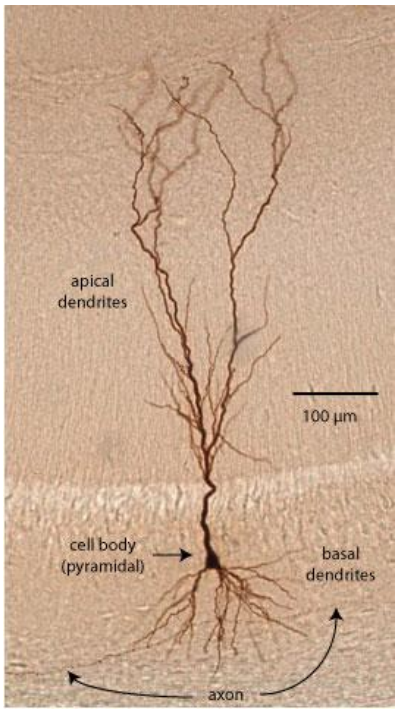

Figure 2.3 Subdivisions of the dendrites of neocortical pyramidal neurons. (Image from Scholarpedia/Shannon Moore, reproduced under the Creative Commons license CC-BY-NC-SA)

The linear mode of integration is associated with the action of synaptic inputs, which are distributed randomly and uniformly throughout the dendritic tree of the neuron (Cash & Yuste 1999; Yuste 2011). The non-linear (supralinear or sublinear) integration of synaptic inputs is associated with synaptic inputs, which are grouped together spatially, a phenomenon known as *synapse clustering*.

2.3 Distributed connectivity and linear integration

The linear integration mode may be particularly useful when synaptic input is dispersed uniformly throughout the dendritic tree, as a result of random connectivity

between neurons that is dictated by anatomical constraints (Braitenberg & Schüz 1998). In this case, the connectivity of neuronal circuits is determined by the overlap of dendritic arbors and axonal processes, as dictated by Peters' rule (Peters et al. 1976). There is evidence that such random connectivity may exist in sensory cortices, however, it is not clear that it arises from random connectivity. In particular, by combining high-speed 2-photon imaging with electrophysiological recordings in the visual (Jia et al. 2010), auditory (Chen et al. 2011) and barrel (Varga et al. 2011) sensory cortical areas, it was shown that synapses on nearby spines in dendrites of pyramidal neurons are responding to seemingly unrelated orientations, sound frequencies or whiskers and whisker combinations, respectively. This indicated that there was no specific organization of synapses at the spatial scale of the dendrite, but instead there is an unstructured mixture of connections. It can therefore be hypothesized that the connectivity pattern from sensory input to these primary sensory cortices supports the distributed/linear integration of sensory signals in the target dendrites. The distributed connectivity and linear summation model has inspired a large volume of artificial neural network research in the past decades (Minsky & Papert 1969; Hopfield 1988). While these artificial neuron models overly simplify the function of neurons by reducing them to point thresholding devices, they have been instrumental in studying memory storage in artificial neuronal populations. These models have established synaptic weight changes as a valid mechanism of learning in artificial neural networks (McClelland & Rumelhart 1986; Hornik et al. 1989).

2.4 Clustering and supralinear integration

The distributed connectivity model presents a simple rule of dendritic connectivity, however, it doesn't capture many of the experimental observations regarding dendritic function. In particular, in several brain areas it has been found that synapses are not randomly placed in dendrites, but tend to form groups or *clusters* of synapses. These clusters of synapses have special significance for synaptic integration: sufficient activation of a number of synapses in a short stretch of dendrite can cause the emergence of a self-regenerating, powerful dendritic spike (Losonczy & Magee 2006). Dendritic spikes are much stronger responses than ordinary excitatory post-synaptic potentials (EPSPs) and thus have the ability to influence the output of the soma, or even induce plasticity at the dendritic level (Spruston 2008; Hardie & Spruston 2009). Several studies have shown that synaptic contacts in many brain areas can group together within a short stretch of the dendritic branch, forming such *anatomical synaptic clusters* (Yadav et al. 2012; Makino & Malinow 2011; Druckmann et al. 2014). In addition, imaging studies have observed that synapses form *functional synaptic clusters*, whereby several neighboring synapses are activated in sync (even if they are not distinctly anatomically clustered), indicating that they carry the same presynaptic information (Takahashi et al. 2012; Kleindienst et al. 2011; Fu et al. 2012). Figure 2.4 summarizes the ways in which synapses cluster together in dendrites. This patterned spatial synaptic arrangement and activation along with concrete evidence of dendritic spike generation both *in vitro* (Schiller et al. 2000; Nevian et al. 2007; Kim et al. 2012; Makara & Magee 2013; Ariav et al. 2003; Häusser et al. 2000; Larkum & Nevian 2008; Losonczy & Magee

2006) and *in vivo* (Smith et al. 2013; Lavzin et al. 2012; Major et al. 2013) endow dendrites with computational capabilities that go beyond the simple linear integration afforded by distributed connectivity. Thus, connectionist models that account only for distributed connectivity, such as the majority of artificial neural network models and spiking neuronal models, are not sufficient to model the function of neurocircuits.

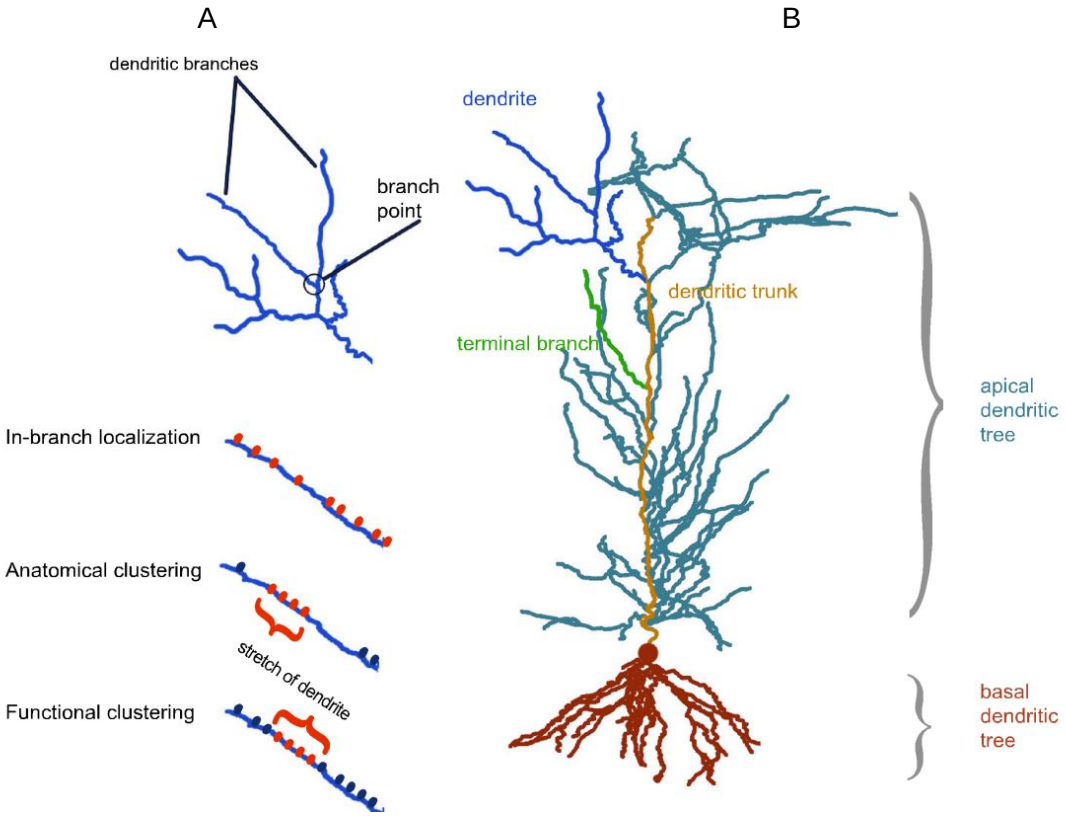

Figure 2.4 Different types of synapse clustering in dendritic surfaces.
A) Clustering within dendritic branches can occur in different ways. B) Different dendritic subdivisions and the terms used to describe them.

The clustering of synaptic inputs within dendrites of both simplified (Mel 1993; Poirazi & Mel 2001) and biophysically detailed neurons (Poirazi et al. 2003b; Poirazi et al. 2003a) was theoretically predicted to influence the dendritic and neuronal output by differentially engaging local conductances. For example, synchronous activation of synapses within the same apical branch of a biophysically realistic pyramidal neuron model was predicted to result in supralinear responses while stimulation of the same number of synapses distributed in different branches resulted in linear summation (Poirazi et al. 2003a). This prediction was verified experimentally in L5 neocortical pyramidal neurons (Polsky et al. 2004). Supralinearity in this case resulted from the induction of dendritic spikes, a phenomenon that was not seen when synapses were stimulated across different branches. Similar supralinear dendritic responses were also found in oblique dendrites of CA1 pyramidal cells upon stimulation of synapses within individual radial oblique branches (Losonczy & Magee 2006). In this case, synchronous stimulation of nearby synapses had the same effect as synchronous stimulation of the same number of synapses distributed uniformly within the radial oblique branch (*in-branch localization*), suggesting that these structures act as single, nonlinear integrative compartments. These dendrites may act as coincidence detectors (Losonczy & Magee 2006; Gómez González et al. 2011; Ariav et al. 2003) and serve as detectors of asynchronous bursting inputs (Gómez González et al. 2011) via the induction of fast or slow, respectively, dendritic spikes.

2.5 LTP cooperativity in nearby inputs

Beyond the integration of synaptic signals, the dendritic depolarization and dendritic spikes can have a strong effect on Long Term Potentiation (LTP), the form of synaptic plasticity, which is believed to play the key role in learning and memory formation. In CA1 pyramidal neurons, local synaptic depolarization that results in dendritic spikes can induce LTP even in the absence of somatic spiking (Golding et al. 2002; Hardie & Spruston 2009). In addition, this form of LTP is stronger when paired synaptic inputs are both located in the apical dendrites than if they are separated in the apical and basal trees. This suggests that the large and long lasting dendritic depolarization generated by the activation of spatially proximal synapses is more effective in inducing strong LTP than the pairing of dendritic input with backpropagating action potentials. This difference possibly arises from the ability of spatially close synapses to undergo plasticity in a cooperative manner.

Cooperativity is the ability of multiple activated synapses to collectively overcome the threshold for plasticity and this characteristic property of LTP is believed to be mediated by NMDA calcium influx (Bliss & Collingridge 1993; Sjöström et al. 2001). Synaptic input, which leads to LTP in dendrites initiates complex biochemical signaling cascades in the dendritic region, triggered by the influx of calcium and the elevation of its local concentration (Baudry et al. 2011). Some of these pathways facilitate the cooperativity of LTP at nearby synapses, and this can lead to the coordinated potentiation of neighboring synapses, promoting synapse clustering. For example, the MAPK (mitogen-activated protein kinase) and mTOR (mechanistic target of rapamycin) cascades remain active for several minutes after their initial

activation (Wu et al. 2001). This prolonged activation allows the spread of proteins and kinases to nearby synapses. The Ras GTPase, which is part of the MAPK signaling pathway and is correlated with increased spine volume during LTP induction, has been shown to spread and invade nearby spines (Harvey et al. 2008). In addition, the RhoA GTPase was found to spread out of stimulated dendritic spines undergoing structural plasticity related to LTP for about 5µm along the dendrite (Murakoshi et al. 2011). These molecular mechanisms support the cooperative potentiation of synapse clusters at the spatial scale of < 20 µm (Winnubst et al. 2012; Patterson & Yasuda 2011; Hering & Sheng 2001).

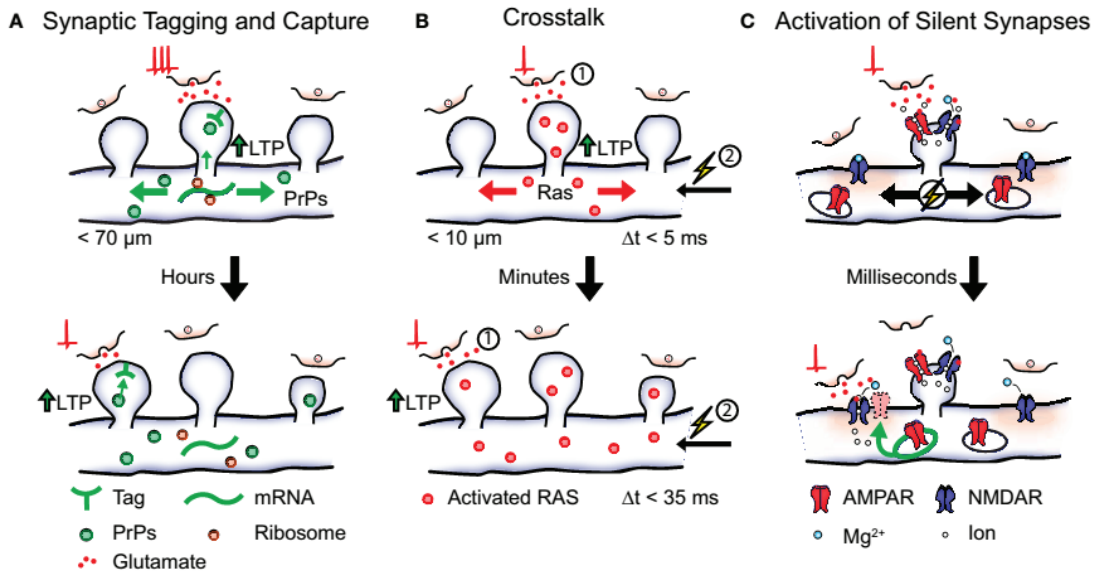

Figure 2.5 Possible mechanisms allowing cooperative LTP and establish synapse clustering.
A) Synaptic tagging and capture allows weakly stimulated synapses to be potentiated within distances < 70µm B) Cross-talk between nearby synapses through molecular pathways allows clustering at the range of 10µm C) Insertion of AMPA receptors allows silent synapses containing only NMDA receptors to become active. PRPs, plasticity-related proteins. Image from

(Winnubst et al. 2012) reproduced under the Creative Commons licence CC-BY.

Another mechanism that enables local cooperativity of LTP is the activation of 'silent' synapses. Silent synapses contain only NMDA receptors, which are blocked by Mg^{2+} ions when the local membrane is in its resting state. The depolarization caused by the activation of nearby synapses, however, can remove the Mg^{2+} block, allowing these synapses to become conductive. Under a Hebbian plasticity protocol, this could eventually lead to the insertion of AMPA receptors in the synapse, 'unsilencing' the synapse (Liao et al. 1995). Figure 2.5 summarizes the ways in which synapse clustering can occur through LTP cooperativity.

Clusters of synapses can also be formed by the addition of new synapses near existing ones (Fu et al. 2012), which effectively changes the wiring diagram, however, such changes are typically slower as they require the restructuring of neural tissue (Trachtenberg et al. 2002; Chklovskii et al. 2004). Since both synapse formation and elimination are processes that persist in the adult brain (Trachtenberg et al. 2002), it may be possible that LTP cooperativity interacts with synapse formation or the conversion of filopodia to dendritic spines and biases the formation of anatomical synapse clusters.

The evidence indicates that LTP cooperativity in nearby synapses can lead to the formation and stabilization of functional and anatomical clusters of synapses within frequently stimulated dendrites. This clustering may serve as a mechanism for effective wiring, whereby connections are established by sharing protein products,

thus saving energy and molecular resources, while at the same time dendritic non-linearities are fully exploited via the selective induction of dendritic spikes (Winnubst et al. 2012). Based on this evidence, the *clustered plasticity* hypothesis has been put forward, which proposes that inputs with correlated activity patterns (presumably sharing some functional features), are more likely to be organized in functional and/or anatomical clusters within the dendrites of pyramidal neurons (Poirazi & Mel 2001; Govindarajan et al. 2006; Harvey & Svoboda 2007). This view has gradually been gaining experimental support, through the advent of modern imaging methods, which allow the detailed mapping of synapses in dendritic arbors. The role of clustering in memory pathologies is currently under investigation. It is proposed that abnormal synapse clustering conditions may be related to psychiatric disease states such as schizophrenia and autism (Kastellakis et al. 2015).

2.6 Plasticity of dendritic excitability

In parallel with synapse clustering, synaptic activity can also cause changes in the conductance of ionic currents, which determine the excitability of neuronal membranes. This dynamic adaptation of the excitability of the dendrite can influence the way in which dendrites integrate synaptic inputs, and consequently affect the neuronal output. Lasting changes in the excitation properties of the membrane are a form of plasticity called *plasticity of intrinsic excitability*, which can be induced by electrical stimulation *in vitro*, or through exposure to an enriched environment. For instance, LTP-inducing excitatory stimulation can persistently down-regulate A-type potassium currents in CA1 pyramidal neurons, increasing the dendritic excitability (Frick et al. 2004). In addition, LTP and LTD protocols in CA1 neurons result in the

increase and decrease, respectively, of the linearity of the summation of postsynaptic responses. This bidirectional plasticity of excitability reflects changes in the hyperpolarization-activated I_h currents and NMDA receptors (Wang et al. 2003).

The plasticity of intrinsic excitability can be locally restricted to dendritic branches via alterations in branch coupling strengths. Repeatedly triggering dendritic spikes in a dendrite *in vitro* leads to a slow but long-lasting increase in the coupling strength of the dendrite to the somatic depolarization, which is mediated by the down-regulation of A-type potassium currents (Losonczy et al. 2008). The regulation of dendritic excitability may thus be exploited as a compartmentalized memory storage mechanism during learning. Indeed, it has been shown that exposure of rats to an enriched environment leads to the enhancement of dendritic spike propagation selectively in a subset of dendritic branches of CA1 neurons (Makara et al. 2009).

In the studies mentioned above, the localized modulation of dendritic excitability was attributed to the activity-dependent regulation of ionic currents. It is not clear, however, if the plasticity of dendritic excitability requires synaptic input or synaptic plasticity. To investigate this issue, a study tested the plasticity of dendritic excitability using photostimulation of hippocampal dendrites in neurons infected with a channelrhodopsin-2 (ChR2) vector (Labno et al. 2014). The pairing of dendritic photocurrent with somatic spiking induced localized *depression* of excitability. This depression was not dependent on synaptic activation or LTP induction, but was sensitive to calcium. Moreover, the depression was conferred by changes in the A-type potassium current, similarly to the case of branch strength potentiation. These

two examples suggest a key role of the A-type K^+ channel in regulating the local intrinsic excitability of pyramidal neuron dendrites.

Taken together, these results indicate that dendritic excitability is a dynamic property, which can undergo long-term potentiation or depression in response to specific stimulation protocols, and it can be dissociated from synaptic plasticity. Therefore, the plasticity of dendritic excitability can serve as a mechanism that modulates localized synaptic activity and contributes to localized memory storage. It is proposed, therefore, that the plasticity of neuronal and dendritic excitability can be considered part of the memory engram (Zhang & Linden 2003; Sjöström et al. 2008; Legenstein & Maass 2011).

2.7 Synaptic Consolidation and Protein Capture

The mechanisms, which determine the effect of synaptic plasticity and the resulting changes in connectivity on memory formation are numerous and complex. Indeed, the induction of synaptic plasticity involves networks of signaling cascades and kinase activation with timescales that vary from seconds to hours (Bhalla 2011; Citri & Malenka 2008). Nevertheless, a high-level model of memory consolidation can capture important aspects of memory encoding and its protein dependence. The synaptic tagging and capture model is such a framework that characterizes the role of late-LTP processes in memory encoding and provides the foundation for localized, clustered memory storage (Govindarajan et al. 2006; Rogerson et al. 2014).

According to the model of synaptic tagging and capture (Frey & Morris 1997; Redondo & Morris 2011), the consolidation of synaptic potentiation occurs in phases.

Initially, synaptic plasticity sets a local synaptic tag in the synapse targeted for potentiation or depression. The synthesis of plasticity related proteins (PRPs), which are required for synaptic potentiation, takes place over a period of hours after learning. Finally, the synapses that were tagged capture the synthesized PRPs, in order to stabilize their synaptic strengths.

The synaptic tagging and capture (STC) model was initially proposed based on LTP experiments, which showed that protein-synthesis-dependent LTP could be induced even under protein synthesis inhibition, if a stimulus is given to a different pathway within a short time window of a few hours (Frey & Morris 1997; Reymann & Frey 2007). According to STC, the up-regulated protein synthesis, which is a result of the stimulation of the second pathway, 'rescues' the LTP because the tagged synapses can readily capture the synthesized PRPs within hours after the tags creation. The phenomenon was observed by the facilitation of late-LTP in weakly stimulated synapses through the activation of a second strongly stimulated set of synapses (Frey & Morris 1997). Weak stimulation alone, normally results in early-LTP, a form of synaptic potentiation that decays after a few hours. As a consequence of the strong stimulus, however, synaptic proteins are synthesized. The weakly stimulated (but still tagged) synapses - which would normally only express early LTP - can capture the PRPs generated by the strong stimulation and consolidate the early-LTP into late-LTP. Interestingly, even an LTD-inducing event is capable of rescuing a weak memory, which seems to imply that late LTP and LTD share molecular pathways or other processes. This type of exchange from LTD to LTP consolidation is termed *cross-capture* (Sajikumar & Frey 2004; Redondo & Morris 2011).

The implications of the STC model for learning and memory concern the interactions that are expected to arise between learning events that occur within a defined time horizon. This interaction was tested in behavioral experiments, which involved pairing a weak learning protocol with a strong form of learning or environmental novelty. By pairing a weak learning protocol, which normally induces short-term memory, with environmental novelty, it was found that novelty –considered a strong learning event- promotes the formation of long-term memory, presumably through the mechanisms of STC (Moncada & Viola 2007; Ballarini et al. 2009; de Carvalho Myskiw et al. 2013). The memory enhancement was prevented when the protein synthesis inhibitor anisomycin was introduced along with the environmental novelty.

2.8 Local Protein Synthesis

Synaptic plasticity involves numerous kinases, phosphatases, as well as various molecular signaling pathways (Citri & Malenka 2008) and the activity of these pathways may be spatially constrained. This suggests that molecular signaling cascades may underlie the cooperativity effects observed in plasticity induction within nearby sites in dendrites (Harvey et al. 2008; Murakoshi et al. 2011; Bhalla 2011; Govindarajan et al. 2010). The PRPs required for plasticity can be synthesized by the protein synthesis machinery that exists in the soma, or they may be translated locally by ribosomes that exist in dendritic arbors. In support of the latter, several studies have established the existence of ribosomes in hippocampal dendrites (Bodian 1965; Sutton & Schuman 2006; Steward & Levy 1982; Bourne & Harris 2011). These ribosome complexes were found to be near synaptic sites, thus positioned appropriately to facilitate plasticity. Moreover, a large number of mRNAs have

been found in hippocampal dendrites and many of those mRNAs code for known synaptic proteins (Steward & Schuman 2007; Cajigas et al. 2012). This evidence suggests that dendrites may support local protein synthesis, which is required for plasticity at the level of the single dendrite. This protein synthesis does not depend on transcription or somatic protein synthesis, and thus allows dendrites to have relatively autonomous synaptic plasticity. Dendritic protein synthesis was identified to be a requirement for rapid synaptic potentiation under exposure to BDNF (Kang & Schuman 1996) and has since been found to be required for other forms of synaptic plasticity (Sutton et al. 2006).

Based on these observations, it has been proposed that the phenomenon of STC may occur at the dendritic level. In this case, it can lead to LTP interactions and to the generation of activity associations at the dendritic level, via the strengthening and stabilization of neighboring synapses, which facilitates synapse clustering (Kelleher et al. 2004; Govindarajan et al. 2006; Rogerson et al. 2014). An *in vitro* study has specifically confirmed that STC can take place at the level of the dendritic branch (Govindarajan et al. 2010). Using glutamate un-caging and two-photon imaging, it was shown that local protein synthesis induced in a synaptic spine could convert the early-LTP of a nearby spine to late-LTP via synaptic capture mechanisms. This conversion of early-LTP to late-LTP was dependent on the time interval between the stimulation and protein synthesis, and on the distance between the two spines. The strength of this synaptic protein cross-capture was inversely proportional to the distance between the site of protein synthesis and the stimulated synapse, and it did not occur for distances larger than 70μm on the same dendrite or larger than 50μm when the synapses were placed in sibling dendrites. In addition, during LTP

consolidation, tagged synapses competed for the capture of available proteins, indicating that the availability of synaptic proteins is a limiting factor for dendritic STC.

While the studies mentioned above support the case for local protein synthesis, it should be noted, that certain forms of LTP require gene transcription, such as the late-phase LTP induced during theta burst stimulation and serotonin application in amygdala slices (Huang & Kandel 2007). It is thus possible that different forms of LTP are employed by different brain areas, and/or under different stages of memory consolidation (Izquierdo et al. 2006), which would lead to differential spatial distributions of potentiated synapses (clustered / non-clustered).

An intriguing consequence of dendritic STC is that it can become a mechanism for associating temporally close memories, which are expected to form memory representations captured by nearby synapses. This mechanism would result to the generation of functional and/or anatomical clusters of synapses that code for memories that are temporally related over large time frames, defined by the temporal overlap between the life time of the synaptic tag and the up-regulation of PRPs. According to such a model, the cross-capture of proteins between synapses that express either LTP or LTD can lead to clustered formation of memory engrams (Govindarajan et al. 2006). As described by previous modeling work, clustered formation of memory engrams, whereby synapses with correlated activity are grouped within dendritic branches, greatly expands the information storage capacity of neural tissue (Poirazi & Mel 2001). Moreover, synapse clustering resulting from

STC has been hypothesized to mediate the cellular and behavioral binding of memories that are temporally related (Rogerson et al. 2014; Silva et al. 2009).

2.9 The role of Inhibition in memory

Inhibition plays a major role in shaping neuronal output throughout the brain, and displays significant variability in its targeting and magnitude (Klausberger et al. 2003). Dendritic-targeting inhibition regulates the input-output-transformations in CA1 pyramidal cells (Cutsuridis & Hasselmo 2012; Lovett-Barron et al. 2012) and increases the threshold for dendritic spiking (Jadi et al. 2012), while perisomatic inhibition controls oscillatory activity (Pouille & Scanziani 2001) and suppresses the amplitude of dendritic spikes. Recent research has highlighted the plastic nature of inhibition through a plethora of inhibitory plasticity mechanisms (Kullmann et al. 2012). Inhibitory plasticity seems to closely match and balance the plasticity of excitation in its structure, possibly enhancing the temporal precision, responsiveness and sparseness of neuronal output. Interestingly, inhibitory synapses have recently been suggested to follow the clustered plasticity pattern of excitatory synapses in the mouse visual cortex (Chen et al. 2012). These lines of research indicate that inhibition plays a significant role in memory formation.

2.10 Regulation of synaptic plasticity by homeostasis

Homeostatic plasticity is a major balancing mechanism, which acts continuously to regulate synaptic plasticity in the long term. Homeostatic phenomena include changes in the intrinsic membrane excitability, the regulation of presynaptic

transmitter release, the balancing between excitation and inhibition as well as alterations in neuronal connectivity and modulation of synaptic strengths (Turrigiano & Nelson 2004). Synaptic scaling, a process that results in neuron-wide changes in synaptic weights, is a well studied homeostatic plasticity mechanism (Turrigiano 2008). Disruption of neuronal activity *in vitro* causes bidirectional uniform scaling of the mini-EPSCs (excitatory postsynaptic current), which represent the quantum of synaptic responses (Turrigiano et al. 1998). Synaptic scaling can cause coordinated modulation of both the AMPA and NMDA currents in synapses (Watt et al. 2000). These studies indicate that neurons can self-regulate their firing rate by adjusting their synapses over long periods of time.

Homeostatic plasticity can be local, thus regulating only the synapses located within a specific branch (Rabinowitch & Segev 2008). Such specificity may be critical for the maintenance of existing memory engrams during the continuous formation of new ones. Recent studies have identified forms of homeostatic plasticity, which operate at the level of the synapse and/or the branch. Hou et al. found that increasing the presynaptic firing that drives a synapse, caused a selective down regulation of GluA1 receptors in the postsynaptic site (Hou et al. 2011). This indicates a synapse-specific homeostatic regulation mechanism that compensates for increased synaptic input. Another study used a combination of two-photon glutamate un-caging and imaging to show that individual synapses compensate for changes in their input via homeostatic regulation that is independent of their neighboring synapses (Béïque et al. 2011). In this case, homeostatic plasticity was found to require the immediate early gene Arc, which is implicated in synaptic plasticity. The functional role of localized or synapse-specific homeostatic plasticity is not straightforward, as it seems

to be a rule that counters the action of LTP in individual synapses, thus leading to erasure of information. A computational study, on the other hand, has shown that a local form of homeostasis which acts on groups of nearby synapses in dendrites can mediate normalization of responses without disrupting synaptic plasticity (Rabinowitch & Segev 2008).

How homeostasis, synaptic plasticity, plasticity of excitability and plasticity of inhibition interact to regulate the action of synapses at the dendritic level is not clear, as these processes have different timescales and roles. Intrinsic excitability appears to positively enhance Hebbian plasticity, while homeostasis provides a form of negative feedback to synaptic action (Sjöström et al. 2008). Interestingly, dendrite-specific LTP coupled with homeostatic depression was computationally predicted to maximize the learning capacity of a medial temporal lobe model implementing online learning (Wu & Mel 2009). The dendritic learning rules led to an order-of-magnitude increase in the capacity of the network compared to Hebbian learning. Homeostatic mechanisms, thus, provide the final touch in the interplay of local and global factors that guide the formation of memory representations, starting at synaptic mechanisms and including dendritic, neuronal and network processes.

Chapter 3.

Methods

3.1 Overview

In order to study the formation of memory engrams, we sought to create a network of neurons with plasticity properties that match the memory-related phenomena described in the previous section. The proposed model consists of excitatory neurons equipped with dendritic subunits and inhibitory neurons. A network of 500 model neurons was implemented, consisting of excitatory integrate-and-fire neurons with dendritic subunits (80%; 400 neurons) and inhibitory point neurons (20%, 100 neurons) (McDonald 1998; Sah et al. 2003). To account for nonlinear dendritic integration reported in pyramidal neurons (Poirazi et al. 2003a; Poirazi et al. 2003b; Polsky et al. 2004; Losonczy & Magee 2006), each excitatory neuron was modeled as a two-layer structure. This was based on prior work, showing that a two-layer artificial neural network model can reproduce the firing rate of a detailed biophysical CA1 pyramidal neuron model under a wide range of stimulus intensities and distributions (Poirazi et al. 2003b; Jadi et al. 2014). Support for such two stage integration in single pyramidal neurons has also been provided by anatomical studies (Katz et al. 2009). In our model, excitatory neurons have 20 dendritic subunits where synaptic integration and synaptic tagging and capture take place independently. The dendritic subunits contribute to the depolarization of the soma, which acts as the

second layer of synaptic integration. Inhibitory neurons are modeled as adaptive integrate-and-fire point neurons. Details about the exact values of the parameters listed in the following equations are provided in Tables 3.1 and 3.2.

3.2 Dendritic integration

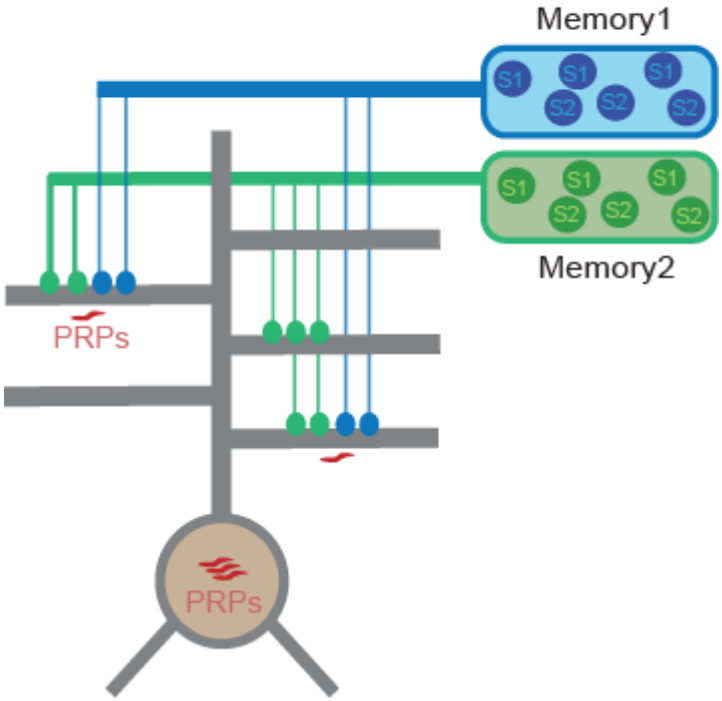

Figure 3.1 Schematic of the delivery of encoding stimuli and synaptic input integration.
PRPs: Plasticity related proteins. S1/S2: Afferent neurons carrying the memory information to be encoded for each memory.

Dendritic subunits integrate incoming synaptic signals independently of each other, acting as independent units of function and plasticity (Branco & Häusser 2010a)

(Figure 3.1). Dendritic EPSPs from synaptic inputs are first scaled according to their synaptic weight (see below) and then summed linearly to calculate the dendritic branch voltage, V_b, which decays exponentially with time constant τ_b, as described by the following equation:

$$\tau_b \frac{dV_b}{dt} = \sum_{i,j} w_j E_{syn}\, \delta\left(t - t_{i,j}\right) - V_b \qquad (3.1)$$

Where $t_{i,j}$ are the times of incoming spikes for synapse j, w_j is the weight of the synapse and E_{syn} is the unitary EPSP. The back propagating action potential V_{bAP} (see below) is summed with V_b to determine the depolarization of the dendrite. When the sum of $V_{b,}$+$V_{bAP,}$ exceeds the dendritic spike generation threshold, θ_{dspike}, a dendritic spike is generated, which causes the voltage of the subunit, $V_{b,}$ to rise instantaneously to V_{dspike}.

3.3 Somatic integration

The V_d of each dendritic subunit is scaled by the branch coupling strength B of the dendrite to calculate its contribution to the synaptic input current that it provides to the soma. The sum of all dendritic currents is added to the total inhibitory current received by the neuron and this provides the total input current to the soma, which is modeled as an integrate-and-fire point unit with adaptation (Jolivet et al. 2006). The branch strength B has been shown to undergo potentiation after repeated dendritic spike elicitation (Losonczy et al. 2008), a phenomenon termed *branch strength potentiation.*

The total current input to the somatic nonlinearity is given by the equation:

$$I_{syn}(t) = g_{syn} \sum_n (B_n V_{b,n}(t)) - IPSC(t) \quad (3.2)$$

where *IPSC(t)* is the total inhibitory input that the neuron receives, g_{syn} is the initial dendritic coupling constant, and B_n is the branch strength potentiation (or depression) of dendrite *n*. The above equation ensures that inhibition modulates the somatic output directly, in accordance with experimental data (Markram et al. 2004). The voltage response of the somatic subunit and its spiking output is modeled as an adaptive integrate-and-fire unit. The somatic membrane potential *V* is given by equations (3.3) and (3.4):

$$C \frac{dV}{dt} = -g_L(V - E_L) - g_{AHP}(V - E_K) + I_{syn}(t) \quad (3.3)$$

$$\tau_{AHP} \frac{dg_{AHP}}{dt} = a_{AHP} \delta(t - t_{spike}) - g_{AHP} \quad (3.4)$$

Where *C* is the somatic membrane capacitance, $g_{L,}$ is the leak conductance, E_L the resting potential, g_{AHP} is the conductance of the afterhyperpolarization (AHP) current and E_K is the AHP reversal potential. Equation (3.4) describes adaptive conductance g_{AHP}, where τ_{AHP} is the adaptation time constant, $a_{AHP,}$ the quantal increase of g_{AHP} after a somatic spike that occurs at time t_{spike} and $\delta(t)$ is the Dirac delta. The time constant τ_{AHP} can have two values, which correspond to the high and low excitability levels of the neuron. Increased neuronal excitability has been observed after learning and overexpression of CREB (Disterhoft & Oh 2006; Zhou et al. 2009). Accordingly, in our model, if a neuron exceeds the Calcium threshold for somatic PRP synthesis (detailed below), it is considered to take part in the memory engram and its excitability is subsequently increased for 12 hours following learning.

Somatic spiking and reset occurs when the somatic voltage reaches a threshold V_T. The backpropagating action potential is modeled by a depolarization component V_{bAP} that is added to all the dendritic subunits. $V_{bAP}\ (t)$ is modeled by an exponential:

$$V_{bAP}(t) = E_{bAP}\, e^{-\frac{t}{\tau_{bAP}}} \qquad (3.5)$$

Where E_{bAP} is the peak of the backpropagating depolarization and τ_{bAP} is the time constant of the *bAP*. The time constant V_{bAP} is large and thus it has a slow tail, which has previously been shown to be required by the calcium control model of plasticity for STDP (Shouval et al. 2002).

3.4 Modeling calcium-mediated processes

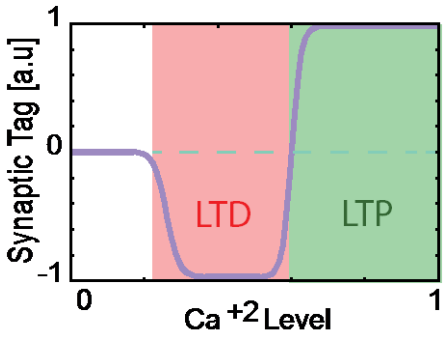

Figure 3.2 Dependence of synaptic tagging on calcium accumulation at the synapse.
Horizontal axis: accumulated synaptic Ca^{+2} in arbitrary units. Vertical axis: Synaptic tag value in arbitrary units.

Calcium acts as the main trigger for the induction of synaptic tags and for the synthesis of PRPs. The total calcium influx to a synapse during a learning event

determines the level of calcium C_{syn}, which models the calcium concentration near each synapse. Each incoming synaptic spike causes a step increase of calcium, which depends nonlinearly on the local depolarization of the dendritic branch where the synapse resides. We assume that calcium influx upon arrival of a presynaptic spike ΔC_{syn} is primarily through NMDA receptors (Higley & Sabatini 2012) and is thus dependent on the depolarization of the dendritic membrane sigmoidally:

$$\Delta C_{syn} = \alpha_{Ca} \frac{1}{1+exp\left(-\frac{V - 30\,mV}{5\,mV}\right)} \tag{3.6}$$

where α_{Ca} is the maximum Ca^{+2} influx and $V=V_b+V_{bAP}$

3.5 Synaptic Tag generation

The strength and the sign (LTP or LTD) of the synaptic tag are determined according to the Calcium Control Model (Shouval et al. 2002), thus low to intermediate levels of Ca^{2+} cause LTD, while higher levels cause LTP (Figure 3.2). After a learning event, the calcium level C_{syn} determines the sign and magnitude of the synaptic tag according to the function *synTag* (Table 3.1). The synaptic tag does not alter the weight of the synapse immediately, but only after the capture of PRPs, which are required for consolidation. Synaptic tags in our model decay exponentially with time constant of 1 hour (Figure 3.4).

3.6 Plasticity related proteins production

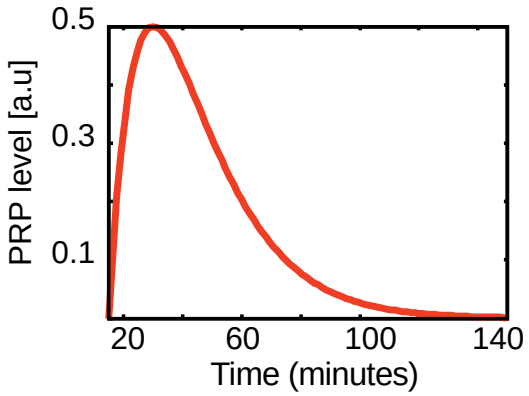

Figure 3.3 Transient concentration of plasticity-related protein after crossing the plasticity threshold
Horizontal axis: Time after the initation of a PRP concentration transient. Vertical axis: Level of PRPs concentration in arbitrary units.

Plasticity studies have identified a crucial role of somatic protein transcription/translation for the consolidation of synaptic plasticity (Frey et al. 1989; Nguyen et al. 1994). Recent studies, however, suggest that under certain conditions, somatic protein translation may not be needed, and instead dendritic protein translation may be crucial (Kang & Schuman 1996; Huber et al. 2000). Dendrites contain protein synthesis machinery as well as an array of mRNAs coding for plasticity-related proteins (Sutton & Schuman 2006; Cajigas et al. 2012). Studies of synaptic tagging and capture have shown that it is possible for the phenomenon to occur at both the somatic and the dendritic level (Frey & Morris 1997; Govindarajan et al. 2010).

We simulate three conditions of protein production in our model: in the first condition, PRPs are presumed to be produced in the soma of the neuron and made available to all dendritic subunits simultaneously. In the second condition, PRP production is restricted in dendritic subunits and is independent of the PRP synthesis in other dendritic subunits. We refer to the first condition as "somatic PRP synthesis" and the second as "local PRP synthesis". For the two conditions, we define separate calcium thresholds for PRP synthesis. The third condition is the combination of the two, such that at every time point the PRPs available to a synapse is the sum of the somatically available PRPs and the locally (branch) available PRPs.

PRP synthesis initiation is modeled as an all-or-none phenomenon. In the case of dendritic PRP synthesis, when the total dendritic calcium level exceeds the dendritic PRP production threshold, $P_{dend,}$, i.e. when $\sum_j C_{syn,j} > P_{dend}$, a PRP transient increase is generated. Accordingly, in the case of Somatic PRP synthesis, a PRP transient is generated when the total calcium level (sum of all dendritic calcium levels) exceeds the somatic PRP production threshold, P_{soma}, i.e. $\sum_n(\sum_j C_{syn,j}^n) > P_{soma}$. The time course of a PRP transient is modeled by alpha functions with different time courses:

$$PRP_{soma}(t) = H(t - 20min)\left(\frac{t-20min}{30\ min}\right) exp\left(1 - \frac{t-20min}{-30\ min}\right) \quad (3.7)$$

$$PRP_{dend}(t) = \left(\frac{t}{15\ min}\right) exp\left(1 - \frac{t}{15\ min}\right)$$

where $PRP_{soma}(t)$ is the stereotypical time course of the protein concentration when somatic protein synthesis is triggered at time t, $PRP_{dend}(t)$ the time course of the

concentration of PRPs in the dendrite when dendritic protein synthesis is triggered at time t and H(t) is the Heaviside step function and models the delay in somatic PRP synthesis(see Figure 3.3). The time course of the alpha functions was chosen based on a previous study of the role of essential kinases in LTP induction (Smolen et al. 2006a), but taking into account more recent evidence regarding the time course of PRP-tag interactions in the dendrite (Govindarajan et al. 2010) and in the whole neuron (Redondo & Morris 2011) . In addition we assumed that somatic PRP synthesis induces a delay of 20 minutes in the availability of proteins which is attributed to second-messenger signaling and protein transport from the soma to the dendrites.

When multiple PRP transients have been generated at different time points $t_{PRP,i}$, the total PRP level at any time point is the saturating sum of PRP transients:

$$PRP_{total}(t) = \sum_i \left(1.0 - PRP_{total}(t)\right) PRP(t - t_{PRP,i}) \qquad (3.8)$$

3.7 Synaptic tag consolidation

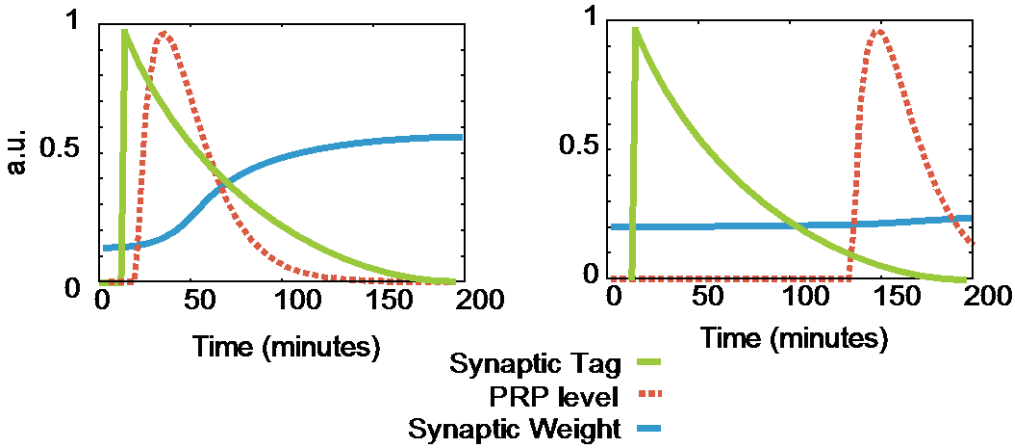

Figure 3.4 Consolidation of synaptic tag into synaptic weight depends on the availability of PRPs.
Left: When synaptic tags overlap temporally with the availability of PRPs (red), the plasticity rule allows the synaptic tag (green) to change the weight of the synapse (blue). Right: In contrast, when PRPs are not available during the lifetime of the synaptic tag, significant synaptic weight change does not take place (right panel).

Synaptic tags are converted to consolidated synaptic weights over time with a rate that is proportional to the value of the tag and the level of PRPs.

$$\Delta w = a_s * synaptictag * PRP_{total}(t) \qquad (3.9)$$

where *synaptictag* is the value of the synaptic tag (positive for LTP, negative for LTD) and a_s is the rate of synaptic tag consolidation. Consolidated synaptic weights are hard-limited in the range [0, 1.0].

3.8 Dynamic neuronal excitability

Learning has been shown to increase the excitability of neurons participating in the formation of a given memory (Disterhoft & Oh 2006; Zhou et al. 2009; Frick et al. 2004; Oh et al. 2003; Sehgal et al. 2014; Silva et al. 2009). Neurons with increased excitability on the other hand are more likely to participate in the formation of a new memory engram (Zhou et al. 2009; Huang et al. 2008; Kim et al. 2013). The activation of transcription factor CREB has also been found to modulate the excitability of neurons (Dong et al. 2006; Han et al. 2006) through the reduction of the afterhyperpolarization (AHP) current (Lopez de Armentia et al. 2007; Zhou et al. 2009). Therefore, it has been suggested that learning makes cells more amenable to be recruited in future learning events through the activation of CREB (Silva et al. 1998; Benito & Barco 2010; Kim et al. 2014; Rogerson et al. 2014; Silva et al. 2009). Finally, it has been proposed that CREB may also induce the downstream activation of its own repressors (Zhou et al. 2009; Silva et al. 2009), which would lead to the reduction of excitability after a certain period, thus creating a time window of increased neuronal excitability. We simulate the increased excitability by reducing the AHP current in the neurons in which somatic PRP synthesis is triggered as shown in Table 3.1 for approximately 12 hours after the learning event (time constant 8 hours).

3.9 Branch strength plasticity

Based on observations of branch-specific changes in intrinsic properties of frequently activated dendrites (Labno et al. 2014; Losonczy et al. 2008), branch coupling

strengths, B_n, were modeled as dynamic, plastic quantities. Branch strength potentiation (BSP) has been found to occur through the repeated elicitation of dendritic spikes (Losonczy et al. 2008) and has important implications for dendritic memory storage (Legenstein & Maass 2011). In addition, a recent study has observed activity-dependent branch strength depression, which was dissociated from synaptic plasticity in hippocampal neurons (Labno et al. 2014).

We model the activity-dependent potentiation of branch strength and, additionally, we incorporate a branch strength normalization rule that prevents saturation of branch strengths (i.e. the strengths of all branches being maximally potentiated). The potentiation and normalization processes are described by equations 3.10 and 3.11. Specifically, the elicitation of a dendritic spike sets a "dendritic potentiation tag", $B_{tag,}$ which causes a slow potentiation in the dendritic branch coupling constant, $B_{n,}$ over the course of the following hours (equation 3.10). Branch coupling strengths are normalized via the use of a normalization term (equation 3.11).

$$\tau_{Btag}\frac{dBtag}{dt} = B_{tag0}\sum_i \delta\left(t - t_{i,dspike}\right) - B_{tag} \qquad (3.10)$$

$$\frac{dB_n}{dt} = \frac{1}{\tau_{BP}}B_{tag}\left(B_{max} - B_n\right) + \frac{1}{\tau_{BH}}B\left(1 - \frac{\sum_n B_n}{N_b}\right) \qquad (3.11)$$

where τ_{Btag}, $B_{tag0,}$ τ_{BP}, B_{max},τ_H, N_b are: the time constant of branch-strength-potentiation tag decay, the stepwise increase in BSP-tag for each dendritic spike, the time constant of branch strength potentiation, the maximum branch coupling strength, the time constant of branch strength normalization, and the total number of branches per neuron, respectively.

3.10 Homeostatic plasticity

The effect of homeostasis on synaptic weights is modeled using a synaptic scaling rule (Turrigiano 2008). According to this rule, the total synaptic weight of a model neuron remains constant. The synaptic weights, $w_{j,}$ of each synapse are normalized according to the following equation:

$$\frac{dw_j}{dt} = \frac{1}{\tau_H}\left(1 - \frac{\sum_j w_j}{w_{init}\, N_{syn}}\right) \qquad (3.12)$$

where w_{init} is the initial synapse weight and N_{syn} the total number of synapses in the model neuron. Homeostatic synaptic scaling has a slow time course determined by τ_H, therefore we introduce a large post-learning period in order to simulate its effect.

3.11 Interneuron model

Interneurons are modeled as integrate-and-fire neurons with adaptation. Interneurons have a different spike adaptation time constant τ_{AHPI} (Washburn & Moises 1992). Inhibitory afferent and efferent connections are not plastic. Interneurons thus provide feedback inhibition to the local circuit.

3.12 Network model and simulation protocol

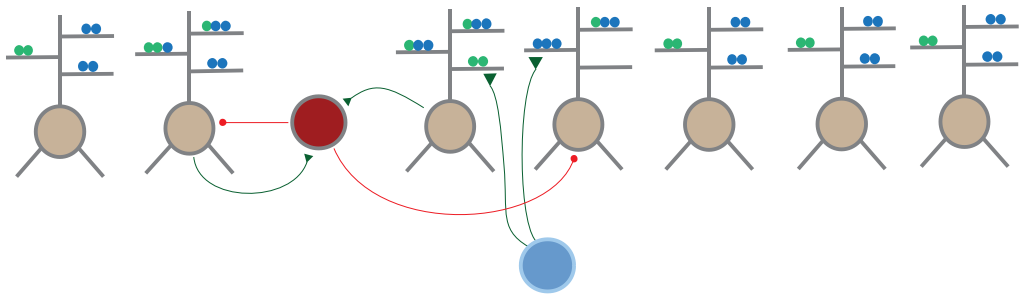

Figure 3.5 Schematic of the network with recurrent feedback inhibitory connectivity.
Excitatory neurons (brown) provide excitation to inhibitory neurons (red) randomly. Inhibitory neurons provide recurrent inhibition to the somatic compartment of excitatory neurons. Stimulus-carrying input neurons representing different memories (green, blue) terminate on random dendritic subunits of the excitatory neurons. Background noise-carrying inputs (blue) provide background excitation to dendritic subunits of excitatory neurons. Only representative excitatory and inhibitory connections (green and red lines respectively) are drawn in this figure.

The network model consists of populations of a) excitatory neurons of a target region, b) inhibitory neurons in the same region c) the stimulus-carrying input neurons and d) background-noise input neurons (Figure 3.5). Conceptually, each memory encoding is performed by the activation of a set of stimulus-carrying neurons, which carry the conditioned and unconditioned stimulus information that represents the memory to be encoded (Figure 3.1). Stimulus-carrying neurons are

grouped in sets of 6 (3 representing stimulus 1 (S1) and 3 representing stimulus 2 (S2)), which fire with an average firing frequency of 30Hz during the training of each memory (S1+S2 neurons) as well as during the recall of each individual event (S1 neurons only). The firing rates chosen induced spiking activity in the excitatory population that resembles the activity of principal neurons in the lateral amygrala (Faber et al. 2001) .

Stimulus-carrying neurons create synapses randomly targeting the dendritic branches of the excitatory neurons. These stimulus-to-excitatory synapses are the only plastic synapses in the network and are initialized to the same initial weight, w_{init}. Feedback inhibition is modeled via random recurrent synaptic connections between the inhibitory and excitatory populations. In addition, a population of background inputs provide continuous background excitation to the excitatory neurons. The background inputs create synaptic contacts to random dendrites and fire with average frequency 0.5 Hz throughout the simulations. The connectivity between neuronal populations in the network model is summarized in Table 3.2.

When encoding multiple associative memories, inter-stimulus intervals (ISIs) are introduced between consecutive memories. During ISI periods, spike dynamics and spiking activity is not simulated; instead, all slow-acting consolidation processes take place (PRP production, synaptic tag consolidation, branch-strength potentiation and homeostasis). After all encoding events, a large consolidation period of 36 hours is additionally introduced, before the memories are recalled, via the activation of the S1 input neurons alone.

In addition to the simulations described in the main text, we performed a simulation in which the memory training was repeated every 24 hours for a period of 4 days. Repeated training of a motor task has been shown to result in increased clustering of synapses in the motor cortex (Fu et al. 2012).

3.13 Calibration of plasticity and connectivity

During amygdala-dependent fear learning, a large percentage of the lateral amygdala neurons (50-70%) are activated (i.e. receive the sensory stimulus) (Guzowski et al. 1999), however, only 25-30% of them undergo plasticity during memory storage (Quirk et al. 1995; Repa et al. 2001; Rumpel et al. 2005; Sehgal et al. 2014). This suggests that although sensory input is widely distributed in the lateral amygdala, only a subset of neurons undergoes plasticity and becomes part of the memory trace.

Accordingly, we calibrated our initial network connectivity and the thresholds of somatic or dendritic Ca^{2+} level that is required for PRP-production so that, after learning of a single memory, its recall of a single memory activates about 30% of this neuronal population. The resulting calibrated parameter values and plasticity thresholds are listed in Tables 2.1 and 2.2.

3.14 Analysis of memory engrams

Successful learning of a given memory is assessed by measuring the spiking properties of the excitatory neuronal population during recall. Due to the diffuse connectivity of the network model, a significant percentage of the excitatory population is active during the recall of each memory. We consider neurons to be coding for a specific memory when their average firing frequency during recall is above 10Hz and refer to these as "coding" neurons.

In order to assess the sparseness of the population response before and after learning we used the population sparseness measure proposed by Treves & Rolls (Treves & Rolls 1991) subtracted from unity so that higher values correspond to more sparseness:

$$S_T = 1 - \frac{(\sum_j \frac{r_j}{N})^2}{(\sum_j \frac{r_j^2}{N})}$$

Where r_j is the average firing rate of neuron j during memory recall, $j=1...N$, and N is the total number of excitatory neurons. The measure is applied on the distribution of firing rates of all pyramidal neurons in the network before and after training. A narrow distribution with a sharp peak represents a sparser encoding than a less sharp, wider distribution.

In addition to the firing properties of the model network, the structure of memory engrams at the subcellular level is assessed by analyzing the distribution of potentiated synapses after memory encoding. The overlap in the population recruited

by different memories is assessed by calculating the ratio of the number of neurons that are activated by both memories over the sum of neurons activated by the two memories. The clustering between different memories in the same branch is assessed by counting the number of branches that contain 2 or more potentiated synapses from both memories over the number of branches that contain at least 2 potentiated synapses from either memories.

A second measure used to assess the similarities in the encoding of memories is the correlation of their distribution of potentiated synapses after memory encoding. For every memory that is successfully encoded by the network, a vector containing the summed synaptic weights of the memory to every branch in the network, and a vector containing the summed synaptic weights of the memory to every excitatory neuron in the network are constructed. Correlations (Pearson's) detected between such vectors for different memories are used to assess the Similarity of synaptic pattern projections to the whole population at the dendritic and the neuronal level. We refer to these vectors as synaptic projection vectors per neuron, and per branch, correspondingly.

Statistic tests were used to assess significance. The paired Student's t-test was used except where otherwise specified.

The following tables list the values of all model parameters, and the connectivity properties of the model network. Time was discretized at 1msec during memory encoding events, and at 60 seconds during the simulation of ISIs. The simulation code was written in C++ and is available upon request from the authors. Analysis of simulation data was performed with MATLAB R2014A (Linux). All computations

were performed in the parallel cluster of the Computational Biology Lab/IMBB (GNU/Linux x86_64, g++, 288 CPU cores).

Table 3.1 : Neuronal and plasticity parameters

Parameter	Description	Model value
τ_b	Passive dendritic integration time constant	20msec
E_{syn}	Maximum unitary EPSP	4.0 mV
θ_{dspike}	Depolarization threshold for dendritic spiking	30mV
V_{dspike}	Dendritic spike max depolarization	50.0 mV
E_L	Somatic leakage reversal potential	0 mV
θ_{soma}	Voltage threshold for somatic spikes	20mV
g_{syn}	Dendritic coupling constant	20 pS
C	Membrane capacitance	200 pF
g_L	Leak conductance	6.67 nS
τ_{AHP}	Adaptation time constant of excitatory neurons	180msec (slow adapting) or 110 msec (fast adapting after learning)
$\tau_{AHP,I}$	Adaptation time constant of interneurons	70 msec
a_{AHP}	Adaptation conductance increase after a spike	0.18nS
E_K	Adaptation reversal potential	-10 mV
τ_{bAP}	Back propagating action potential time constant	15msec
E_{bAP}	Back propagating action potential max amplitude	30 mV
a_{Ca}	Calcium influx rate	0.1msec^{-1}
synTag (x)	Sign of synaptic tag as a function of [Ca^{2+}] (Calcium control model)	$\left(\frac{1.3}{1+exp(-10(10x-3.5.))}\right) - \left(\frac{0.3}{1+exp(-19(10x-2.0))}\right)$
P_{dend}	Calcium threshold for PRP production in the case of dendritic protein	2.0 (arbitrary units)

	synthesis	
P_{soma}	Calcium threshold for PRP production in the case of Somatic protein synthesis	18.0 (arbitrary units)
a_s	Rate of synaptic tag consolidation	6.7 minutes
B_{tag0}	Unitary change in synaptic strength 'tag'	0.2
τ_{Btag}	Branch strength potentiation tag time constant	10 minutes
τ_{BP}	Branch strength potentiation time constant	2 hours
τ_{BH}	Branch strength normalization time constant	3 hours
B_{max}	Maximum branch strength	1.0
τ_H	Time constant of homeostatic synaptic scaling	7 days
w_{init}	Initial synapse weight	0.2
τ_{CREB}	Time constant of increased excitability (due to CREB activation)	8 hours

Table 3.2: Network connectivity

N_n	Number of neurons	500
N_{pyr}	Number of excitatory neurons	400
N_{inh}	Number of inhibitory neurons	100
$N_{branches}$	Number of branches per excitatory neuron	20
$N_{background}$	Background-stimulation input neurons	10
N_{event}	Number of stimulus-carrying input neurons per memory	6 (3 S1 inputs / 3 S2 inputs)
$N_{pyr \rightarrow inh}$	Total number of connections from pyramidal neurons to inhibitory neurons	3200
$N_{inh \rightarrow pyr}$	Total number of connections from inhibitory neurons to pyramidal neurons	4800
$N_{stim \rightarrow pyr}$	Total number of plastic synaptic connections from each set of 6 memory encoding neurons to excitatory neuron dendritic subunits	12800
$N_{background \rightarrow pyr}$	Total number of synaptic connections from background input neurons to excitatory neuron dendritic subunits	1600

Chapter 4.

Results I: Memory trace formation in the model network

In the first part of the simulations we assessed the model's ability to encode a single associative memory composed of two events or stimuli (S1 and S2). This encoding was achieved by the concurrent activation for 4 sec of the afferent synaptic inputs representing each stimulus. These events could, for example, represent a pair of conditioned and unconditioned stimuli, as in the case of classical fear conditioning. As shown in Figure 3.1 the encoding stimuli were delivered from a pool of six stimulus carrying neurons. Half of the neurons were assumed to carry the S1 and the other half the S2. During the encoding phase both the S1 and S2 neurons are firing with average firing frequency 30Hz. The stimulus carrying neurons were initially connected with random excitatory neuron dendrites with low initial synaptic weights (Table 3.1). The successful formation of an associative memory between S1 and S2 was indicated after learning (recall) by the enhanced response of the network to the presentation of the first associated stimulus (S1), as observed experimentally in both fear conditioning (Quirk et al. 1995; Maren & Quirk 2004) and other forms of

associative memory (Weinberger 2007). Recall was assessed 24-hours post-training, to allow for typically slower homeostatic processes to take place.

4.1 Network responses to S1 increase after learning

The network response to the presentation of the S2 (i.e. the conditioned stimulus) was increased after learning. This is in line with experimental data (Maren & Quirk 2004; Kang & Schuman 1996), which show that learning increases the responsiveness to the conditioning stimulus. This indicates that the two stimuli S1 and S2 became associated in our network.

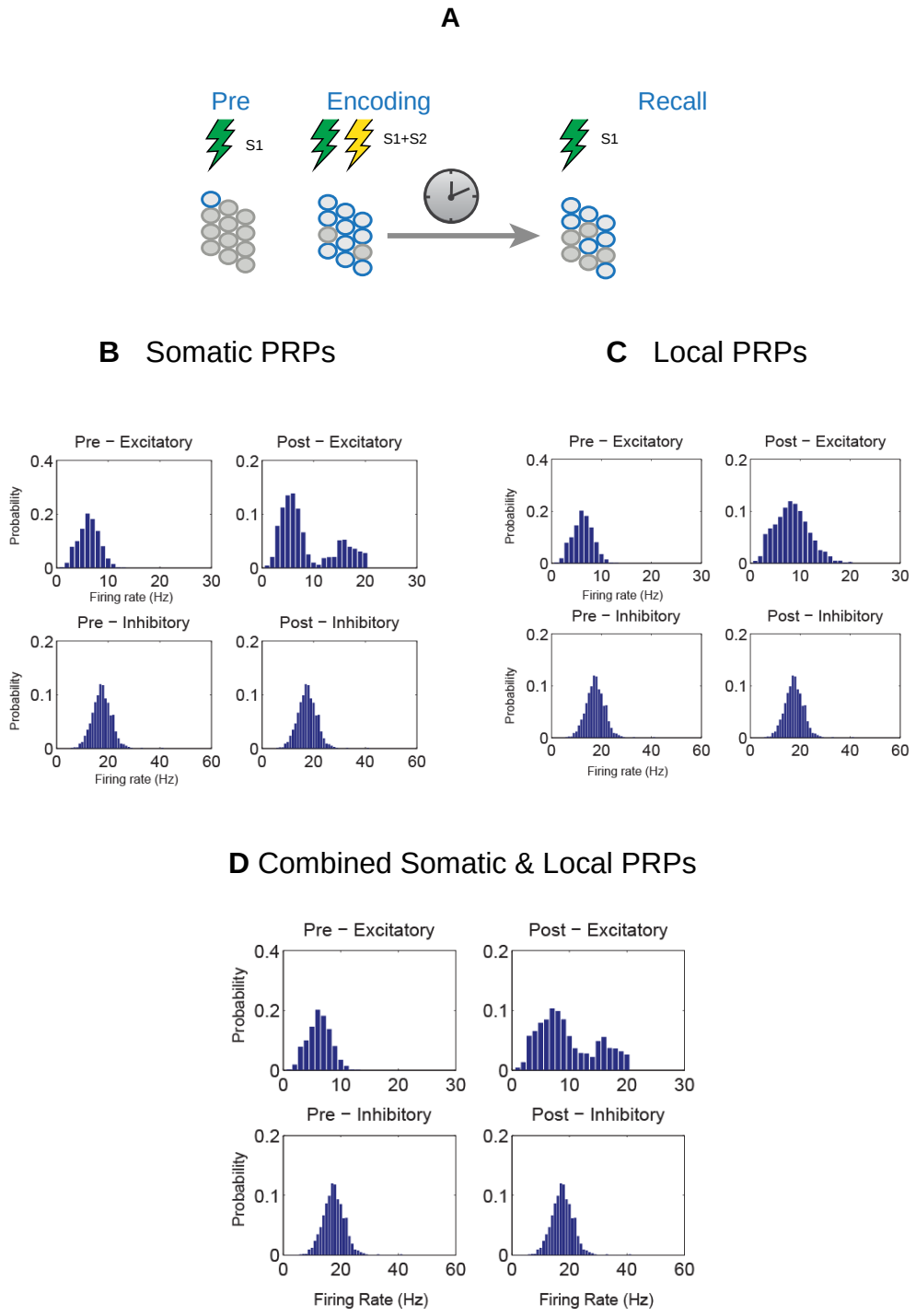

Figure 4.1 Firing rates after memory encoding

A) Schematic of the memory encoding simulation. B) Firing rates of neuronal excitatory and inhibitory populations during presentation of S1 before (Pre) and after learning (Post) in the case of Somatic PRP synthesis. C) Firing rate distributions for the case of local PRP synthesis. D) Firing rates under combined Somatic and Local PRP synthesis condition (S&L).

We observed that the distribution of firing rates of the excitatory population after learning was different under the two conditions (Figure 4.1). In the case of Somatic PRP synthesis the distribution of firing rates , indicating the existence of a neuronal population that responds vigorously to the encoding stimulus (Figure 4.1B). In the case of local PRP synthesis (Figure 4.1B), the activity was more evenly distributed among the neurons receiving potentiation.

During recall, the percentage of *coding neurons* - excitatory neurons firing above 10Hz - as well as their average firing rate (Figure 4.2), increased significantly for all three PRP conditions (Somatic, Local and S&L). The percentage of coding neurons for the memory (Figure 4.2) increased from 0.9±0.1% before training (Pre) to 29.7±0.9% under Somatic, 21.9±0.7% under Local and 33.4±0.9% under S&L PRP conditions, respectively. One-way ANOVA with Bonferroni's post-hoc test found the differences between all groups (conditions) to be significant ($p<0.01$). The average firing rate of these coding neurons in response to S1 presentation increased from 10.8±0.3Hz before training to 15.5±0.3Hz under Somatic, 12.3±0.2Hz under Local and 14.9±0.3Hz under S&L PRP conditions ($p<0.05$ one-way ANOVA with Bonferroni's posttest).

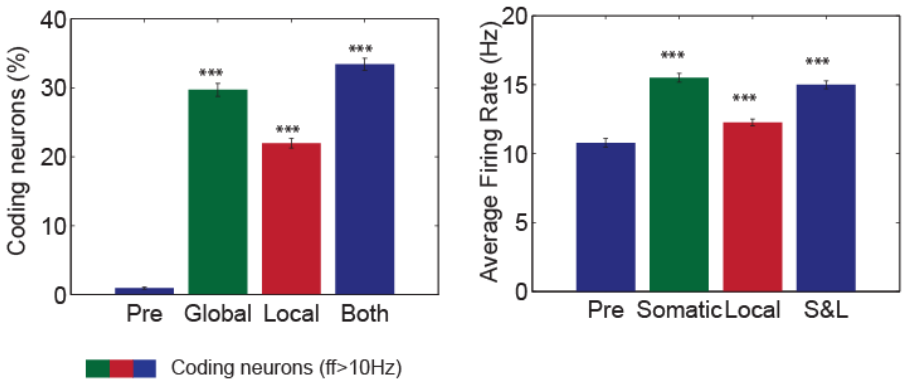

Figure 4.2 Percentage of coding neurons during recall

The cases of Somatic (Left), Local & S&L PRP synthesis and average firing rate of the coding population (Right) are shown.

Error bars indicate the SEM for 10 simulation trials. ***p < 0.05 one-way ANOVA with Bonferroni's posttest.

These results indicate that in both cases there was sufficient neuronal activation and synaptic plasticity to consolidate the synaptic weights under both cases of somatic and local PRP synthesis. In both cases the percentage of coding neurons is increased significantly, albeit in the case of local PRP synthesis the increase is smaller. Thus, besides somatic plasticity local plasticity could also contribute to memory encoding. The distribution of firing rates, however, shows that the two cases lead to different expression of the memory when recalled in terms of population dynamics. As we shall see later this arises from structural differences in the allocation of synapses in the two cases.

4.2 Sensitivity of memory allocation to model parameters

The model parameters used in these simulations (listed in tables 3.1 & 3.2) were calibrated according to experimentally observed values, where available. A number of parameters however, are under constrained, as they model phenomenologically processes which are complex in nature. In addition, the molecular mechanisms mediating these processes are not known.

The molecular and structural nature of the synaptic tag or the group of synaptic plasticity proteins required for long-term synaptic potentiation is not yet known, and as such only phenomenological descriptions of the theory exist. As such, we based our calibration of the related time constants for synaptic tag formation and protein capture on constraints set by relevant experimental in vitro studies.

The time course of synaptic tagging and capture in the case where different pathways provide the tagging and the protein-producing stimuli is roughly known from related in vitro experiments (Frey & Morris 1997; Sajikumar & Frey 2004; Redondo & Morris 2011), even though it is only approximately possible to separate the time courses of synaptic tag and synaptic protein availability. There is as of yet only one study, which examines the synaptic tagging and capture phenomenon at the dendritic level (Govindarajan et al. 2010). This study allowed the more precise measurement of the time course of interaction between the two processes (synaptic tagging and protein capture) and established that the synaptic tag lasts longer than PRPs. We thus calibrated the relevant time constants (Table 3.1) according to this study. We should note that the observations for both somatic and dendritic STC roughly agree on the time course of the STC phenomenon (1-3 hours somatic, 1-2 hours dendritic). The

dendritic STC studies have shown that the time constant of the tag is actually larger than the time constant of PRPs (Govindarajan et al. 2010).

The mechanisms via which CREB increases the excitability and the time course of its effect, is also not well characterized by the literature. Neuronal excitability is shown to be elevated rapidly, and remains high for more than 24 hours in vivo (Moyer Jr et al. 1996). CREB levels, on the other hand, have been shown to increase rapidly but drop between 30 minutes and a few hours later (Stanciu et al. 2001; Trifilieff et al. 2007) and to have a second, prolonged phase (Trifilieff et al. 2007). Additionally, it is proposed that CREB activation may include a wave of activation and a wave of inactivation, as CREB activates its own repressors (Silva et al. 2009).

As such, the model parameters were calibrated to best match the experimentally observed phenomena of memory allocation and in particular the percentage of coding neurons, which is shown to be about 1/3 of the entire population in the lateral amygdala. In order to test the sensitivity of the model to the choice of parameters, we performed an exploration of the parameter space by perturbing the values of specific model parameters. We adjusted the parameters shown in Figure 4.3 by scaling them in a range from 50% to 150% of the values listed in Tables 3.1 & 3.2. We evaluated their effect in the size of the coding population.

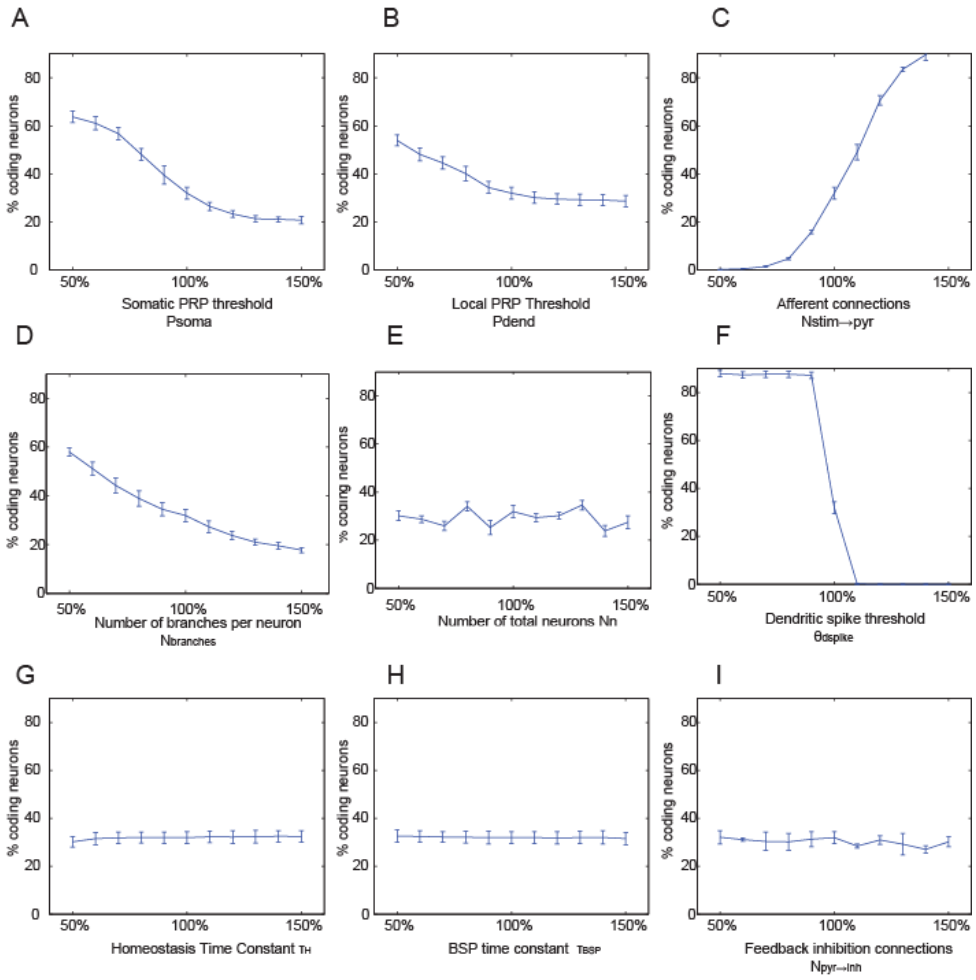

Figure 4.3 Sensitivity of the coding population size to model parameters. A) Dependence on somatic PRP synthesis threshold B) Dependence on local PRP Threshold C) Dependence on number of stimulus-carrying synapses D). Dependence on number of branches per neuron E) Dependence on total number of neurons F) Dependence on the voltage threshold for dendritic spike generation θ_{dspike} G) Dependence on the time constant of homeostatic scaling τH H) Dependence on the time constant of branch strength potentiation τ_{BSP} I) Dependence on the number of feedback inhibitory connections. Error bars indicate the SEM for 10 simulation trials.

The results indicate that certain properties of the model are crucial for the formation of a memory engram. The sharp dendritic spike threshold (Figure 4.3F), a sufficient initial afferent connectivity (Figure 4.3C) and the dendritic spike threshold (Figure 4.3F) strongly affect the size of the coding population, and are required in order to have a coding population size that agrees with the observed one. The plasticity thresholds, for both somatic and local PRP synthesis (Figure 4.3 A&B) have a large effect in the coding population size. In contrast, the time constants of slow processes, as well as the level of feedback inhibition, does not alter significantly the coding population size (Figure 4.3 G-I). It is therefore evident that the initial connectivity and the threshold for nonlinear dendritic response are crucial for the formation of a memory trace in the population modeled here.

4.3 Population activity becomes sparser after learning

Studies of associative fear conditioning have shown that learning is accompanied by a sparser firing of the population encoding the conditioned stimulus. A study that used two photon *in vivo* calcium imaging to measure the response of neurons in the somatosensory cortex found that it enhanced the sparse population coding of the conditioning stimulus (whisker stimulation). Thus, fewer neurons were responsive to CS presentation after learning (Gdalyahu et al. 2012), but they had a stronger response. As we saw before, the encoding of a memory in our network can lead to such a condition in the case of Somatic PRP synthesis, in which the distribution of firing rates in the population is bimodal, indicating that a distinct subset of neurons

fires vigorously to S1 presentation. In order to estimate the sparseness of the population coding of the excitatory model neurons before and after learning, we applied the Treves-Rolls metric (Treves & Rolls 1991). This measures the steepness of the firing rate distribution (Figure 4.4). In this figure, we have plotted a summary histogram of the firing rates of all the excitatory neurons for 10 different simulation trials, sorted by firing rate. The distributions show that before learning, and after learning in the case of Local PRPs the firing rates form a continuum with few neurons having high firing rates. In the case of Somatic PRPs (and consequently in the combined S&L condition) however, the distribution has a sharper cutoff that separates neurons with high firing rate from neurons with low firing rate (Figure 4.4 B,D). We applied the Treves-Rolls metric to these data in order to quantify the sparsity of the population coding.

As shown in Figure 4.5, the population activity sparseness is significantly larger after learning for all PRP conditions. Our data suggest that sparseness will be greatest under Somatic and smallest under Local PRP conditions. The combined S&L condition presents an intermediate case in which the cutoff of high firing frequencies is still present (Figure 4.5B), yet, it is overshadowed by the more diffuse connectivity provided by local PRP synthesis (Figure 4.4C).

The differential distribution of firing rates can be attributed to the way in which Somatic PRP capture differs from dendritic PRP capture. In the former case, neurons that cross the calcium threshold for PRP synthesis will have all their synaptic tags converted to consolidated synaptic weights in all their dendrites simultaneously, leading these neurons as a whole to have a more markedly elevated firing rate

compared to other responsive cells. In the Local PRP case, only synapses tagged within PRP producing dendrites will be potentiated. As such, neurons may have potentiated synapses in only a few of their dendrites, which are nevertheless enough to lead to neuronal firing. This leads to a broader firing rate distribution. Under S&L PRP conditions, many neurons will have dendrites with strengthened synapses, and thus various levels of increased activity. However, some coding neurons will have much higher firing rates due to Somatic PRPs, leading to an intermediate level of activity sparseness.

Note that activity sparseness should correspond to signal-to-noise ratio in memory recall, with less sparseness resulting in more interference between stored memories (high noise).

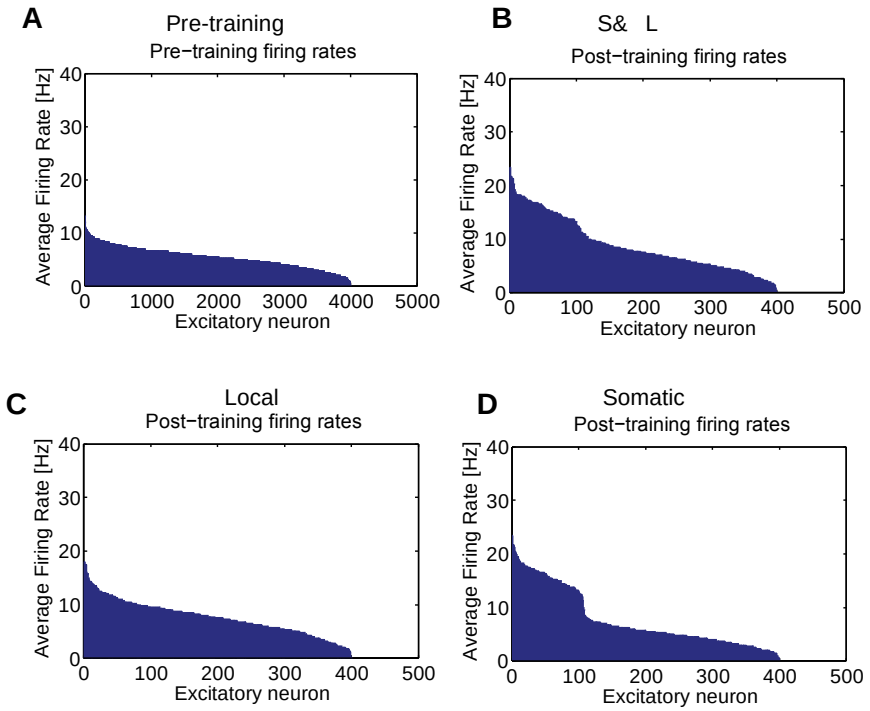

Figure 4.4 Histograms of firing rates

Histograms of (A) pre-recall and post-recall (B,C,D) of the memory under local (C), somatic (D) and combined S&L (B) PRP synthesis

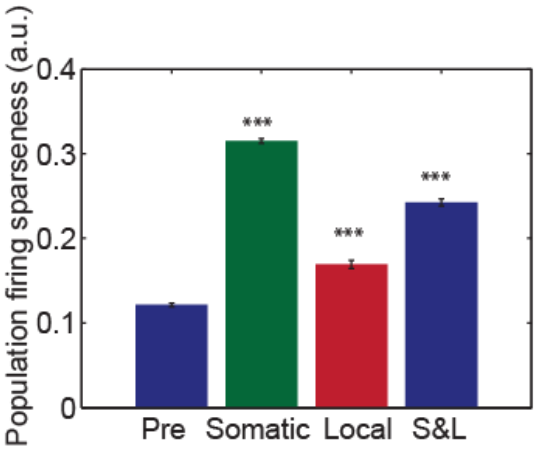

Figure 4.5 Population firing sparseness during recall under different PRP synthesis conditions.
Conventions as in Figure 4.2.

4.4 Cellular and sub-cellular features of the learned memory differ between PRP conditions

As we saw in the previous section, the population firing, which is the expression of a learned memory is determined by the subcellular structure of the synaptic potentiation. It is therefore interesting to characterize the distribution of allocated and potentiated synapses to different neurons and to different dendritic subunits.

Our results show that the mode of PRP availability will affect the sub-cellular properties of the memory trace. Specifically, we found that the total number of potentiated synapses after learning is the smallest under Local, larger under Somatic

and largest under S&L PRP conditions (Figure 4.6A). Moreover, under these three different conditions, potentiated synapses are distributed in different ways among neurons and their branches.

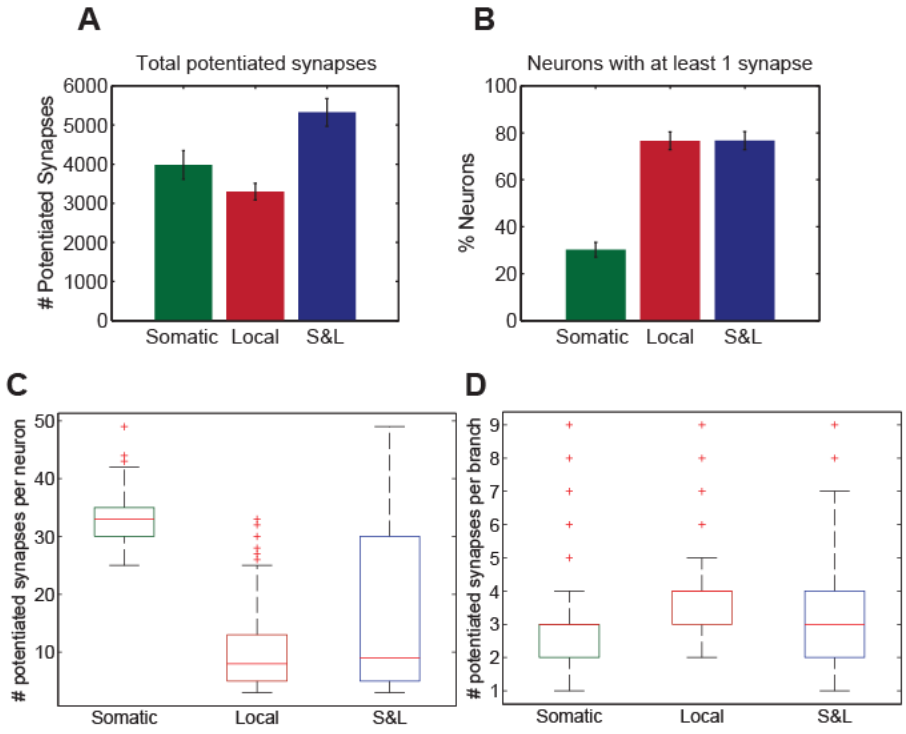

Figure 4.6 Subcellular characteristics of synapse distribution for different PRP synthesis conditions.

A) Total number of potentiated synapses for the whole excitatory neuronal population B) Percentage of excitatory neurons with at least 1 potentiated synapse C) Box plot of the number of potentiated synapses per neuron over 10 simulations D) Box plot of the number of potentiated synapses per branch over 10 simulations. Conventions as in Figure 4.2.

Under Somatic conditions, potentiated synapses are restricted to approximately one third (29.2±2.5%) of the excitatory neurons (Figure 4.6B), while under Local and S&L conditions they are found in the majority of excitatory neurons (Figure 4.6B). One-way ANOVA with Bonferroni post-test indicates that the Local and S&L cases are different from the Global case ($p<0.01$), but not between them. It should be noted that the above numbers correspond to neurons containing at least *one* potentiated synapse after learning. The percentage of neurons that actually code for the memory (i.e. respond during recall) is much lower (20-35%, Figure 4.2A).

Within each neuron, more synapses are potentiated on average under Somatic (32.9±4.5) PRP conditions, compared to Local (10.8±6.5) and S&L (17.4±13.1) ($p<0.01$ between conditions, one-way ANOVA with Bonferroni post-test). Looking at the distribution of the number of potentiated synapses per neuron, we can see that the cases of Somatic and Local PRPs lead to different outcomes. As shown in Figure 4.7, in the case of Somatic PRPs the neurons that undergo plasticity have a large number of potentiated synapses ranging from 20 to 50 per neuron. Kruskal-Wallis one-way analysis of variance indicated that the distributions of synapses per neuron were different ($p<0.01$) and Bonferroni posttest indicated that the between conditions means were different ($p <0.01$). This observation is in accordance with the STC hypothesis, which allows all tagged synapses of a neuron to capture the available PRPs when the PRP synthesis is presumed somatic. This is not the case in the condition of dendritic (Local) PRP availability. In this case, the number of potentiated synapses per neuron has a wider range with neurons receiving as few as 5 potentiated synapses. The S&L case appears to be a combination of the two other cases (Figure 4.7).

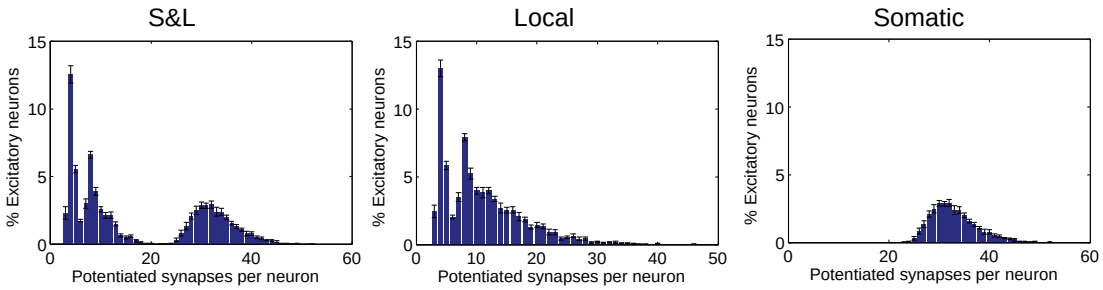

Figure 4.7 Distribution of the number of potentiated synapses per neuron after learning under different PRP synthesis conditions.

Looking at the dendritic level, we can also see that the condition of protein synthesis alters the distribution and the clustering properties of the synapses. The average number of potentiated synapses per branch is significantly different between conditions ($p<0.01$ one-way ANOVA followed by Bonferroni post-test ($p<0.01$)), is largest under Local conditions (3.9±0.9 synapses, Figure 4.6D) and smaller under Somatic and S&L conditions (2.8±1.0, Figure 4.6D). While these differences do not appear dramatic, the distributions of potentiated synapses per branch are significantly different ($p<0.01$ Kruskal-Wallis one-way analysis of variance followed by Bonferroni post-test) reveal that under Local PRP conditions, synapses are potentiated in groups of at least 3 (Figure 4.8), reflecting synapse clustering, while under Somatic or S&L PRP conditions potentiation can also be observed in single synapses.

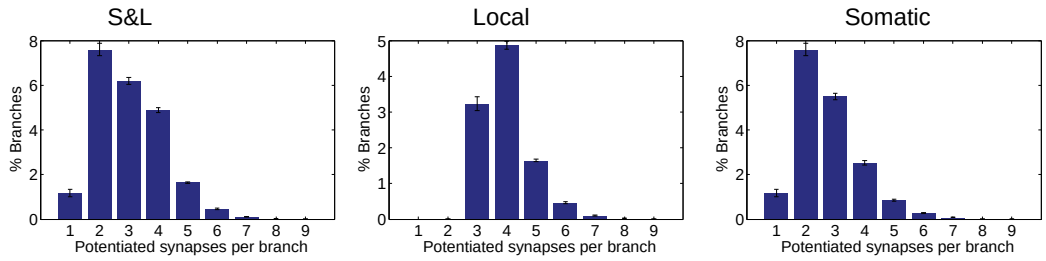

Figure 4.8 Distribution of the number of potentiated synapses per branch after learning under different PRP synthesis conditions.

4.5 Discussion

In this chapter we analyzed the main components of a model for predicting the cellular and subcellular components of a long-term memory trace. We show that, by taking into account the basic rules known to apply to long-term LTP, and changes in excitability taking place during learning we can predict and analyze the structure of memory engrams.

One important distinction concerns the locus of plasticity-related protein synthesis. While multiple studies have shown that protein synthesis is required for the consolidation of synaptic potentiation to late-LTP (Reymann & Frey 2007; Nguyen et al. 1994; Moncada & Viola 2007), the nature of the proteins required for synaptic strengthening/weakening, the cellular location where these are synthesized and the mechanism that delivers them to synapses that need to be potentiated are unknown. Different RNA transcripts induced by synaptic activity are implicated in memory functions and these include transcription factors, neurotransmitters, receptors, scaffolding proteins, structural proteins and others (Abbott & Nelson 2000). More

recently, it has been shown that plasticity-related RNAs are found in dendrites, where they are thought to play a role in synapse modification and maintenance. A study found a surprisingly high number of dendritic RNAs in CA1 neurons, many of which code for known plasticity proteins such as ligand-gated receptors (Cajigas et al. 2012). Since it is currently unknown how these RNAs are activated and how the protein products are incorporated in newly generated, potentiated or de-potentiated synapses, the synaptic tagging and capture model provides a model that can explain many of the observed phenomena related to the protein-synthesis dependence of LTP without explicitly modeling molecular dynamics. Thus, despite the success of the STC theory in explaining the associativity of late-LTP under many different protocols, the molecular components that mediate the function of synaptic tagging and subsequent protein transport remain elusive.

The activity-induced signaling from the synapse to the nucleus that leads to the synthesis of PRPs is believed to be slower than the time required for the expression of Initial Early Genes (IEGs). For example, the IEG Arc is expressed in CA1 neurons as early as 2 minutes after neuronal activity (Guzowski et al. 1999). Studies have shown various signaling pathways from the synapse to the nucleus such as TORC1, CREB2 and ERK1/2, however none of them can cause nuclear activation in such short timescales. It is proposed, thus, that depolarization caused by EPSPs or action potentials in combination with “pre-charging” of the promoter regions of IEGs with RNA polymerase II act to accelerate the process of IEG expression in the nucleus (Saha et al. 2011). At the dendritic sites, it is not yet known how dendritically-targeted mRNAs are docked in synaptic sites. It has been shown that there is bidirectional transfer of proteins within dendrites with rates that are compatible with

transport through microtubules (Tübing et al. 2010), thus supporting the idea that these mRNAs can be transported between synapses within a dendritic compartment. The studies mentioned above have shown that plasticity-related proteins could be synthesized both in the nucleus and in the soma, and it is not yet known which factors determine the locus of synthesis. It is possible that different forms of late-LTP in different brain areas have different requirements (Izquierdo et al. 2006), therefore it is possible that somatic and dendritic synthesis are engaged differentially.

The nature of the structural or molecular changes mediating the setting of a synaptic tag is also still under active investigation. Actin remodeling is believed to play a role in initiating structural changes in a synapse that will later lead to synapse strengthening during protein capture and LTP consolidation. The enzyme CaMKII is believed to play a key role in the initial steps of this process. CaMKII consists of two subunits CaMKIIα, a subunit translated locally at active synapses, and the regulatory subunit CAMKIIβ that is translated at the soma. CaMKIIα could thus serve as an initial tagging marker that later captures CAMKIIβ, which in turn initiates downstream pathways in order to create the synaptic tag. Interestingly, it has been shown that Arc activity, in tight interaction with CaMKIIβ acts as an "inverse tag", which leads to the removal of AMPA receptors, thus preventing the synapse from being potentiated, or causing de-potentiation (Okuno et al. 2012). Thus, somatically-synthesized CaMKIIβ along with Arc could prevent potentiation in untagged synapses, while synapses with CaMKIIα can capture CaMKIIβ and continue to normally generate a synaptic tag.

Despite the evidence provided above, very little is known about the downstream components that lead to synaptic capture and tagging. There have been previous attempts to model networks of molecular pathways that implement STC (Bhalla & Iyengar 1999; Smolen et al. 2006b). The complexity of these models however, and the fact that large parts of the molecular pathway are unknown (Smolen et al. 2006b) does not allow them to be used in models where plasticity is driven by electrical activity. Taking this into account, we sought to use a simplified phenomenological STC description using deterministic equations.

Previous models of STC have suggested different approaches to the modeling of STC. Clopath et al (Clopath et al. 2008), for example suggested an STC model that is not based on calcium dynamics but rather on voltage dynamics, bi-stability and spike-timing-dependent plasticity. The model was successful in reproducing findings regarding synaptic tagging and capture, however it cannot be used in a generic model of plasticity since it is based on specific assumptions that don't have a biophysical correlate, such as a bi-stable LTP consolidation switch and stochastic rate transitions. Another model of STC proposed by Barrett et al. (Barrett et al. 2009) also proposes stochastic transitions between synapse states as a correlate of STC. STC experiments however have shown that synaptic tags do not transition stochastically, and that, in contrast, the phenomenon of STC can be induced in very short stretches of dendrites deterministically (Govindarajan et al. 2010). In addition, the evidence suggests in all cases the calcium influx through NMDA receptors is the major first step that determines the course of synaptic plasticity (Graupner & Brunel 2012; Rubin et al. 2005; Weisskopf et al. 1999; Hao & Oertner 2011; Bauer et al. 2002; Shouval et al. 2010). Taking into account these modeling and experimental findings, we based our

modeling of synaptic tagging on a deterministic, calcium-dependent model of plasticity.

Calcium-dependent plasticity rules have been shown to provide a generic framework for understanding different forms of plasticity, including Hebbian LTP/LTD (Cooper & Bear 2012). In addition, with regards to spike-timing dependent plasticity (STDP), it has been shown that this form of plasticity can be considered a consequence of more fundamental, calcium-dependent plasticity rules rather than a fundamental rule in itself (Shouval et al. 2010). The Calcium Control model of synaptic plasticity by Shouval et al. (Shouval et al. 2002) is such a proposed fundamental model. Our synaptic tagging model is based on the Calcium Control model of bidirectional plasticity (Figure 3.2). Low or baseline Ca^{2+} concentration causes no change in synaptic strength, while intermediate levels cause LTD. High levels of Ca^{2+} influx cause potentiation (LTP). The calcium influx required for plasticity is dominated by the NMDA-dependent influx of calcium during stimulation in our experiments, although the gating function of the NMDA (Eq. 3.6) can be adapted to accommodate non-NMDA sources of calcium influx such as voltage gated calcium channels. As shown by the results of the sensitivity analysis (Figure 4.3C), dendritic spike events often overshadow the sub threshold depolarization through NMDAs. Thus, as it is shown in Figure 4.3C, a model without dendritic spikes or one where the dendritic spike threshold is much higher than our parameter choice, would require different choices in plasticity thresholds in order to yield similar results, (e.g. a coding population size that is compatible with experimental evidence). On the other hand, the requirement for dendritic spikes is in agreement with experiments in CA1 hippocampal neurons which show that dendritic spikes are more effective than back-

propagating action potentials in inducing LTP (Hardie & Spruston 2009). Dendritic spikes can induce LTP in a single burst, without requiring the repeated rhythmic stimulation that is typically induced in LTP experiments (Remy & Spruston 2007). Thus, we conclude that the modeling of dendritic spikes is essential in order to reproduce aspects of LTP that are found experimentally mainly in hippocampal neurons.

Given that the locus of protein synthesis during LTP consolidation is still an open question, our model allowed us to explore the outcomes of different choices for the locus of PRP synthesis. In summary, we predict that dendritically restricted protein capture (Local) would result in a *lower contrast* memory engram compared to the cases where PRPs are available throughout the neuron (Somatic and S&L conditions). This is evident by the larger number of neurons containing potentiated synapses (Figure 4.6B) the smaller number of potentiated synapses per neuron (Figure 4.6C) and the larger width of the distribution of potentiated synapses per neuron (Figure 4.7). Engrams that are formed via compartmentalized and independent PRP synthesis in dendrites have thus synapses more distributed throughout the neuronal population. This allows the neurons of the resulting engram to have a more graded response to the encoding stimulus (Figure 4.4C). This is a property that is compatible with linear models of synaptic integration, which do not depend on nonlinear phenomena for the determination of the output of the neuron. On the other hand, our results indicate that even though the neuronal population has graded response, the synapses do need to be potentiated in groups, which might lead to synapse clustering. As shown in Figure 4.8, local PRP synthesis requires the concerted action of multiple synapses in order to be induced. This requirement is

exacerbated by the emergence of dendritic spikes, which, in our model, requires the activation of at least four incoming synapses or the synergy of a backpropagating action potential depolarization. As a result, under local PRPs, there are no branches with less than three potentiated synapses. This is compatible with observations of clustered plasticity in neurons within spatial distances that are roughly the size of a dendritic subunit considered here (<70μm) (Makino & Malinow 2011; Takahashi et al. 2012; Govindarajan et al. 2010). Nevertheless, the large distribution of the engram throughout the population comes at a cost to the sparsity of the neuronal response during recall (Figure 4.5).

The case of Somatic PRPs, on the other hand, allows the network to respond differently. In this case, synaptic tagging and capture can dominate the entire neuron, thus leading to a more sharply defined population of coding neurons. The resulting engrams have thus higher population firing sparseness, driven by mass synaptic action throughout their entire dendritic population. Synapses in this case don't need to form clusters, even though even in this case, LTP cooperativity dominates, as coincidences of 2-3 potentiated synapses are the most common (Figure 4.8).

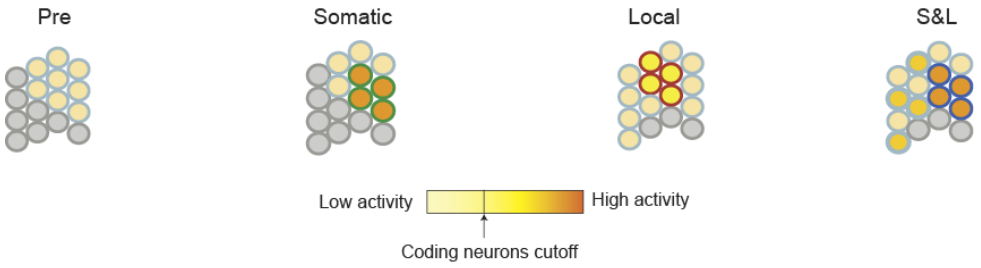

Figure 4.3 Schematic: properties of the associative memory trace under different PRPs synthesis conditions.

The case of combined S&L PRP synthesis shows that the two STC locations do not act antagonistically against each other. Indeed, the S&L acts as a combination of the other two at the subcellular level, while at the population coding level, it is dominated by the large distribution afforded by Local PRPs, a wider distribution of potentiated synapses per branch and a bimodal distribution of the number of synapses per branch. Therefore, in the S&L case, the consequences of increased LTP consolidation that result from the fact that PRPs are available from two sources, are counterbalanced by neuronal inhibition, so that the average size of the coding population and its firing rate does not change dramatically (Figure 4.2).

Since the sources of PRP synthesis are not yet clear from experimental studies, our results suggest that observations of the subcellular structure of the memory engram can be used to determine their source. For example, plasticity markers such as pHluorin-tagged glutamate receptors (Zhang et al. 2015) and phosphorylated cofilin (Lynch et al. 2014), as well as two-photon *in vivo* imaging (Fu et al. 2012; Makino & Malinow 2011), could be used to test the distributions of potentiated synapses after learning. Evidence for widespread plasticity across a majority of neurons, with localized clusters of potentiated synapses within a small subset of their dendritic branches, would indicate that Local (as opposed to Somatic) PRP mechanisms predominate during associative memory formation.

Chapter 5.

Results II: Memory storage during behavioral tagging

5.1 Background

For long-term memories (LTM), it has been established that they are not fixed immediately, but after a period of consolidation (Nadel et al. 2012). Synaptic and cellular consolidation of the memory takes place within the first few hours of the memory formation, , and this is believed to be mediated by multiple molecular and cellular mechanisms (Dudai 2004). During this period, the memory is in a labile state, which allows consolidation to be disrupted or affected by other factors such as stress, arousal, motivation and reward. These factors can either improve or impair the memory. Memories that are stored in the brain, however, are not all long-term. Short-term memory (STM) refers to forms of memory that last for a short time and then fade. A crucial finding regarding short-term memories is that they are not affected by protein synthesis inhibitors. In contrast, protein synthesis and/or transcription has been found to be required for the consolidation of long-term memories (Quevedo et al. 2004).

Long-term memory is believed to be mediated through long-term potentiation, and since the consolidation of LTP is governed by the mechanisms of synaptic tagging

and capture, STC has implications for the encoding of long-term memories. The in vitro studies of synaptic tagging and capture have shown that the proteins required for the consolidation of a long-term memory need not originate from the same stimulus event that initially sets the synaptic tag, but that PRPs may be supplied by another stimulus that causes protein synthesis within a few hours before or after the tag-setting input (Sajikumar et al. 2005). Surprisingly, the phenomenon is bidirectional between LTP and LTD, so that an LTP tag can be consolidated by proteins originating from an LTD-inducing stimulus (Sajikumar & Frey 2004). On the grounds of this in vitro observation, it has been suggested that the protein sharing mechanisms may be more broadly applied to the consolidation of short term memories. It is proposed that a short-term memory can be converted to a long-term memory by capturing protein products from another, unrelated, but long-term memory, which induces protein synthesis. If the analogy with in vitro STC is to hold, then it is expected that the phenomenon will occur only within a few hours before or after the short-term memory.

A *weak memory*, is a short-term memory that does not persist beyond a few hours. Weak memories can result behaviorally from learning that is limited in time or is mild, so that it causes the behavioral expression of a memory only temporarily. Experimentally, this can be achieved, for example, by shortening the duration or the number of the learning trials in a fear conditioning experiment, in which case the expression of fear response returns to baseline a few hours later (Maren 2005). On the other hand a long-term memory is termed *strong memory* and its acquisition in general requires protein synthesis (Moncada & Viola 2007).

Scientists have put the hypothesis of the implications of STC at the behavioral level to the test, and the resulting experiments are referred to as *behavioral tagging* experiments. In these experiments, the weak memory is believed to set a *behavioral tag*, which is presumed to be correlated with the synaptic tagging mechanism, and the protein products required for the strengthening of the weak memory are provided by a second, strong memory. These experiments have found that when a weak memory is paired with a learning event that is known to lead to long –term memory (and thus is presumed to cause PRP synthesis), the weak memory can be promoted to a long-term memory, and this strengthening is dependent on protein synthesis (Ballarini et al. 2009; de Carvalho Myskiw et al. 2013). The long-term memory must be presented within minutes to hours *before or after* the weak learning event in order to allow for the interaction between the two memories to occur. Ballarini and colleagues (Ballarini et al. 2009) showed that behavioral tagging can be observed by pairing two learning events. The weak memory in this case was a spatial object recognition task, while the strong memory was the exploration of an open field. It was shown that the weak object recognition memory can be strengthened and promoted to long-term memory when combined with the open-field learning for up to 2 hours before or after the weak memory (Ballarini et al. 2009; Moncada & Viola 2007). This is in accordance with STC in vitro experiments which predict that weak stimulation that normally causes only transient synaptic potentiation (i.e., early-LTP), can be converted to late-LTP if a stronger stimulation, capable of inducing late-LTP, precedes or follows within an interval of approximately 2 hours (U Frey & Morris 1998; Reymann & Frey 2007). Importantly, the enhancement of the weak memory was protein-dependent, and was blocked by the protein synthesis inhibitor

anisomycin. This evidence is taken to point to the behavioral analog of synaptic tagging and capture. A number of experiments have examined the applicability of the behavioral tagging paradigm to other forms of learning. As shown in Figure 5.1, the behavioral experiments in general confirm the applicability of behavioral promotion of memories to many different learning paradigms in both mice and in humans. It is worth pointing out that in all the rat/mouse experiments the phenomenon was found to be protein-dependent. This dependence is a strong indicator that the underlying mechanism is related to the synaptic tagging and capture of proteins at the cellular and neuronal level.

Learning task (training)	Time course (min) of training/event association: effects on LTMs −240	−180	−120	−60	0	+60	+120	+180	+240	Associated events	PRP synthesis dependency	Model
Inhibitory avoidance	—	—	LTM	LTM	LTM	LTM	LTM	LTM	LTM	—	—	Novel OF, SKF33893, dobutamine	Yes	Rat Mouse
Contextual fear conditioning	—	—	—	LTM	—	—	—	—	—	Novel OF	Yes	Rat
Extinction of contextual fear conditioning	LTM	LTM	LTM	LTM	LTM	LTM	LTM	LTM	LTM	LTM	LTM	Novel OF	Yes	Rat
Spatial object recognition	LTM	—	LTM	LTM	LTM		LTM	LTM	—	LTM	Novel OF, reconsolidation, extinction	Yes	Rat
Conditioning taste aversion	—	—	—	LTM	LTM	LTM	LTM	—	LTM	—	Novel flavor	Yes	Rat
Event arena	—	—	—	LTM	—	LTM	—	—	LTM	LTM*	Novel OF, rewarded T-maze	Yes	Rat
Water maze + footshock	—	—	—	—	LTM	— LTM	—	—	—	LTM#	Novel OF	Yes	Rat
Memory of story	LTM	—	—	LTM	—	LTM	—	—	LTM	Novel science or music lesson	—	Human
Memory of a draw	LTM	—	—	LTM	LTM	LTM	—	—	LTM	Novel science or SE lesson	—	Human
Visual memory	—	—	—	—	LTM	LTM	LTM	—	—	—	—	Pavlovian fear conditioning	—	Human

LTM Long-term memory promotion/improvement.
LTM No promotion/improvement.
— Not determined.

#/∗ Associated 5/6 h after training.
OF Open field.
SE Sexual education.

Figure 5.1 Behavioral tagging as observed in different learning tasks and animal models.

The effects on long-term memory formation are shown for different learning tasks that follow the behavioral tagging paradigm. Learning task is the “tagging” memory while the memory event presumed to provide the PRPs for

consolidation is the associated event. The associated event is shown at different times relative to the training session. Long-term memory is generally measured 24 h after training, and it could be promoted/improved, or not. The dependence of the phenomenon on protein synthesis was tested in most of these experiments as shown in column 4. Figure adapted from (Moncada et al. 2015) under the Creative Commons license CC-BY.

A second factor that can affect the plasticity of related memories is the plasticity of excitability. It has been shown that neurons that participate in learning have higher excitability. On the one hand studies show that excitability in the hippocampus is increased for hours to days after learning (McKay et al. 2013). On the other hand, studies of CREB activity following learning have identified a bi-phasic pattern, showing a rapid increase of CREB within hours, followed by a trough, and a second phase hours later (Trifilieff et al. 2006; Stanciu et al. 2001). Given CREB's role in increasing the excitability of neurons (Zhou et al. 2009), it has been suggested that the activation of CREB may create "windows" in time, which allow for memory strengthening when a second memory arrives (Rogerson et al. 2014; Silva et al. 2009). The first memory of the pair is presumed to create a subpopulation of neurons with higher excitability. When the second memory of the pair arrives, these neurons will be more likely to be activated, thus also more likely to express plasticity (Figure 5.2). This mechanism is thus presumed to allow an increased allocation of the second memory than if the first memory had not occurred. This mechanism could, for example, be related to *emotional tagging*, i.e. the strengthening of unrelated memories due to a strongly emotional event (Silva et al. 2009).

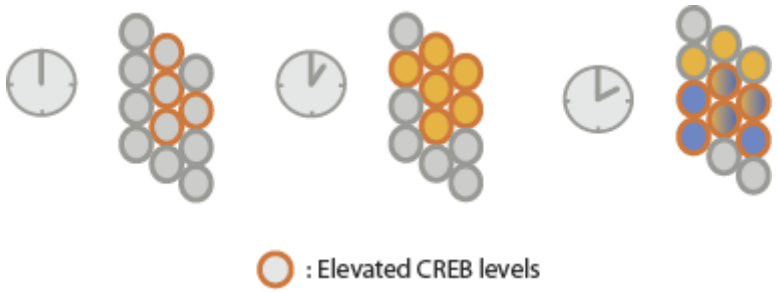

Figure 5.2 Memory trace overlaps may be promoted by increased excitability.
Increased activity of CREB is postulated to lead to increased excitability of neurons after a learning event. Learning in the following hours is preferentially allocated in these neurons with increased CREB activity (middle). The population of the memory trace will in turn be engaged in subsequent learning of another memory that comes within hours (right). This mechanism creates overlaps between the memory traces of memories stored within hours from each other.

The phenomena of behavioral tagging and of excitability-dependent strengthening are related, in the sense that they both result in the strengthening of a memory via pairing, although the two rely on different biophysical mechanisms. It is worth noting that the contribution of CREB in weak memory rescuing is not directly discriminated from the contribution of STC mechanisms, due to the fact that they overlap in their effects and time course, and also because they may share molecular pathways. Using modeling, however, we can discriminate the effects of the two mechanisms as we shall see in the next sections.

5.2 Memory rescuing through synaptic cross-capture

We sought to simulate the pairing of a strong and weak learning in order to show how the strengthening of the memory arises through synaptic plasticity and protein capture, and to study the properties of the resulting synaptic memory traces of the strong and weak memory. We used the network model outlined in Chapter 3 to study the effect of weak-strong memory pairing on the strength of memories. Weak learning, by definition, should not result in long-term memory. Therefore, we used a protocol in which the weak memory was encoded by giving the encoding stimulus for a shorter duration of time. In particular, we presented the encoding stimuli for a duration of 2700msec. In our simulations, this led to almost none of the neurons receiving enough stimulation to begin somatic protein synthesis (under the somatic PRP synthesis conditions) (2.1±(?)1.8% of pyramidal neurons). Both the STC mechanism and learning-induced enhancement of intrinsic excitability (McKay et al. 2013) could potentially affect how weak and strong memories interact. To evaluate the contributions of these two factors, we performed simulations where STC was implemented and the neuronal excitability of recruited neurons was either Enhanced or remained Static. In the case of Enhanced excitability, the crossing of the somatic PRP threshold for a neuron increased its excitability for a period of 12 hours. Under the Static excitability condition, there is no enhancement of excitability after learning.

We chose various intervals between the strong and weak memory ranging from 24 hours up to 1 hour before and after the strong memory. In order to assess the weak memory rescuing, we considered the coding population of the weak memory as a measure of the strength of the memory. After pairing a weak memory with a strong one, we observed an increase in the size of the weak memory. As we will see, the

strengthening is dependent on the conditions of PRP synthesis and excitability that are considered.

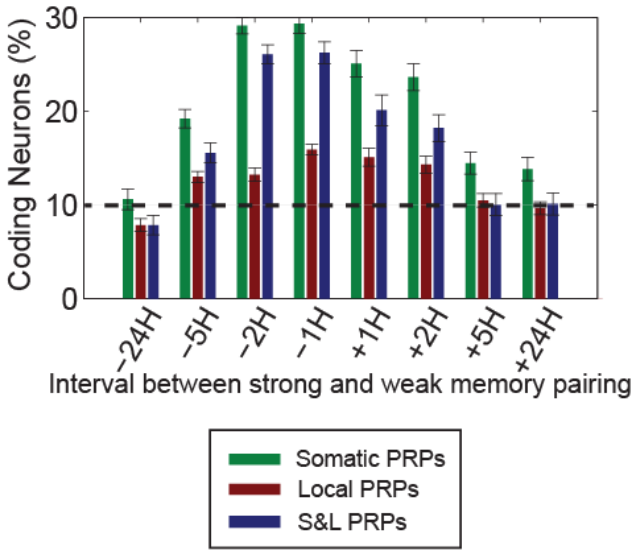

Figure 5.3 Percentage of coding excitatory neurons for the weak memory as a function of the interval between the strong and weak memories.
Error bars indicate the SEM for 10 simulation trials

As shown in Figure 5.3, the coding population for the weak memory is significantly higher in all three PRP conditions (Somatic, local and combined) for 1-2 hours between memories compared to the 24 hours interval*. Rescuing, in this case, depends strongly on PRP conditions, and also on neuronal excitability. Specifically, under S&L PRP conditions, the population of coding neurons representing the weak memory (Figure 5.3) is much larger (up to 27.8±1.5%* , at -1 hour) within the 2-hr

window compared to baseline (9.2±0.9%* , at 24 hours). The size of the weak memory trace, assessed by the coding population, is slightly larger for Somatic PRP conditions and drops dramatically for Local conditions (dotted line represents baseline levels at 24 hours for the S&L condition).

In the case of Local PRP conditions, there is a lower probability that tagged synapses (representing the weak memory) will be co-localized in the same dendritic branches with strong synapses that produce PRPs (representing the strong memory). This is due to the fact that the population of dendritic subunits is much larger than the neuronal population. The probability of a tagged synapse being in a dendritic branch that produces PRPs is lower than the probability that a synapse is in a *neuron* that produces PRPs. In addition, as synapses are scattered across more neurons in the case of local PRP synthesis (as explained in chapter 3), it is less likely that a neuron will have a large enough number of potentiated synapses in order to drive its firing during memory recall. These simulations thus predict that under Local PRP conditions, rescue of the weak memory by the strong memory would be less effective and probably restricted to smaller pairing windows (e.g. < 1 hour). In the case of Somatic PRPs, the capture of proteins by the tagged synapses of the weak memory is more effective, given that the all the synapses tagged by the weak memory in a neuron that produces PRPs get potentiated. This provides an advantage to somatic protein synthesis in terms of the ability to potentiate a weak memory.

---

* $p < 0.01$ one-way ANOVA followed by Bonferroni post-test

Experiments of behavioral tagging have shown that the dependence of memory rescuing on the time between the two memories is approximately symmetric, although only a few time points are being investigated in all the behavioral tagging studies. Our results show, however, that the increase of excitability after learning will induce an asymmetry in the time-dependence of weak memory rescuing. As shown in Figure 5.3 the rescuing effect is stronger at -1 , -2 and -5 hours compared to at +1, +2 and +5 hours in the cases of Somatic and S&L PRPs ($p < 0.01$ one-way ANOVA with Bonferroni post-test). In this case, the strong memory precedes the weak one, creating a population of neurons with increased excitability. As a result the weak memory is further strengthened at -2 hours and at -5 hours, but it is not at +2 hours and +5 hours. This effect is, however, only significant in the case where somatic or combined S&L PRP synthesis takes place. In the case of local PRP synthesis, the increased excitation is not enough to significantly alter the neuronal population. As we explained previously, in the Local PRP case, the rescuing is dependent on the coincidence of tagged synapses and PRP producing branches. Since neuronal excitability is a property that affects the somatic output of the cell (i.e. the adaptation part of our somatic compartment model), it does not affect the local AHP current in dendrites. Therefore, the increase of excitability through AHP current adaptation does not affect the local excitability in the dendrite, and thus does not lead to increased probability of PRP synthesis through increased calcium influx. That is the reason why we do not see an asymmetric increase in the coding population within the window of 2 hours.

Regarding the strong memory, our model shows that the pairing with a weak memory increased the size of its coding population only slightly. This is shown in Figure

5.4, where there are no significant differences between inter-stimulus intervals except for the ISI of +2H and +1H compared to 24 hours ($p < 0.01$ one-way ANOVA with Bonferroni post-test). The increase in coding neurons, however, in this case is relatively small.

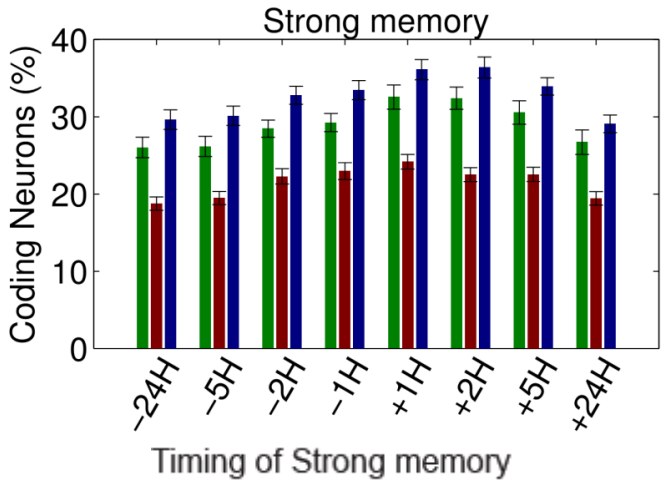

Figure 5.4 Percentage of the coding population for the strong memory for different time intervals between strong and weak memory.
Conventions as in Figure 5.3.

We next examine the structure and relationships between the memory engrams encoding the strong and weak memories. We find that the two neuronal populations expressing the memories are highly overlapping. The overlap is evident within the entire window of time that the weak memory is strengthened. This is shown in Figure 5.5 in which the percentage of neurons expressing the memory that are common between the two memories is shown. The overlap in the population is particularly high in the case of somatic PRP synthesis. This result agrees with the larger coding population for the weak memory (Figure 5.3). The phenomenon in this case is

evident even at 5 hours, indicating that even at near the end of the lifetime of synaptic tags and PRPs there are interactions between the two enough to cause synaptic potentiation. As before, the overlap between the two populations has an asymmetry in time as indicated by the significant differences between ISIs of 2H and 1H ($p<0.01$ one way ANOVA followed by Bonferroni post-test), which are a result of the action of increased excitability.

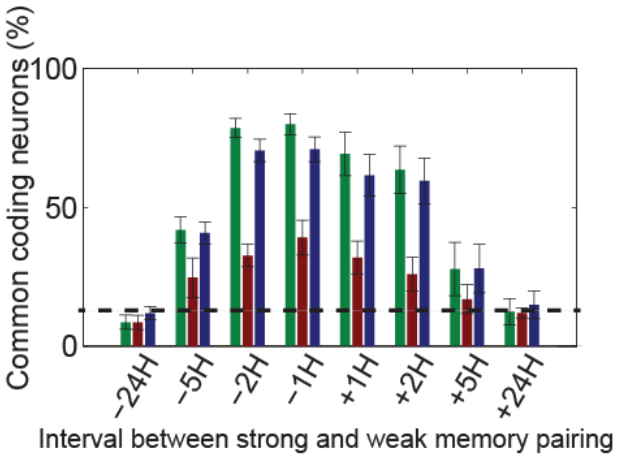

Figure 5.5 Percentage of common coding neurons of the weak-strong memory pairing.
Bars indicate percentage of neurons that code for both memories. Dotted line indicates the average level of co-allocation at +24 hours under Somatic PRPs, considered as baseline. Conventions as in Figure 5.3.

We find that the memory engrams of the strong and weak memory are overlapping not only at the coding population but also at the firing rate level (Figure 5.6). In order to assess the similarities between the firing pattern of the population during recall of the strong and weak memories, we used the Pearson correlation between their population firing vectors. A population firing vector contains the average firing rate

of the excitatory population during the recall of either the strong or weak memory. We find that the population firing rate vectors of the strong and weak memory are significantly correlated ($p<0.001$ for the null hypothesis of zero correlation) for ISIs less than 5 hours, however they were not correlated at 24 hours ($p>0.1$) during the window for which we have rescuing of the weak memory. This is shown in Figure 5.6 in which the correlation between the firing patterns of the population for the two memories is shown.

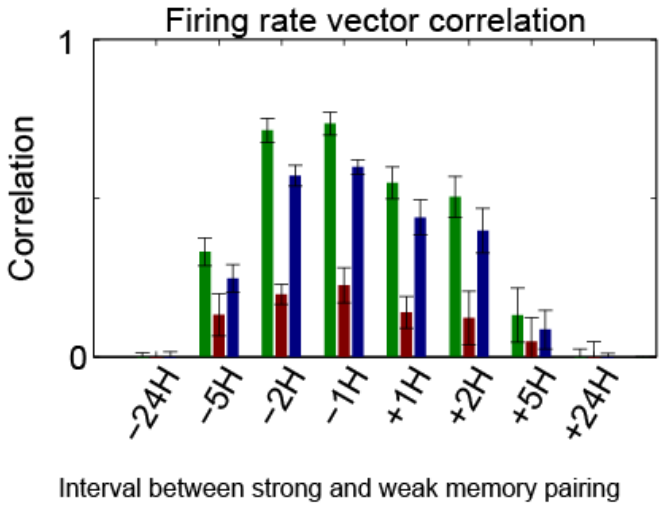

Figure 5.6 Similarity (Pearson correlation) of firing rate vectors between the strong and weak memories under enhanced excitability.
Conventions as in Figure 5.3.

This correlation at the population firing level corresponds to a binding of the two memories at the synaptic and neuronal level. We assessed the correlation of two vectors related to the allocation of the memory. First the correlations between the vectors of the number of potentiated synapses representing each memory follow the same pattern, with a significant ($p<0.001$) and high correlation during the

association window of 5 hours but low and non-significant correlation at 24 hours ($p>0.05$). The same observation can be made at the dendritic level. The vectors of the number of potentiated synapses per branch have significant and high value of correlation during the rescuing window ($p<0.001$). These results are shown in Figure 5.7.

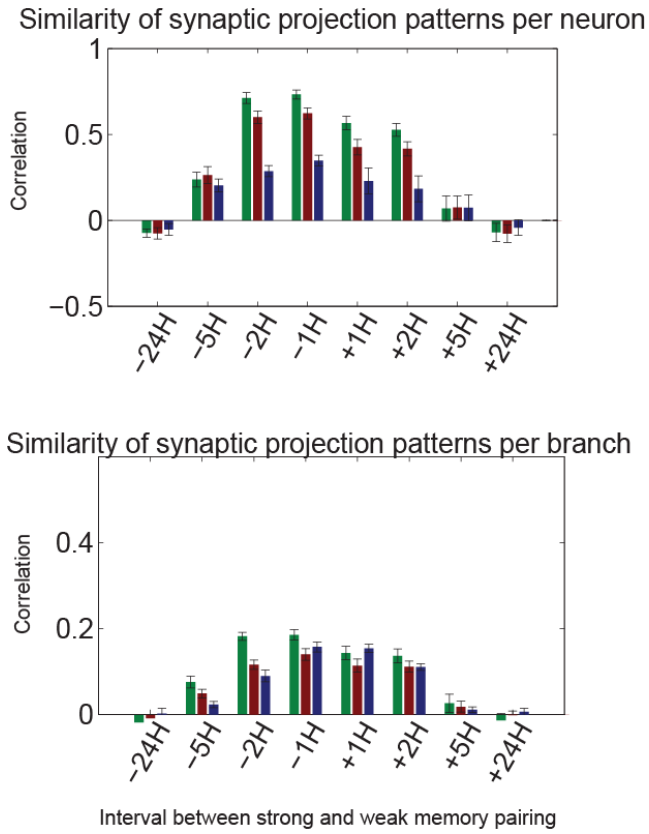

Figure 5.7 Synaptic weight vector similarities under enhanced excitabiltiy. Top: Pearson correlation between synaptic weight vectors per neuron. Bottom: Pearson correlation between synaptic weight vectors per dendritic branch. Conventions as in Figure 5.3

In order to characterize the co-allocation at the dendritic level, we also measured the proportion of branches that encoded both memories and contained 2 or more potentiated synapses from each memory. This is a measure of the number of clusters created that contain both memories, since each such cluster must contain at least 4 synapses, at least 2 from each memory. Figure 5.8 shows the percentage of dendrites containing such clusters. The co-allocation in dendrites had similar characteristics as the co-allocation at the population level, and wass significantly higher for ISIs < 5 hours ($p<0.01$ one-way ANOVA, Bonferroni post-test) under somatic PRP synthesis. Under Local PRP synthesis it was significantly higher for ISIs < 2H ($p<0.001$ one way ANOVA, Bonferroni correction).

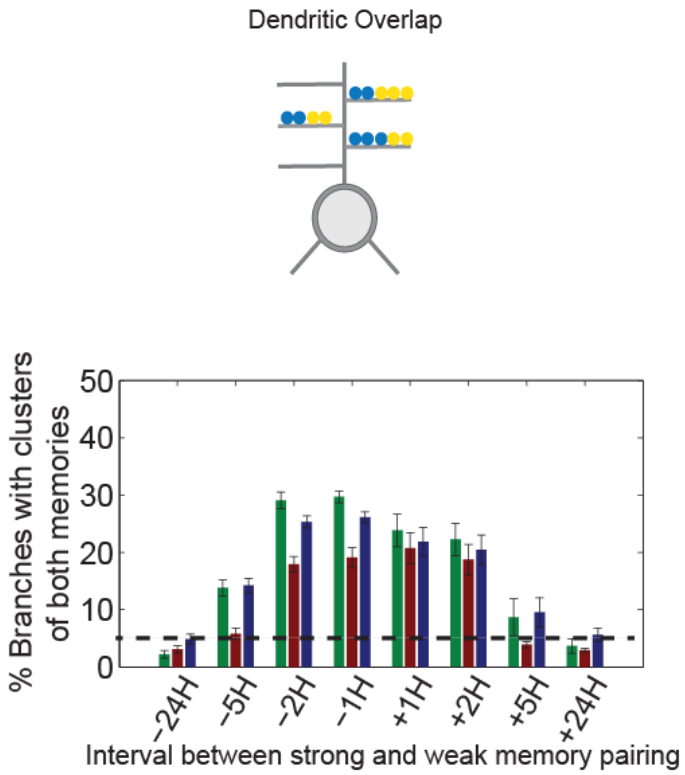

Figure 5.8 Co-allocation properties of the weak-strong memory pairing in dendrites.
Only the dendritic subunits that include *at least 2* potentiated synapses from each memory are included (Top). Dotted line indicates the baseline level, which is considered at 24 hours. Conventions as in Figure 5.3.

In order to separate the effect of synaptic cross-capture from the effect of increased excitability, we repeated the same experiments without the effect of enhanced excitability. In this case the asymmetry observed in Figure 5.5 is removed ($p>0.05$ one-way ANOVA, Bonferroni post-test). In the case of Global PRPs there is a reversal of the asymmetry, as there is a smaller but significant increase activation at

+1H and +2H compared to -1H -2H ($p < 0.001$ one-way ANOVA, Bonferroni post-test). This is attributed to the fact that synaptic tags have a larger time constant that PRPs: this extends the interaction time between PRPs and synaptic tags when the tagging stimulus is given before the PRP inducing stimulus. These results are shown in the coding population of the weak memory in Figure 5.9. Therefore, we propose that manipulations that attenuate or block the enhancement of neuronal excitability such as drugs that enhance the slow after-hyperpolarization, should blunt or eliminate this asymmetry revealed by Somatic and S&L PRP modes. In addition, there are not significant differences between -5H and -24H or +5H and +24H ($p > 0.05$ one-way ANOVA , Bonferroni post-test), indicating that the removal of enhanced excitability restricts the rescue of the weak memory by the strong one to the 2-hr window.

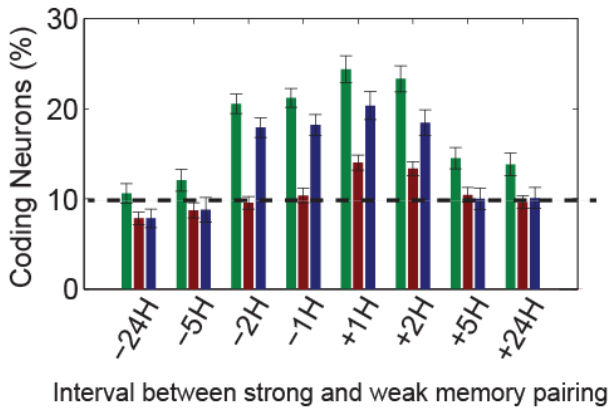

Figure 5.9 Coding population of the weak memory without enhanced excitability

Conventions as in Figure 5.3.

Similar findings regarding the asymmetry of memory allocation can be observed at the synaptic level. Figure 5.10 shows the number of common coding neurons and the percentage of cluster where memory is co-allocated without enhanced excitability.

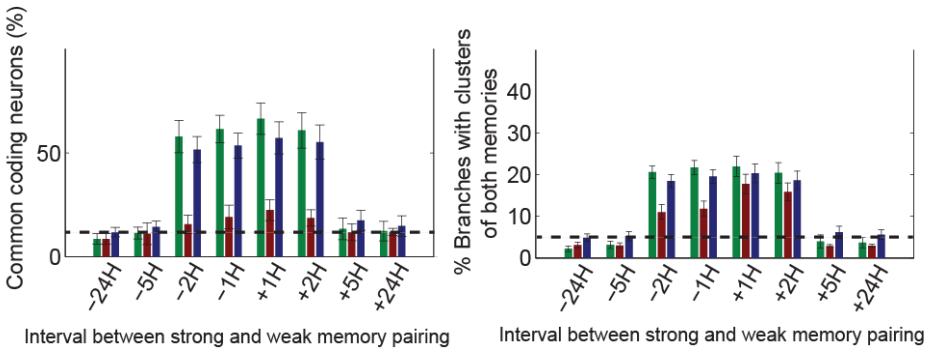

Figure 5.10 Co-allocation properties of the weak-strong memory pairing without increased excitability
Conventions as in Figure 5.3.

By looking at the similarity between the firing rate vectors of the population we can observe that the correlation beyond a 2 hour window is not significant ($p>0.1$). In addition the similarities in the synaptic projection patterns per neuron and per branch are not significantl beyond the same 2 hour window ($p>0.05$). Figure 5.11 summarizes these results. This indicates that, even though both memories have coding populations at 5 hours (Figure 5.9), there is no underlying connection between the weak and strong memory.

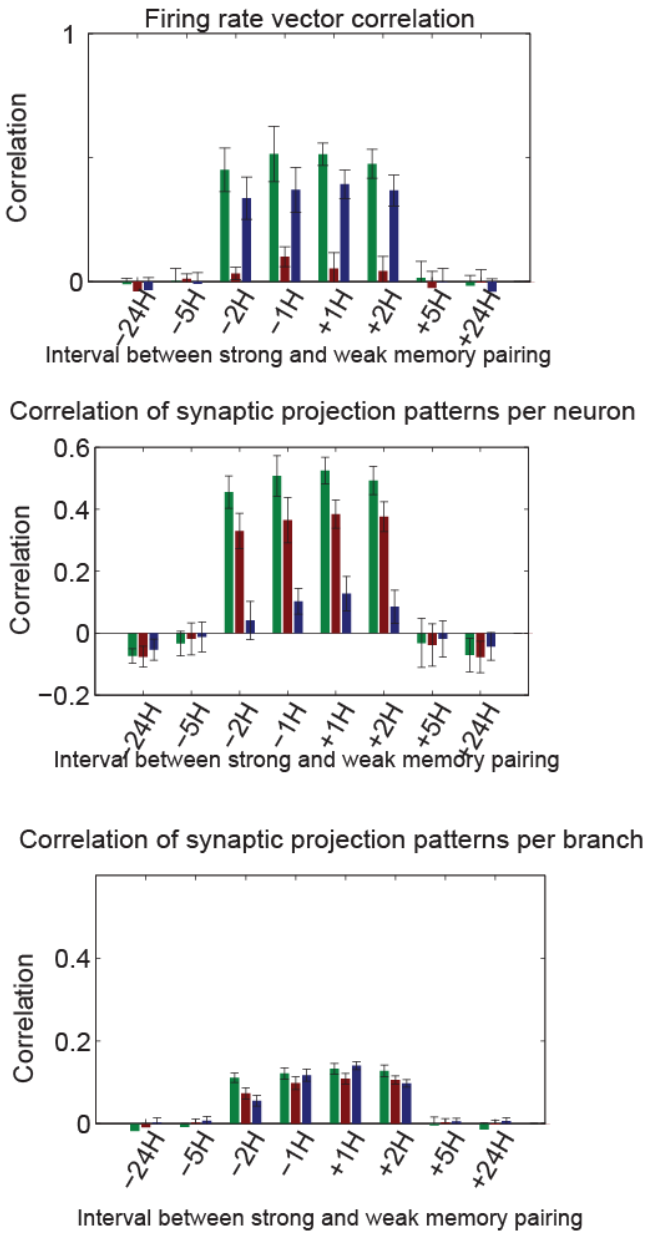

Figure 5.11 Co-allocation properties of the weak and strong memory with static (not enhanced) excitability.

Top: Pearson correlation of firing rate vectors between the strong and weak memories under static excitability. Middle: Correlation between synaptic weight vectors per neuron Bottom: Correlation between synaptic weight vectors per dendritic branch. Conventions as in Figure 5.3.

5.3 Interactions between 3 weak and strong memories

Given that neuronal and dendritic co-allocation underlie the association of information in the prior simulations, we next investigated whether these mechanisms also allow the linking of multiple weak or strong memories across time, where recall of one memory increases the probability of recall of the others (Silva et al. 2009). Three subsequent memory-triggering events (weak or strong) were presented in two different orders: "strong-weak-strong" or "weak-strong-weak". The ISIs between the memories tested were 1, 2, 5 or 24 hours. The interactions between these memories across time were assessed during recall. This particular simulation incorporated conditions of combined (S&L) PRP availability as well as the increases in excitability described above, since the available experimental evidence suggest that this scenario likely reflects *in vivo* conditions.

The results are summarized in Figure 5.12. When a weak memory-causing event is placed between 2 strong ones (i.e. strong-weak-strong scenario), the size of the neuronal ensemble encoding the weak memory increases dramatically (from 7.7±0.4% at ISI=24 hrs to 32.3±1.3% at ISI=1hr, $p<0.01$ one-way ANOVA with Bonferroni post-test), essentially turning the weak memory into a strong one. This increase in memory strength, measured as an increase in the size of the neuronal ensemble encoding that memory, is significantly** ($p<0.001$) larger than that observed when a weak memory-causing event is paired with a single strong one (maximum size 27.8±1.5 at -1 hour), since both strong memories share PRPs with the weak memory. Furthermore, with a 1 hr ISI, the degree of overlap of the neuronal

ensembles representing all three memories (Figure 5.12 B) is high, which could likely result in memory interference. Importantly, there is significant co-clustering of synapses representing all three memories (Figure 5.12 D), including the weak memory (Figure 5.12 C), which is significantly higher for all timings compared to +24H ($p < 0.001$). This is due to the enhancement of excitability of the neurons that encode for the first memory, which lasts for 12 hours, thus recruiting many of these neurons into the memory traces of both the weak and the second strong memory.

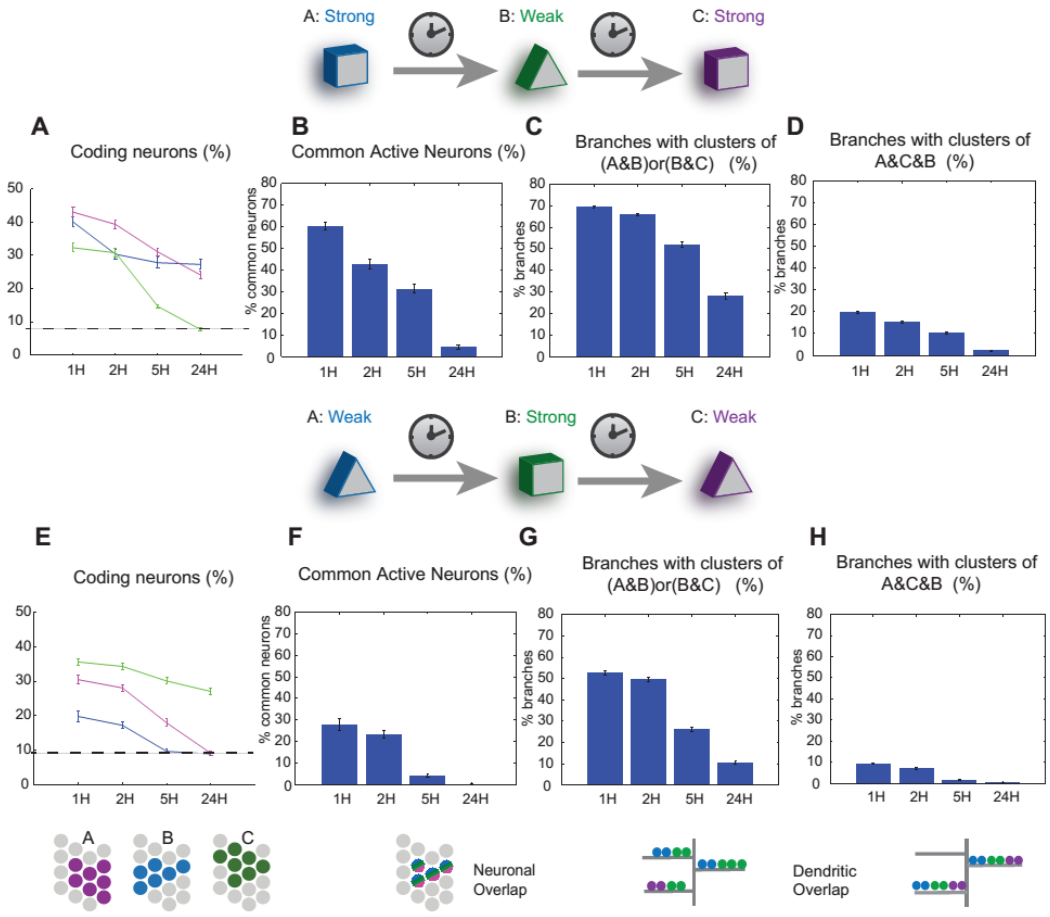

Figure 5.12 Memory interactions between 3 memories – combination of strong and weak memories.

A) Size of each memory (coding neurons). Line colors in this figure indicate the order in which memories are encoded. Blue: Memory A (strong), Green: Memory B (weak), Magenta: Memory C (strong). B) Percentage of the coding neurons of memory B that also code for memory A and memory C. C) Percentage of branches containing clusters (2 or more synapses) of the second memory which are co-allocated with a cluster (2 or more synapses) of the first memory or a cluster of the third memory. D) Percentage of branches containing clusters (2 or more synapses) of the second memory which are co-allocated with a cluster (2 or more synapses) of the first memory AND a cluster of the third memory. E-H) As in (A-D), for the case of a weak memory followed by a strong and then by a second weak memory. The simulations in this figure were performed under the S&L condition with enhanced excitability. Error bars indicate the SEM for 10 simulation trials.

When a strong memory-inducing event is flanked by 2 weak memory-triggering events (weak-strong-weak scenario) the result is a strengthening of both weak memories at ISIs 1H and 2H ($p<0.01$ one-way ANOVA with Bonferroni post-test), however the effect is both more pronounced and stable for the second weak memory in the series (Figure 5.12 E, magenta). Compared to the first weak memory (Figure 5.12 blue) the coding population is significantly different ($p<0.001$) for ISIs 1-5H The second weak memory thus benefits from the enhanced excitability of neurons coding for the strong memory. For all ISIs tested, the strong memory is encoded by a larger ensemble than the two weak memories, and the overlap between the three memories is moderate (Figure 5.12 E,F). Interestingly, while co-clustering of the synapses representing the strong memory with those of either weak memory is high (Figure 5.12 G), the probability of co-clustering of the synapses representing all three memories is low (Figure 5.12 H). This is because weak memories have very few

neurons with enhanced excitability and interactions are limited to STC time windows.

In summary, our model predicts that a weak memory-causing event can be strengthened if placed between strong memory-causing events, even if the intervals used are clearly outside of the 2 hr window used in STC experiments. However, our model suggests that memory interference may be a significant factor when shorter intervals are used. Additionally, our model suggests that the rescue and linking effects we studied are less effective when a strong memory is placed between two weak ones (as compared to the strong-weak-strong scenario), due to smaller neuronal overlaps. In this case short ISIs (e.g., 1 hr) appear to maximize linking and rescue effects. These simulations once again confirm the essential role of neuronal co-allocation and synapse clustering in memory linking and make a number of interesting predictions that could be tested using simple behavioral approaches.

5.4 Discussion

Overall, our model makes the following predictions regarding weak-strong memory interactions: First, weak-strong memory pairing within a window of 2 hrs can lead to rescuing of the weak memory, as shown experimentally (Moncada & Viola 2007; Ballarini et al. 2009). Second, rescue of the weak memory is achieved through neuronal co-allocation and synaptic co-clustering of the two memories, irrespective of the source of the PRPs. Third, this rescue should be more effective if PRPs are available throughout the neuron. Fourth, the rescue should be asymmetric and

extended to a 5-hour window, if the strong memory is acquired first and if it leads to an increase in neuronal excitability within this time frame.

This could be conceivably tested experimentally by conditions that would inhibit primarily somatic, rather than dendritic, protein synthesis. This may be feasible with localized manipulations of protein synthesis in brain regions, such as the pyramidal fields of the hippocampus, where somatic and dendritic layers are not in complete juxtaposition. Moreover, we predict that rescue would be more effective if the strong memory *precedes* the weak one, as this would result in a larger population of neurons responding to the weak memory, especially if Somatic or S&L PRP modes are dominant (shown by the asymmetry in green/blue bars in Figure 5.3). This asymmetry could be a mechanism for detecting the order (sequence) of events, and is predicted to rely on the enhancement of neuronal excitability that follows learning (Disterhoft & Oh 2006).

Chapter 6.

Results III: Memory overlaps between two strong memories

6.1 Background

The process of memory allocation to neuronal circuits reveals aspects of memory storage that were hitherto unknown and suggests possible links that could bind temporally related memories together. Studies have proposed that the co-allocation of two memories to an overlapping population of neurons links the two memories by increasing the probability of co-recall (Zhou et al. 2009). According to this hypothesis, CREB-dependent transcription in the neurons encoding the first memory results in temporary increases in excitability (Stanciu et al. 2001; McKay et al. 2013) that, for a time, bias the allocation of subsequent memories to many of the same neurons that encoded the first memory (Viosca et al. 2009; Zhou et al. 2009). This creates the possibility for neuronal overlaps between memories. We saw that in the case of weak-strong memory pairing this overlap is very high. The fact that the weak memory on its own will have very little long-term consolidation contributes to this. This is a result of the dependence of weak memory strengthening on synaptic cross-capture of proteins: The weak memory is dependent on the neurons where the strong

memory is encoded for its allocation, and therefore the resulting overlaps in populations are high.

It is possible, however, that this kind of memory co-allocation can occur even when both memories are strong. Recent studies have begun to identify mechanisms that can bind together the memory traces of two separate memories. Garner et al. used transgenic mice that express a designer receptor exclusively activated by designer drug (DREADD) to address this question (Garner et al. 2012). The DREADD is activated by the artificial ligand clozapine-N-oxide (CNO), which triggers strong depolarization and spiking. The authors conditionally expressed the DREADD under the control of the activity dependent Fos promoter and the tetracycline-inducible system. The receptor was expressed in a manner that is inducible and activity-dependent. The researchers expressed DREADD in the neurons activated while mice were in a context A. Later, the mice were fear conditioned in a context B, while simultaneously the neurons that had been activated in context A were being reactivated with CNO. As a result of this procedure, the fear response was expressed behaviorally only when both CNO was given *and* the mouse was in context B, but not when the mouse was in context B without CNO (or in context A). This indicates that a synthetic memory trace was created, which required both the normally activated population of context B and the chemically reactivated population of context A to be active in order to be expressed. In another experiment, researchers used optogenetics to mark dentate gyrus or CA1 neurons of the hippocampus during exposure in context A and then proceeded to fear condition the mice in context B while activating the neurons of context A (Ramirez, Liu, et al. 2013). During fear recall, the mice in this case showed freezing in context A, even though they had not

been fear conditioned there. This mechanism of "false memory" creation is believed to rely on the overlap between the neurons expressing the two memories (Figure 6.1). These studies suggest that memory allocation mechanisms are the reason why recalling a memory while encoding a different one can result to the linking and integration of the two memories (Howard & Kahana 2002).

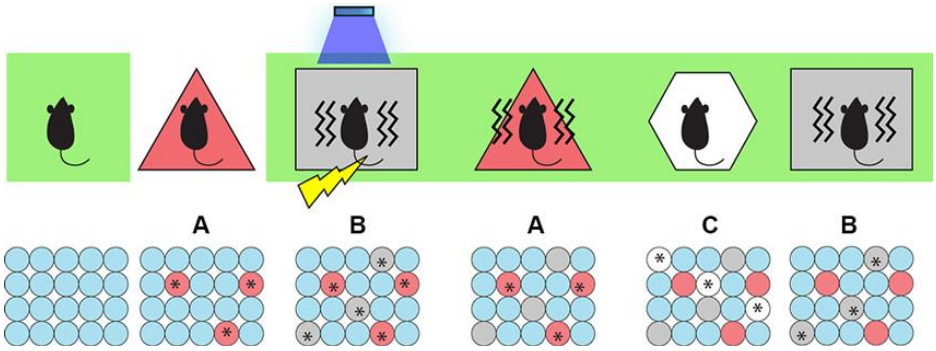

Figure 6.1 Creation of a "false memory" through optogenetic activation in a different context.
Mice were conditioned in context A and the activated neurons were tagged with ChR2. Subsequently they were fear-conditioned in context B while simultaneously the neurons tagged in context A were being activated with light. As a result, the mice expressed fear in context A even though they had not been fear conditioned in that context, while they did not express fear in a novel context C. As expected, they expressed fear recal in context B. Top panel: experimental conditions, Bottom panel: putative populations of neurons activated (asterisks) in contexts A (red), B (grey) and C (white). Figure taken from (Ramirez, Tonegawa, et al. 2013) reproduced under the Creative Commons licence CC-BY.

We saw in chapter 3 that the rescuing of a weak from a strong memory creates overlap between the two memories. We used a similar memory pairing, but for strong

memories in order to study the overlaps created when the two memories are both strong and identified the properties of their overlapping allocation.

6.2 STC and excitability bind together strong memories

We presented two strong (capable of producing PRPs) learning events to our model population separated by Inter-Stimulus-Intervals (ISI) that ranged between of 1 and 24 hours. The recall of the memories was tested 24-hrs later by measuring responses to one of the two stimuli associated with each of the memories. Simulations were performed under all three PRP conditions (Somatic, local and S&L), with and without enhanced neuronal excitability.

As shown in Figure 6.2, interactions between the two strong memories were observed for ISIs of 1-5 hours. Specifically, for ISIs of 1-2 hrs, training with both memories led to large enhancements in the number of neurons encoding each memory (> 40% increase at 1 hour, $p<0.01$ one-way ANOVA with Bonferroni post-test). Interestingly, for an ISI of 5 hrs, only the second memory was enhanced ($p<0.01$) (Figure 6.2, Right) while the first memory was not ($p>0.1$). This asymmetry was driven by the increase in excitability caused by the first memory, since blocking this enhancement eliminated the asymmetry (Figure 6.5).

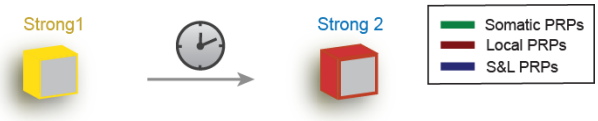

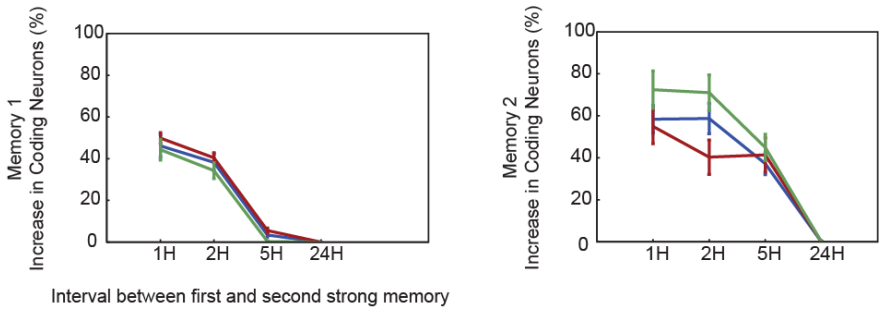

Figure 6.2 Increase in the percentage of the population of coding neurons for the two strong memories of the pair compared to baseline (24 hours).
Left: first memory , Right: second memory of the pair. Error bars indicate the SEM for 10 simulation trials.

Memory enhancements were accompanied by an increase in the overlap between the neurons and the dendritic segments encoding the two memories (Figure 6.3), which was characterized by increased clustering of synapses onto common branches. In the absence of increases in excitability, overlap between the two memories was restricted to ISIs of 1-2 hrs ($p<0.01$ one-way ANOVA followed by Bonferrroni correction) as opposed to 5 hrs, (Figure 6.5) suggesting that the role of neuronal excitability is to prolong the interaction window between memories. The restriction of PRPs to dendritic branches led to a smaller degree of neuronal co-allocation between the two memories (41.3±1.0% under Global, 22±1.5% under Local, $p<0.01$ one-way ANOVA), but comparable levels of synapse clustering (29.5±1.6% and 24.9±1.2% respectivel,y $p<0.01$ one-way ANOVA).

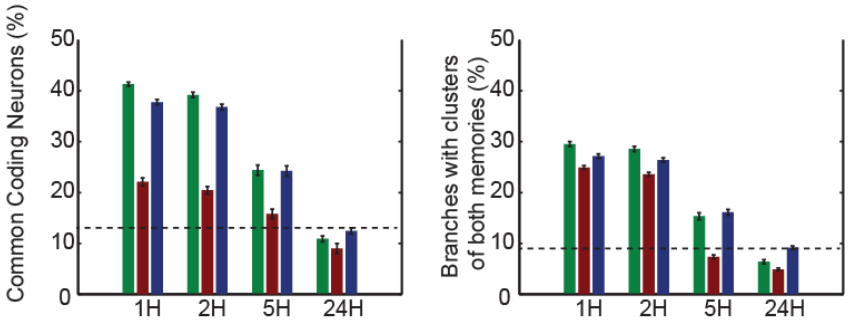

Figure 6.3 Overlapping properties of memory allocation for the case of two strong memories being encoded.
Percentage of common coding neurons (left) and branches containing >2 synapses of each memory (right) under the condition of static excitability. Conventions as in Figure 6.2

The overlapping nature of the allocation of the two memories is more prominent in the correlations of synaptic allocation at the firing rate population level, and the encoding population level. This is shown in Figure 6.4, in which the correlation between the population firing rate vectors during the recall of the two memories is plotted for different memory intervals. Both somatic and local PRP conditions create similarities, although they are more prominent under Somatic PRPs. The correlation is significant up to 5 Hours ($p<0.01$) but not to at 24 hours ($p>0.1$).

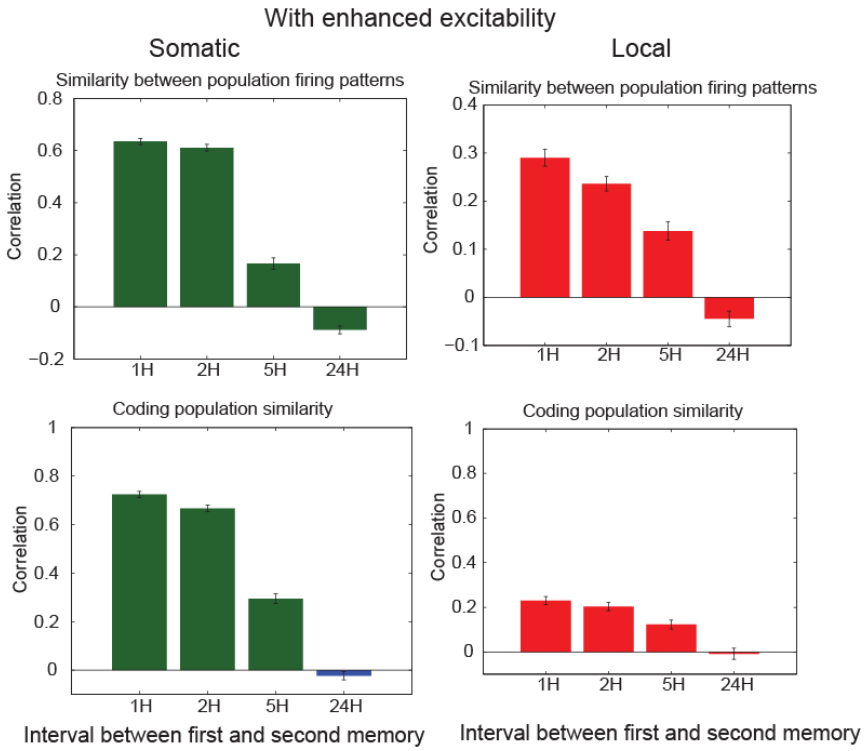

Figure 6.4 Pearson correlation in the neuronal allocation of two strong memories under the condition of enhanced excitability.

Top: Correlation in population firing rate vectors of the two memories. Bottom: Correlation in coding neuronal population (i.e. correlation between binary vectors representing the coding populations for the two memories). Conventions as in Figure 6.2

The enhanced excitability extends the association window of the two memories provided by STC to the ISI of 5 hours, as shown before. We repeated the simulations removing the effect of enhanced excitability in order to isolate its contribution. The results are shown in Figures 6.5 and 6.6. Two main conclusions are driven by these results: 1) the strengthening of the memories at 5 hours is reversed as there is now not significant difference between 5 and 24 hours ($p>0.1$ one-way ANOVA) and 2) the enhancement of the second memory under local PRPs is greatly impaired without

enhanced excitability. This indicates a synergistic effect between excitability and STC when PRP synthesis is dendrite-restricted.

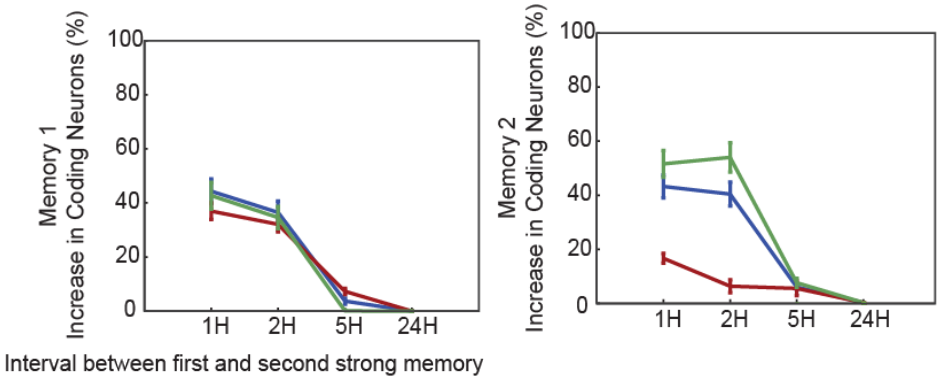

Figure 6.5 Increase of the coding population for the two strong memories under the Static excitability condition compared to baseline (24H).
Left: first memory , Right: second memory of the pair. Conventions as in Figure 6.2

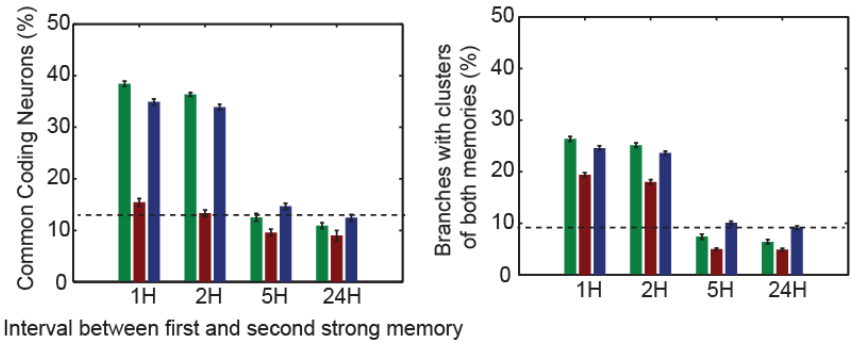

Figure 6.6 Common coding neurons and branches under static excitability.
Common coding neurons (left) and branches containing more than 2 synapses of each memory (right) under the condition of static excitability for the three different PRPs synthesis conditions.
Conventions as in Figure 6.2

As before, these effects become more pronounced when quantified by the correlation of the firing rate vectors and the coding population vectors. Figure 6.7 shows the abrupt change of the similarities between 2 and 5 hours.

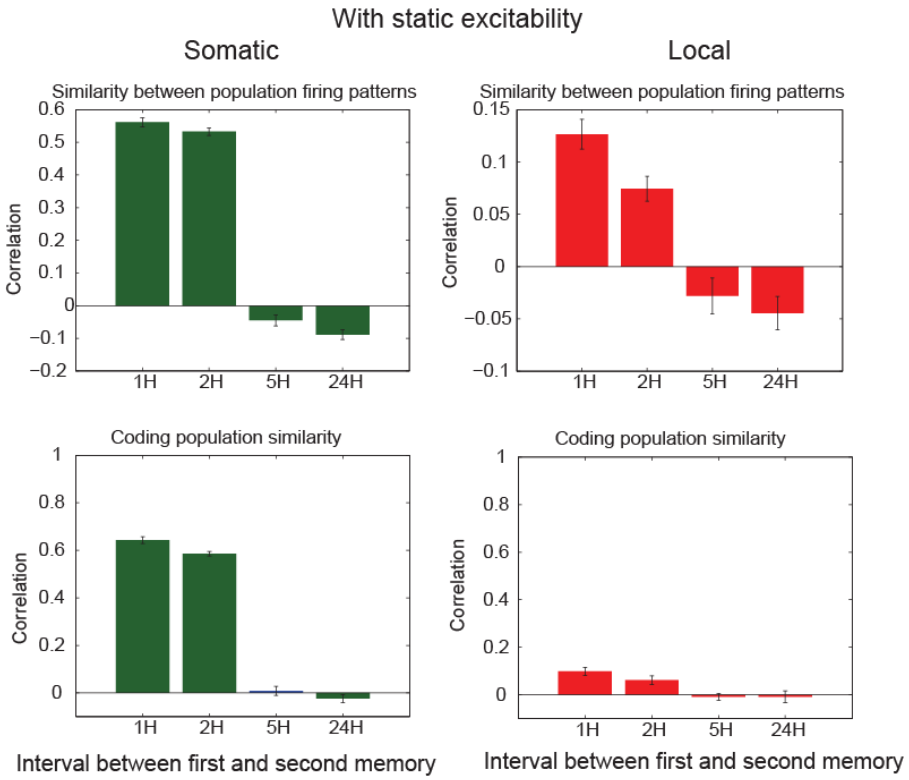

Figure 6.7 Pearson correlation in the allocation of the two memories for the case of static excitability.
Top: Correlation in population firing rate vectors of the two memories. Bottom: Correlation in coding neuronal population for the two memories.

6.3 Discussion

Overall, our model makes the following predictions regarding the interactions between two strong memories:

First, our simulations support the hypothesis that changes in excitability lead to co-allocation of memories separated by several hours (Rogerson et al. 2014; Silva et al. 2009).

Second, our model also supports the hypothesis of clustered plasticity mediated by STC (Govindarajan et al. 2006).

Third, pairing of two strong memories can affect both memories, but only the second memory is enhanced when long ISIs (i.e., 5 hours) separate the two memories.

Fourth, our model suggests that the asymmetric enhancement of the second memory is due to increases in neuronal excitability following the acquisition of the first memory, and predicts that blocking this increase in excitability should eliminate this asymmetry and possibly restrict memory enhancement to a 2-hour interval.

Fifth, for ISIs smaller than 2 hrs, the high overlaps between the neuronal ensembles representing both memories under Somatic and S&L PRP conditions may lead to memory interference (Robertson 2012). Restricting PRPs to dendritic branches (e.g., by reducing transcription), should reduce neuronal co-allocation and therefore decrease interference.

Finally, our model studies suggest that in all cases, interactions between strong memories are mediated by neuronal and dendritic co-allocation that drive co-clustering of synapses representing both memories.

Chapter 7.

Results IV: Creating memory episodes by binding memories via population overlaps

7.1 Background

The prediction that timely pairing of strong memories can create associations between them via their allocation to overlapping neuronal populations suggests that this may be a general mechanism for binding together a sequence of memories that occur over relatively long time periods, thus creating memory episodes.

Episodic memory is comprised of serially associated memories that need to be both stored separately, in order to be distinguishable, but also connected with each other in order to be able to be associated during recall. The mechanisms of increased excitability and/or STC suggest a way for binding memories together in overlapping population. This mechanism has characteristics that are favorable for the creation of memory episodes: 1) the mechanism binds together memories in a time-dependent way so that the closer the memories are in time, the higher their co-allocation, and 2) the increase of excitability (modeled by the condition of enhanced excitability here) creates an asymmetry in the strengths of two subsequent memories being encoded (as discussed in chapter 6).

The overlapping storage hints to a mechanism that favors the simultaneous recall of two related memories: During recall of the first memory, the neurons activated are also a large subset of the neurons required for the recall of the second memory. Thus, the hypothesis that memories bound in this way through overlaps are likely to be recalled together (Rogerson et al. 2014; Silva et al. 2009). Although this hypothesis has not yet been experimentally verified, it is important to study the implications of neuron engram overlaps that result from STC and CREB/excitability (Rogerson et al. 2014).

7.2 Serial memories become associated through overlapping allocation

We examined the effect of consolidation mechanisms in the storage of a string of memories that are encoded serially in the same neuronal population. We simulated a series of 10 memories that are separated 1 hour from each other and studied the relationships between the resulting memory traces. As before, we evaluated both the somatic PRP and the dendritic PRP synthesis conditions, and additionally, we repeated the simulations without the effect of increased excitability (enhanced excitability) in order to distinguish it from the effect of STC.

As shown in Figure 7.1A, STC and enhanced excitability introduce overlaps in the populations coding the 10 encoded memories in the case of Somatic PRP synthesis. The overlaps are strong between memories that are encoded one or two hours apart, and less strong for longer ISIs, even though the overlaps extend to the entire span of

the memories (10 hours). The average overlap between the populations against the time between memories is plotted in Figure 7.1B. Looking at the dendritic branch level, we observe that co-clustering of subsequent memories is more prominent, and that the probability of co-clustering remains high even for memories separated by 5 or more hours (Figure 7.1 B). As shown in figure 7.1B the probability of co-clustering drops approximately linearly as the interval between two memories is increased. This indicates that co-allocation of memories is prominent, and this is shown in figure 7.1C where the number of memories represented in a branch (having at least 1 potentiated synapse, as opposed to 2 which is the criterion we use for co-clustering), The average number of memories represented per branch is 3.9 ±1.9.

In general these results indicate that 1) STC and excitability act as general mechanisms that cause overlapping storage of memories through large time spans, and 2) that the magnitude of the correlation is dependent on the time courses of STC and excitability.

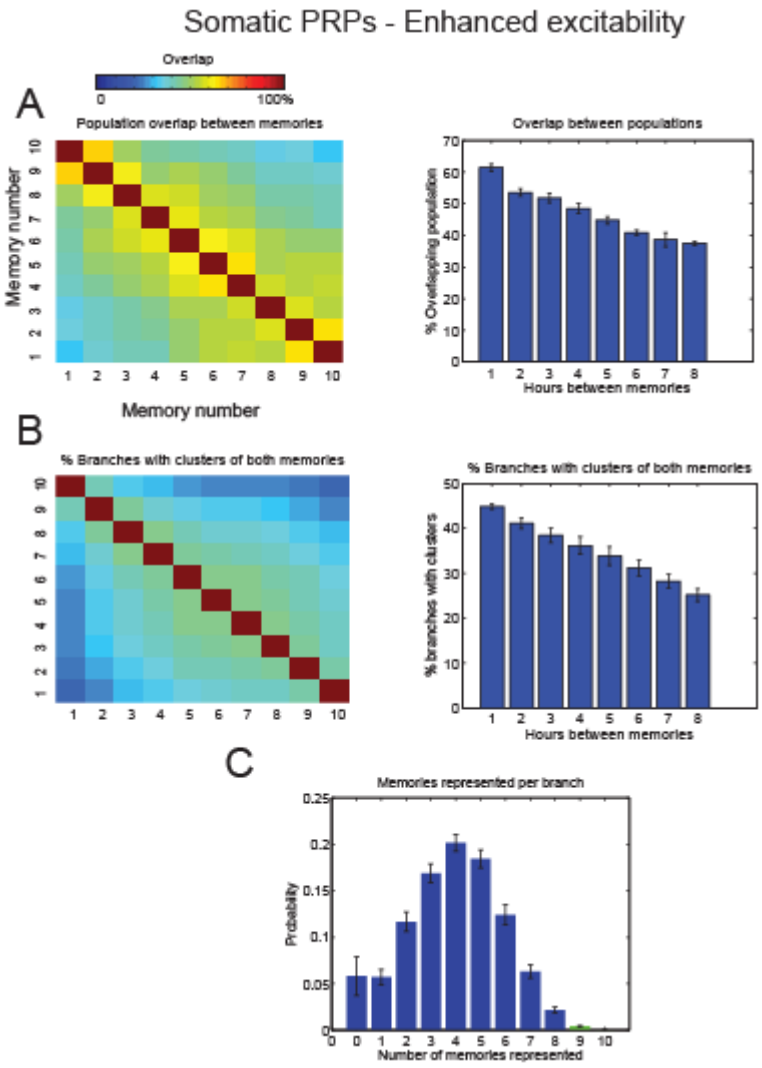

Figure 7.1 Co-allocation of memories under Somatic PRP synthesis and enhanced neuronal excitability conditions.

A) Left: coding population overlap between different memories (ratio of percentage of neurons coding for both memories / neurons coding for either memory). Right: average overlap as a function of time between memories. B) Left: percentage of branches with clusters of 2 memories for all combinations of memories. Right: Average percentage as a function of the time between memories. C) Probability distribution of the number of memories per branch

(i.e. number of memories that have at least 1 potentiated synapse in a branch). Error bars indicate SEM for 10 simulation trials.

In the case of Local PRPs and enhanced excitability, the overlapping allocation is much less prominent for all the intervals between memories, as shown in figure 7.2 ($p<0.001$ one-way ANOVA between the two PRP). Additionally, dendritic branches have an average of 2.2±1.7 memories per branch (Figure 7.2). Kruskal-Wallis one-way analysis of variance shows that the distribution is different from the case of Somatic PRPs ($p <0.001$).

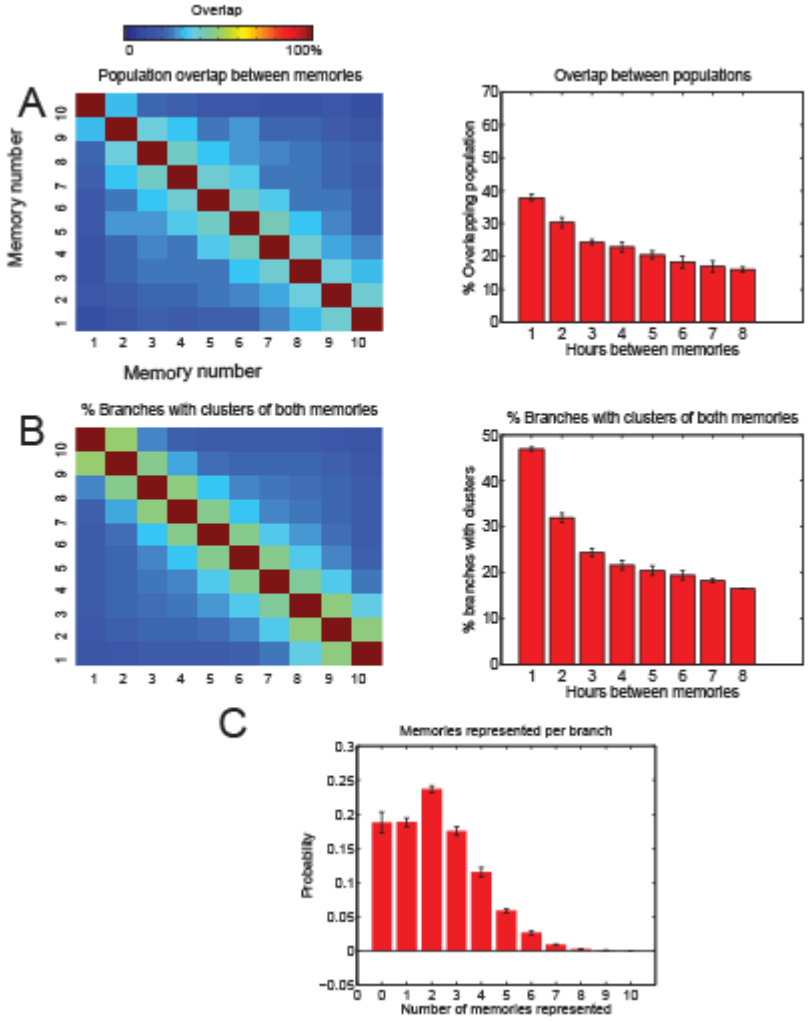

Figure 7.2 Co allocation of memories under Local PRP synthesis and enhanced neuronal excitability conditions.
Conventions as in Figure 7.1.

In order to isolate the effect of STC, we repeated the same simulation without the effect of enhanced excitability (static excitability). The results are shown in Figures 7.3 and 7.4, and indicate that STC by itself can still create large overlaps for the intervals of 1 hour. In this case the both the neuronal overlap and the percentage of

branches with both memories is significantly different from the case of enhanced excitability ($p < 0.001$ one-way ANOVA) indicating that there is a "drop" in the overlap at 3 hours window. Thus, enhanced excitability increases the temporal window for co-allocation.

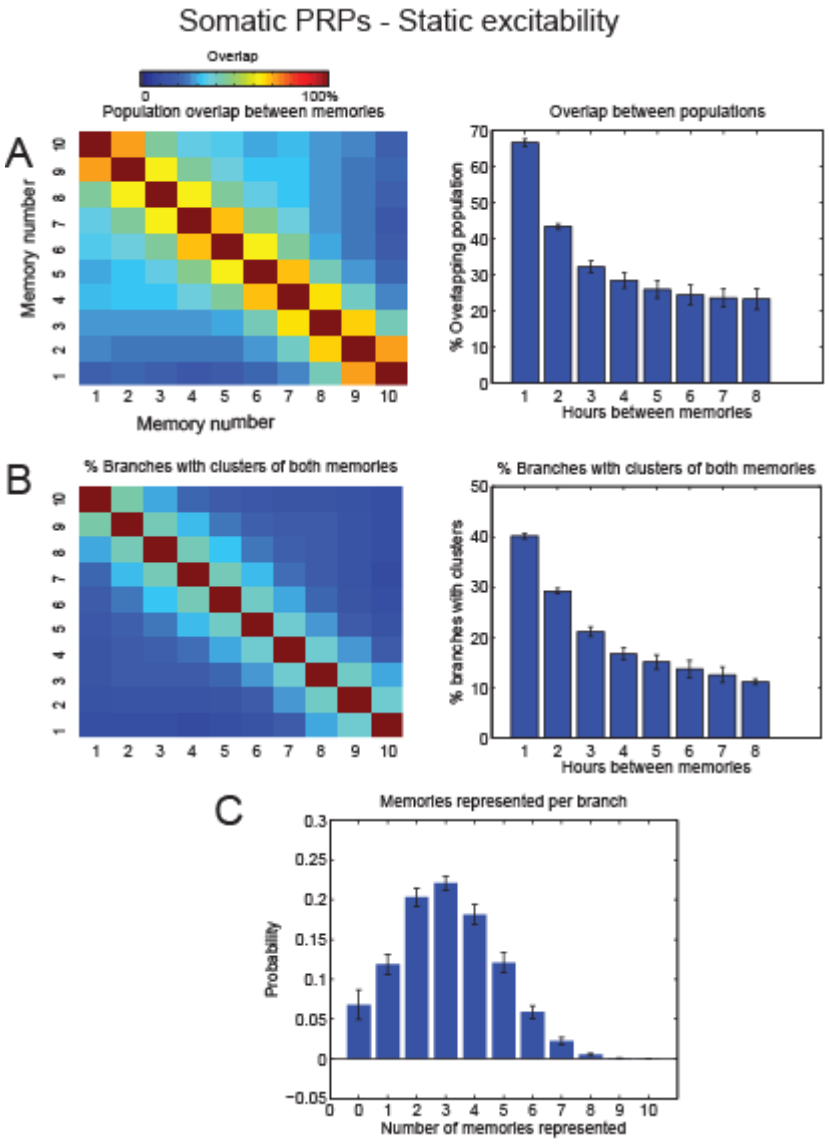

Figure 7.3 Co allocation of memories under Somatic PRP synthesis and Static neuronal excitability conditions.
Conventions as in Figure 7.1

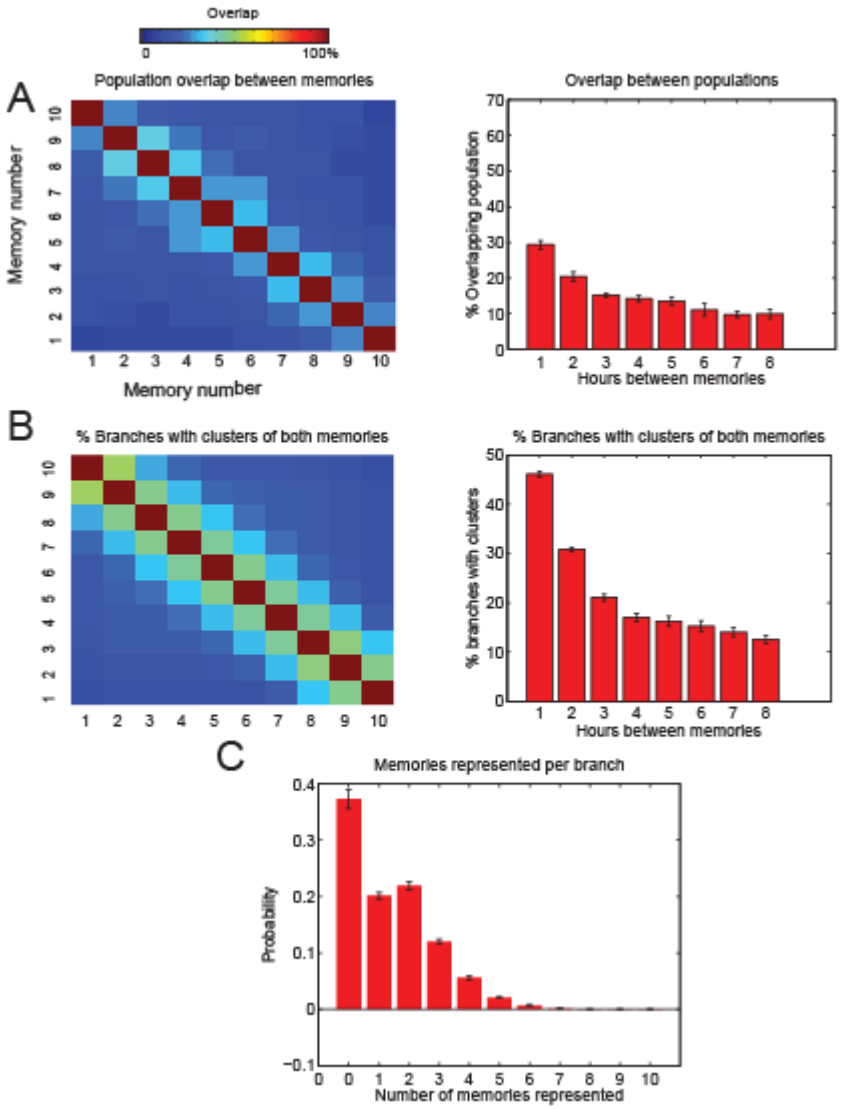

Figure 7.4 Co-allocation of memories under Local PRP synthesis and Static neuronal excitability conditions.
Conventions as in Figure 7.1

In sum, these simulations predict that subsequent memories spaced 1-2 hours apart will be strongly associated with each other and that the recall of one memory will lead to the recall of multiple memories that are part of a given ‘episode’. However, since the overlaps are symmetric, the information about the sequence of encoding cannot be recovered under this episodic memory formation model.

Chapter 8.

Results V: Repeated learning leads to increased clustering of synapses

8.1 Background

Studies investigating the synaptic potentiation due to learning at the subcellular level have provided evidence about the distribution of synaptic potentiation in dendrites after learning. Using two-photon microscopy, Fu et. al. (Fu et al. 2012) investigated the formation of new synapses during the learning of new motor skills and the addition of new spines over days of repeated learning. Their findings suggest that the synapses formed during repeated training tend to cluster together in dendrites, thus supporting the clustered plasticity hypothesis. By imaging the formation of spines in motor cortex dendrites, the researchers analyzed the spine changes that occur during the learning of a motor task that was repeated over multiple days (Fu et al. 2012). During this learning protocol, the majority of new spines that were formed in adjacent positions in the dendrite were more clustered than control spines (in distances < 5μm), and the process was dependent on the activation of NMDA receptors. This showed that newly formed spines are highly likely to be added to the existing clusters rather than being allocated randomly, thus contributing to the refinement or reinforcement of motor learning. In addition, clustered spines were

more stable than isolated ones, implying that the arrangement of synapses in clusters may promote the stability of long-term memories. Increased anatomical clustering of potentiated synapses has also been observed in an *in vitro* study, which simulated spatial learning in the hippocampus (Kramár et al. 2012).

8.2 Repeated learning without synapse reorganization

We simulated this type of repeated learning by repeatedly training the same memory in our population with a 24h interval between each training event for 1 to 4 days, and under the condition of both somatic and dendritic PRP synthesis. The encoding protocol was the same in each simulated repeated learning, while the intervening 24 hour period allowed for homeostatic and excitability-related consolidation changes to take place. After each simulated training day, we assessed the coding population of the memory by recalling it as described in chapter 2. We used the percentage of dendritic subunits with more than 2 potentiated synapses as a measure of clustering in the model. The simulations were performed under both Somatic and Local PRP synthesis cases, under the condition of enhanced excitability.

Our results show an increase of coding population from 25±2.7 % in the first day to 33.1± 3.0% in the 4^{th} day of repeated training for the case of Somatic PRP synthesis ($p<0.001$ one-way ANOVA). Under Local PRPs, there is a more dramatic increase in the coding population, from 18.1±2.1 % to 40.9±2.5% ($p<0.001$). However, we observed little change in the clustering properties of this memory encoding, as there was only a small change in the average percentage of branches with more than 2 potentiated synapses (one-way ANOVA followed by Bonferroni post-test found

significant differences between day 1 and days 2-4 ($p<0.01$) but not between days 2-4 ($p>0.05$)). The number of potentiated synapses per branch changed from 3.36±0.46 after day 1 to 4.17 ± 0.23 after day 4 of training under Somatic PRPs . These results are shown in Figure 8.1.

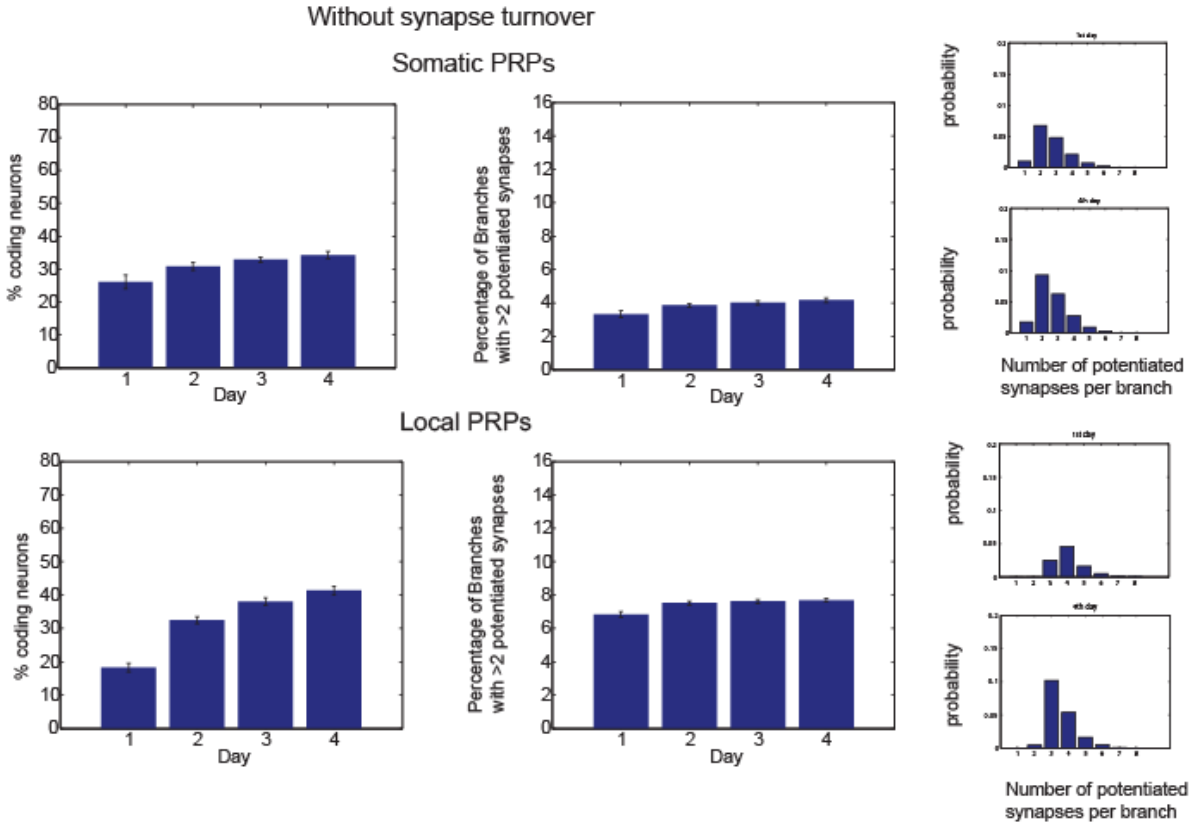

Figure 8.1 Repeated training of the same memory does not lead to increased clustering when synapse reorganization does not occur.
Left column: The coding population under somatic (top) and local (bottom) protein synthesis. Middle column: Clustering assessed by the percentage of of branches with > 2 potentiated synapses. Right column: Histograms of the number of potentiated synapses per branch in day 1 and day 4 of training. Error bars indicate SEM of 10 simulation trials.

8.3 Synapse reorganization leads to increased clustering

We reasoned that the absence of increased clustering of the same memory after repeated training is due to the lack of synapse reorganization in our model. Synapse reorganizations are typically slow in the brain and consist mainly of the turnover of weak synapses and the formation of new filopodia or immature synapses between axons and dendrites that were not previously connected (Holtmaat et al. 2005; Trachtenberg et al. 2002). We thus proceeded to simulate synapse reorganization to our model.

Synapse formation and elimination closely follows the structural changes of dendritic spines, which are known to change in long timescales. In the cortex, spine generation and elimination persists into adulthood (Trachtenberg, Chen et al. 2002, Holtmaat, Trachtenberg et al. 2005). New spines are continuously formed and old spines turn over. However, large spines (which are also functionally strong (Matsuzaki, Honkura et al. 2004, Noguchi, Nagaoka et al. 2011)) persist much longer than small ones (Trachtenberg, Chen et al. 2002). New filopodia are continuously formed and eliminated in young adult or adult mice, and give rise to spines, which are stable over time, with larger (strengthened) spines being more stable (Grutzendler, Kasthuri et al. 2002, Zuo, Lin et al. 2005). Since new spine formation and spine elimination results in the remodeling of synaptic connectivity, we simulate the turnover and *de novo* formation of a small percentage of weak synapses in our network. We simulate the spine formation as follows: out of the synapses that have not undergone potentiation (i.e. synapses with weight less than w_{init}), we randomly select a subset containing 0.5% of them every hour. The synaptic connections are removed, and replaced with

new, random connections from the afferent axons to the dendrites of excitatory neurons. This allows the constant remodeling of the afferent connectivity in the network over long periods of time.

The results of the simulations, which include dynamic synapse formation and elimination are shown in Figure 8.2. In the case of somatic PRP synthesis, our results indicate that such repeated training leads to an increase of the coding population as the training is repeated compared to the first day ($p<0.01$ one-way ANOVA). This indicates that newly formed weak synapses are potentiated with repeated learning. New synapses indeed seem to cluster with the existing ones with every new training, as shown in figure 8.2, right column, which shows the distribution of the number of synapses per branch increasing from after 1 day of training and after 4 days of training ($p<0.01$ one-way ANOVA followed by Bonferroni correction). The increase in the number of branches that contain more than 1 potentiated synapses indicates that synapses cluster on dendritic branches after the first day. The number of potentiated synapser per branch increased from 3.17 ± 0.48 after day 1 to 5.85 ± 1.51 after day 4 of learning ($p<0.001$ one-way ANOVA). Thus in this case we observed increased clustering of synapses with repeated learning compared to the case without synapse reorganization ($p<0.01$ one-way ANOVA). The phenomenon of increased synapse clustering also occurs under the local PRP synthesis condition. This is also shown in Figure 8.2. The number of potentiated synapses per branch in this case increased from 6.77 ± 0.37 after day 1 to 10.46 ± 1.90 after day 4 of learning ($p<0.001$ one-way ANOVA).

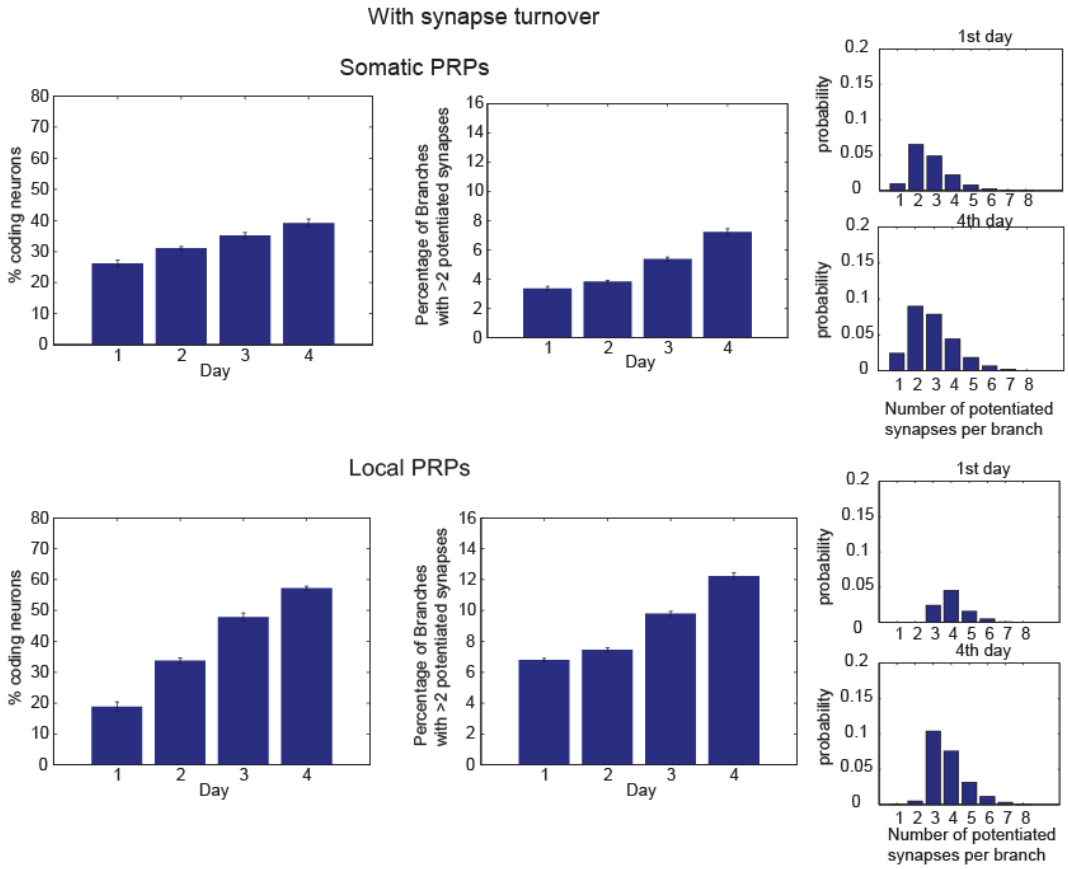

Figure 8.2 Repeated training of the same memory leads to increased clustering when synapse turnover and new synapse formation are allowed in the network.

In this figure, synapse elimination and formation is allowed in the network. Left column: The coding population under somatic (top) and local (bottom) protein synthesis. Middle column: Clustering assessed by the number of branches with > 2 potentiated synapses. Third column: Distribution of synapses per branch after day 1 training and after day 4 training. Error bars indicate SEM of 10 simulation trials.

8.4 Discussion

In this chapter we applied the model of memory formation in order to examine a particular experimentally observed aspect of memory: increased clustering, which follows learning. In the experiment by Fu et al. (Fu et al. 2012), the experimenters used transcranial two photon microscopy to follow the development of new spines in layer 5 pyramidal neurons of the motor cortex of mice that practiced novel forelimb skills. The authors observed that one third of the synapses formed were formed in clusters of nearby synapses, which most of the time were synapse pairs. Importantly, the authors followed the emergence of new spines while the mice were being re-trained in the same motor learning every day. They found that the newly formed spines tended to cluster with the spines that were formed the first day, thus strengthening even further the clusters that were formed in the first day. In contrast, under control conditions, when a different task was learned in different days, the newly formed synapses did not tend to cluster with the older ones. The authors suggest that clustering was induced by repetitive firing and provided a structural basis for spatial coding of motor memory.

In our experiments, using the original model in which there is no synapse reorganization, we observed a relevant strengthening of the memory after repeated learning, which is reflected by the higher coding population under both Somatic and Local PRPs (Figure 8.1). We did not observe, however, an large increase in the number of clustered synapses, which would indicate that new synapses are being added to existing clusters, or that new clusters are being formed. This is attributed to the static nature of the connectivity of the model: the connections were allocated at random before the first day of training and can only be strengthened from there on. The learning of the memory strongly induces plasticity in these synapses, so that

subsequent learning has little effect, as there are few synapses that are left un-potentiated. This is indicated by the small increase in the number of branches with more than 2 potentiated synapses in figure 8.1, right.

In contrast, when synapse reorganization is allowed in the model, new weak synapses can be formed in the network even after the first simulated day of training. This creates a reserve pool of weak synapses that have the ability to be potentiated further via re-training by virtue of being within the same neurons as the synapses that were generated in day 1. As shown in figure 8.2, apart from the increase in the coding population, which indicates a strengthening of the memory via re-training, the number of branches containing more than 2 synapses increases with every simulated day of training. This is true both under somatic and local PRP conditions. Local PRP conditions, as we saw in chapter 2 facilitate the formation of larger synaptic clusters by virtue of the requirement for strong depolarization to induced plasticity, which can only be brought about by the synergistic action of 3 or more synapses in the same branch. As shown in the rightmost column of Figure 8.2, the number of synapses per branch is greatly amplified after learning between day 1 and day 4.

In conclusion, our results regarding the increase of clustering via repeated learning suggest that the increased clustering observed experimentally is conferred by newly formed contacts rather than the potentiation of existing but un-potentiated ones, thus there is a requirement for dynamic synapse formation, which is normally balanced by elimination. This is in agreement with (Fu et al. 2012), who reported that repeated learning resulted in the addition of new spines and not the potentiation of pre-existing but un-potentiated ones. Thus, we suggest that an experimental intervention that

abolishes the formation of new synapses would abolish the increased synapse clustering observed with repeated learning.

Chapter 9.

Summary and beyond

In this thesis, we explored theoretically through the use of computational modeling how we can predict the structure of memory engrams being formed in cortical circuits, and the possible ways in which the allocation and distribution of synapses in the dendrites of the network can affect the expression of memories.

9.1 Summary

In Chapters 3 & 4 we outlined the components of a model of memory that corresponds to our current knowledge about memory engrams and used it to study the structure of a memory engram. It should be noted that previous studies have not attempted to integrate the multitude of mechanisms that affect memory trace formation as a whole, but have rather examined each mechanism separately for its consequences (Barrett et al. 2009; van Rossum & Shippi 2013; Clopath et al. 2008; Smolen et al. 2012; Bhalla & Iyengar 1999; Legenstein & Maass 2011; O'Donnell et al. 2014). We presented a strategy to take into account the independence of dendritic subunits that is computationally tractable while still allowing for the nonlinear phenomena, which participate in memory, such as dendritic spikes.

Our major finding is that such a model can replicate experimentally observed properties of the memory engram such as its limited but distributed population size,

the clustering of synaptic inputs and the increased sparseness of the resulting population code. Importantly, we identify a link between the subcellular locus of protein synthesis and these properties. We thus propose two hypotheses from these data:

a) Given that different forms of long-term memory may require different molecular mechanisms, including different locus of PRP synthesis and different molecular cascades for their consolidation (Izquierdo et al. 2006), we propose that these differences will be evident in the distribution of firing rates in the population during recall (Figure 4.1), on the average firing rate (Figure 4.2), on the sparseness of the engrams and the clustering properties of the synapses participating in learning (Figure 4.5).

b) Manipulations that block or interfere with protein synthesis in specific compartments of the neuron, in particular the soma or the dendrites will interfere with the properties of the memory engram leading to either more sharply defined population coding (in the case of Somatic PRPs) or more broadly distributed and clustered synaptic memory allocation (in the case of Local PRPs).

In Chapter 5 we examined the putative processes, which are believed to underlie the behavioral tagging experimental paradigm. We show that the dependence on protein synthesis creates different conditions that lead to different outcomes regarding the expression of the memory. We propose that weak learning that is dependent on somatic LTP (such as learning that involves the hippocampus) will be:

a) more easily consolidated to long-term memories by other memories which provide the PRPs

b) asymmetrically strengthened due to the action of CREB/increased excitability

c) more likely to overlap with a strong memory, thus increasing the possibility for either common recall of the memory or memory interference.

In all cases, we expect that the weak and strong memories must be strongly co-allocated at the dendritic branch level. This hypothesis can be tested readily via calcium imaging after behavioral tagging experiments.

In Chapter 6 we proposed that even strong memories being encoded within appropriate times can be strengthened in a cooperative way, leading to co-allocation of the memories, and consequently to co-expression. This may be considered as a mechanism that underlies two known psychological findings:

a) The "emotional tagging" of memories links together memories that are unrelated by virtue of the fact that one of the memories has a strong emotional component. This leads to the increased expression of the memory and may be mediated, for example, by the modulatory action and activation of the amygdala (McGaugh 2004).

b) Context-dependence of memory is the improved recall of memory in the context in which it was encoded, even when the context is irrelevant to the memory task (Smith & Vela 2001) (e.g. improved performance in a test when the test is given in the same environment where the subject studied). In this case, context information that is constantly provided by the medial temporal lobe may be readily incorporated as part of a memory engram by virtue of being co-active with the memory being learned.

Our results suggest that the increase of excitability allows memory strengthening asymmetrically, by promoting the second memory for longer intervals beyond 5 hours. This finding can be readily tested experimentally with behavioral experiments. In addition, if the time course of memory pairing is found to extend beyond the 5 hours window, this can be taken as evidence that enhanced excitability/CREB contribute to the consolidation of memories.

In chapter 7, we showed that a group of memory events can be co-allocated if they occur in sequence, in a way that may facilitate their parallel recall. This property is favorable for the formation of episodic memories, which must be both associated, in order to form a coherent memory, and separated enough in order to avoid memory confusion. We show that the locus of protein synthesis affects the way in which memories can be bound in an episode, and find that somatic protein synthesis promotes the association of entire strings of memories, while local protein synthesis tends to bind memories up to 3 hours. At this point, very little is known about the structure of episodic memory engrams and the relationships between the individual memories that comprise them. Our results thus provide putative hypotheses, which, via investigation through behavioral or imaging experiments, can reveal the properties of the underlying long-term LTP mechanisms that enable episodic memory formation.

In chapter 8 we examined a different property of memory engrams that has been found experimentally: the clustering of synapses results from repeated learning. The increased clustering in this case is believed to be correlated with refinement of a motor memory learning, which is achieved through the repeated learning. We find

that, when the neural circuit is allowed to reorganize through the continuous turnover and new synapse formation in a way that is compatible with experimental observations (Trachtenberg et al. 2002), our model replicates the finding of increased clustering that follows repetitive-learning. We thus hypothesize that increased clustering is a property that enables improved learning when increased turnover of synapses (and new naive synapse formation) takes place, such as in response to novel sensory experience (Trachtenberg et al. 2002).

9.2 Extending the current model

In this thesis we opted to take a broad strategy in order to model long-term memory formation that is based on the hypothesis that it is mediated via late-LTP processes. This is currently a widely accepted hypothesis about the storage of long-term memories, and its NMDAR-dependence and protein-dependence are both well established (Wang et al. 2013; Patterson & Yasuda 2011). The contribution of synaptic tagging and capture in late-LTP consolidation is now also well established (Uwe Frey & Morris 1998; Redondo & Morris 2011; Morris 2006), as is the contribution of homeostatic mechanisms (Pozo & Goda 2010; Bartlett & Wang 2011). The contribution of branch-specific potentiation or CREB-dependent is less studied in terms of its effect on memory, although both phenomena have been presumed to play important roles in memory (Rogerson et al. 2014; Legenstein & Maass 2011). In general, while certain parts of the cascades leading to memory trace formation are understood, the entire process is extremely complex at the molecular level and involves hundreds of proteins. At this point, there have been few attempts to model these molecular pathways (Smolen et al. 2006b; Bhalla & Iyengar 1999;

Kotaleski & Blackwell 2010), however the task of mapping the entire molecular machinery that is responsible for memory trace formation is still considered an intractable problem (Abbott & Nelson 2000; Bhalla 2014). A major reason for that is the lack of constraints in the parameters of the models is due to the sheer large number of parameters and the difficulty of obtaining their values from experiments. In general, an entirely detailed model of memory engram formation would require the modeling of molecular and electrical activity at multiple spatial scales and temporal scales, and the identification and characterization of the entire molecular machinery implicated in late-LTP processes (Bhalla 2014).

On the other hand, models that capture the essential characteristics of plasticity functions are instrumental in delineating the contributions of plasticity rules in specific aspects of memory, such as the role of STC (Clopath et al. 2008; O'Donnell & Sejnowski 2014) or the role of branch-strength potentiation (Legenstein & Maass 2011). In this thesis, we followed such a phenomenological approach to describe synaptic plasticity, in a way that allows us to make useful conclusions without making unrealistic assumptions about the nature of the underlying mechanisms. Regardless, aspects of the model can be improved by future knowledge of the nature of the plasticity mechanisms we incorporate. For example, the role of calcium in the initiation of synaptic tagging and plasticity-related protein synthesis is not well known, although progress is being made in characterizing the process via which CaMKII may initiate the synaptic tagging mechanism (Okamoto et al. 2009). Similarly, little is known yet about the role of dendritic plasticity in memory, despite investigations that span two decades. Dendritic plasticity may have a complementary role in memory or it may be the main mechanism in different forms of LTP or

different brain regions (Steward & Schuman 2007), however the cascades that lead to its initiation are not yet known. We opted thus to model dendritic plasticity separately in order to identify the differences in memory trace formation. Our model would benefit greatly from research in the processes that lead to PRP synthesis. Such knowledge can be readily incorporated in our current model, as it already performs multi-scale modeling of electrical and molecular processes. Knowledge of the pathways initiating plasticity would greatly enhance the ability of the model to generate detailed predictions about the expected structure of memory traces.

The mechanism of synaptic tagging and capture is better understood, mainly due to its simple phenomenological description. For example, the time courses of synaptic tagging or synaptic capture have been studied in detail at the dendritic level (Govindarajan et al. 2010), allowing us to make more confident choices of the model parameters. Still, more studies are needed to verify whether the results of the in vitro study can be extrapolated in the general case. Similar model parameter validation is needed for the action of increased excitability/CREB. While CREB has been found to have an important role in memory, it is not clear what the time course of its action is. The action of CREB is too broad to be practical to model in detail; therefore studies that specifically identify the molecular pathways downstream of CREB will be particularly valuable in future computational studies of its role in memory. Nevertheless, the phenomenological strategy we used in the current thesis is in agreement with recent experimental observations of the time course of CREB activation (Cai et al. 2016; Rashid et al. 2016).

There are many other ways in which the current model can be expanded to provide a more accurate prediction of memory trace formation:

a) Increase in the number of neurons simulated is important to study the mass action of large populations of neurons, as well as the possible contribution of population-wide processes such as neural synchrony.

b) Separation of the populations of excitatory and inhibitory neurons in different nuclei can enable the modeling of specific types of memory, such as fear learning in the basolateral amygdala, in a more precise way, by incorporating specific connectivity constraints. It should be noted that the model is in its current form able to model such separate populations.

c) Stimulation protocols for more complex forms of memory learning can be used. In its current form the model utilizes rate-based coding of incoming stimuli in order to simulate the most general case of coincidence-based learning that can take place, for example, during fear learning in the lateral amygdala or in the hippocampus. More complex stimulation protocols could allow the simulation of rule-based learning or sequence-based learning such as auditory learning. These forms of learning might require the simulation of a timing-based plasticity protocol such as STDP. It should be noted, however, that STDP can be derived from a calcium-based plasticity model such as the one that we already use in the model (Shouval et al. 2010).

d) Detailed knowledge of the process of synaptic tag formation, PRP synthesis and their calcium-dependence would allow a more accurate description of the subtleties

involved in long-term memory interactions. Currently, these parameters are still under intense investigation by experimentalists.

e) Better characterization of the branch-strength potentiation phenomenon would allow more accurate modeling. Currently, only the potentiation of branch strengths has been studied in relation to LTP (Losonczy et al. 2008), while branch-strength depression has been shown to be independent of plasticity (Labno et al. 2014). Our model would benefit from a more detailed description of the phenomenon.

f) Recurrence of network connections would be expected to greatly expand the storage capacity of the current network. We limited our model to non-recurrent connectivity, as we were interested in modeling the strengthening of afferent connectivity that follows learning, which has been characterized experimentally (Humeau et al. 2005; Murayama et al. 2009). Recurrent connectivity reorganization is not well studied with relation to long-term LTP studies. Regardless, recurrent connectivity allows different network states to occur and provides a link between biophysical and artificial neural networks. (e.g. (Churchland et al. 2012)). The model can be readily used to study recurrent connectivity in its current form.

g) Dendritic synaptic plasticity can be studied in more detail by adding an additional rule about the spatial dependence of LTP cooperativity. This would allow distance-dependent LTP within the same dendrite and would offer a better characterization of the synapse clustering that follows. A detailed measurement of the resulting synaptic clusters would allow to better characterize the probability of such clusters eliciting dendritic spikes, or undergoing cooperative plasticity.

Model extensions like the ones mentioned above would allow us to make more confident and accurate predictions about sub-cellular synaptic plasticity and its relation to memory. As the relevant field of memory studies, which examine particular memory engrams at the neuronal and sub-neuronal level is very active, more comparisons with experimental studies will be possible, which will allow further improvements that capture the essential characteristics of memory traces. Developments in optogenetics, imaging and molecular methods allow for increasingly better understanding of the memory traces underlying simple forms of learning. As the experimental evidence expands to include more complex forms of learning, models of memory can incrementally provide further predictions, test new hypotheses and guide further research in the field.

Bibliography

Abbott, L.F. & Nelson, S.B., 2000. Synaptic plasticity: taming the beast. *Nature neuroscience*, 3 Suppl, pp.1178–83.

Ariav, G., Polsky, A. & Schiller, J., 2003. Submillisecond precision of the input-output transformation function mediated by fast sodium dendritic spikes in basal dendrites of CA1 pyramidal neurons. *The Journal of neuroscience*, 23(21), pp.7750–8.

Ballarini, F. et al., 2009. Behavioral tagging is a general mechanism of long-term memory formation. *Proceedings of the National Academy of Sciences of the United States of America*, 106(34), pp.14599–604.

Barrett, A.B. et al., 2009. State based model of long-term potentiation and synaptic tagging and capture. *PLoS computational biology*, 5(1), p.e1000259.

Bartlett, T.E. & Wang, Y.T., 2011. Illuminating Synapse-Specific Homeostatic Plasticity. *Neuron*, 72(5), pp.682–685.

Baudry, M. et al., 2011. The biochemistry of memory: The 26year journey of a "new and specific hypothesis". *Neurobiology of learning and memory*, 95(2), pp.125–33.

Bauer, E.P., Schafe, G.E. & LeDoux, J.E., 2002. NMDA receptors and L-type voltage-gated calcium channels contribute to long-term potentiation and different components of fear memory formation in the lateral amygdala. *The Journal of neuroscience : the official journal of the Society for Neuroscience*, 22(12), pp.5239–5249.

Béïque, J.-C. et al., 2011. Arc-dependent synapse-specific homeostatic plasticity. *Proceedings of the National Academy of Sciences*, 108(2), pp.816–821.

Benito, E. & Barco, A., 2010. CREB's control of intrinsic and synaptic plasticity: implications for CREB-dependent memory models. *Trends in neurosciences*, 33(5), pp.230–40.

Bhalla, U.S., 2011. Multiscale interactions between chemical and electric signaling in LTP induction, LTP reversal and dendritic excitability. *Neural networks : the official journal of the International Neural Network Society*, 24(9), pp.943–9.

Bhalla, U.S., 2014. *Multiscale modeling and synaptic plasticity.* 1st ed., Elsevier Inc.

Bhalla, U.S. & Iyengar, R., 1999. Emergent properties of networks of biological signaling pathways. *Science (New York, N.Y.)*, 283(5400), pp.381–7.

Bliss, T. V & Lomo, T., 1973. Long-lasting potentiation of synaptic transmission in the dentate area of the anaesthetized rabbit following stimulation of the perforant path. *J Physiol*, 232(2), pp.331–356.

Bliss, T.V.P. & Collingridge, G.L., 1993. A synaptic model of memory: long-term potentiation in the hippocampus. *Nature*, 361(6407), pp.31–39.

Bodian, D., 1965. A suggestive relationship of nerve cell RNA with specific synaptic sites. *Proceedings of the National Academy of Sciences of the United States of America*, 53(2), p.418.

Bourne, J.N. & Harris, K.M., 2011. Nanoscale analysis of structural synaptic plasticity. *Current opinion in neurobiology*, 22(3), pp.1–11.

Braitenberg, V. & Schüz, A., 1998. Cortical architectonics. In *Cortex: Statistics and*

Geometry of Neuronal Connectivity. Springer, pp. 135–137.

Branco, T., Clark, B.A. & Häusser, M., 2010. Dendritic discrimination of temporal input sequences in cortical neurons. *Science (New York, N.Y.)*, 329(5999), pp.1671–5.

Branco, T. & Häusser, M., 2011. Synaptic integration gradients in single cortical pyramidal cell dendrites. *Neuron*, 69(5), pp.885–92.

Branco, T. & Häusser, M., 2010a. The single dendritic branch as a fundamental functional unit in the nervous system. *Current Opinion in Neurobiology*, 20(4), pp.494–502.

Branco, T. & Häusser, M., 2010b. The single dendritic branch as a fundamental functional unit in the nervous system. *Current Opinion in Neurobiology*, 20(4), pp.494–502.

Cai, D.J. et al., 2016. A shared neural ensemble links distinct contextual memories encoded close in time. *Nature*, In Press.

Cajigas, I.J. et al., 2012. The Local Transcriptome in the Synaptic Neuropil Revealed by Deep Sequencing and High-Resolution Imaging. *Neuron*, 74(8379), pp.453–466.

de Carvalho Myskiw, J., Benetti, F. & Izquierdo, I., 2013. Behavioral tagging of extinction learning. *Proceedings of the National Academy of Sciences of the United States of America*, 110(3), pp.1071–6.

Cash, S. & Yuste, R., 1999. Linear summation of excitatory inputs by CA1 pyramidal neurons. *Neuron*, 22(2), pp.383–94.

Chen, J.L. et al., 2012. Clustered dynamics of inhibitory synapses and dendritic spines in the adult neocortex. *Neuron*, 74(2), pp.361–73.

Chen, X. et al., 2011. Functional mapping of single spines in cortical neurons in vivo. *Nature*, 475(7357), pp.501–505.

Chklovskii, D.B.B., Mel, B.W. & Svoboda, K., 2004. Cortical rewiring and information storage. *Nature*, 431(7010), pp.782–788.

Churchland, M.M. et al., 2012. Neural population dynamics during reaching. *Nature*, pp.1–8.

Citri, A. & Malenka, R.C., 2008. Synaptic plasticity: multiple forms, functions, and mechanisms. *Neuropsychopharmacology : official publication of the American College of Neuropsychopharmacology*, 33(1), pp.18–41.

Clopath, C. et al., 2008. Tag-trigger-consolidation: a model of early and late long-term-potentiation and depression. *PLoS computational biology*, 4(12), p.e1000248.

Cooper, L.N. & Bear, M.F., 2012. The BCM theory of synapse modification at 30: interaction of theory with experiment. *Nature Reviews Neuroscience*, 13(11), pp.798–810.

Cui-Wang, T. et al., 2012. Local zones of endoplasmic reticulum complexity confine cargo in neuronal dendrites. *Cell*, 148(1-2), pp.309–21.

Cutsuridis, V. & Hasselmo, M., 2012. GABAergic contributions to gating, timing, and phase precession of hippocampal neuronal activity during theta oscillations. *Hippocampus*.

Dash, P.K., Hochner, B. & Kandel, E.R., 1990. Injection of the cAMP-responsive element into the nucleus of Aplysia sensory neurons blocks long-term facilitation. *Nature*, 345(6277), pp.718–21.

Disterhoft, J.F. & Oh, M.M., 2006. Learning, aging and intrinsic neuronal plasticity. *Trends in neurosciences*, 29(10), pp.587–99.

Dong, Y. et al., 2006. CREB modulates excitability of nucleus accumbens neurons. *Nature neuroscience*, 9(4), pp.475–7.

Druckmann, S. et al., 2014. Structured Synaptic Connectivity between Hippocampal Regions. *Neuron*.

Dudai, Y., 2004. The neurobiology of consolidations, or, how stable is the engram? *Annual review of psychology*, 55, pp.51–86.

Faber, E.S., Callister, R.J. & Sah, P., 2001. Morphological and electrophysiological properties of principal neurons in the rat lateral amygdala in vitro. *Journal of neurophysiology*, 85(2), pp.714–23.

Frey, U. et al., 1989. Long-term potentiation induced in dendrites separated from rat's CA1 pyramidal somata does not establish a late phase. *Neuroscience Letters*, 97(1), pp.135–139.

Frey, U. & Morris, R.G.M., 1998. Synaptic tagging: implications for late maintenance of hippocampal long-term potentiation. *Trends Neurosci*, 21(5), pp.181–188.

Frey, U. & Morris, R.G.M., 1998. Weak before strong: dissociating synaptic tagging and plasticity-factor accounts of late-LTP. *Neuropharmacology*, 37(4), pp.545–552.

Frey, U. & Morris, R.G.M.G., 1997. Synaptic tagging and long-term potentiation. *Nature*, 385(6616), pp.533–6.

Frick, A., Magee, J. & Johnston, D., 2004. LTP is accompanied by an enhanced local excitability of pyramidal neuron dendrites. *Nature neuroscience*, 7(2), pp.126–35.

Fu, M. et al., 2012. Repetitive motor learning induces coordinated formation of clustered dendritic spines in vivo. *Nature*, 1(7387), pp.92–5.

Garner, A.R. et al., 2012. Generation of a synthetic memory trace. *Science (New York, N.Y.)*, 335(6075), pp.1513–6.

Gdalyahu, A. et al., 2012. Associative fear learning enhances sparse network coding in primary sensory cortex. *Neuron*, 75(1), pp.121–32.

Golding, N.L., Staff, N.P. & Spruston, N., 2002. Dendritic spikes as a mechanism for cooperative long-term potentiation. *Nature*, 418(6895), pp.326–331.

Gómez González, J.F., Mel, B.W. & Poirazi, P., 2011. Distinguishing Linear vs. Non-Linear Integration in CA1 Radial Oblique Dendrites: It's about Time. *Frontiers in computational neuroscience*, 5, p.44.

Govindarajan, A. et al., 2010. The Dendritic Branch Is the Preferred Integrative Unit for Protein Synthesis-Dependent LTP. *Neuron*, 69(1), pp.132–146.

Govindarajan, A., Kelleher, R.J. & Tonegawa, S., 2006. A clustered plasticity model of long-term memory engrams. *Nature reviews. Neuroscience*, 7(7), pp.575–83.

Graupner, M. & Brunel, N., 2012. Calcium-based plasticity model explains sensitivity of synaptic changes to spike pattern, rate, and dendritic location. *Proceedings of the National Academy of Sciences*, 109(10), pp.3991–3996.

Guzowski, J.F. et al., 1999. Environment-specific expression of the immediate-early gene Arc in hippocampal neuronal ensembles. *Nat Neurosci*, 2(12), pp.1120–1124.

Han, J.-H. et al., 2007. Neuronal competition and selection during memory

formation. *Science (New York, N.Y.)*, 316(5823), pp.457–60.
Han, J.-H. et al., 2009. Selective erasure of a fear memory. *Science (New York, N.Y.)*, 323(5920), pp.1492–6.
Han, M.-H. et al., 2006. Role of cAMP response element-binding protein in the rat locus ceruleus: regulation of neuronal activity and opiate withdrawal behaviors. *The Journal of neuroscience*, 26(17), pp.4624–4629.
Hao, J. & Oertner, T.G., 2011. Depolarization gates spine calcium transients and spike-timing-dependent potentiation. *Current Opinion in Neurobiology*, 22(3), pp.509–515.
Hardie, J. & Spruston, N., 2009. Synaptic depolarization is more effective than back-propagating action potentials during induction of associative long-term potentiation in hippocampal pyramidal neurons. *The Journal of neuroscience : the official journal of the Society for Neuroscience*, 29(10), pp.3233–41.
Harnett, M.T. et al., 2012. Synaptic amplification by dendritic spines enhances input cooperativity. *Nature*, 491(7425), pp.599–602.
Harvey, C.D. et al., 2008. The spread of Ras activity triggered by activation of a single dendritic spine. *Science (New York, N.Y.)*, 321(5885), pp.136–40.
Harvey, C.D. & Svoboda, K., 2007. Locally dynamic synaptic learning rules in pyramidal neuron dendrites. *Nature*, 450(7173), pp.1195–200.
Häusser, M. & Mel, B., 2003. Dendrites: bug or feature? *Current Opinion in Neurobiology*, 13(3), pp.372–383.
Häusser, M., Spruston, N. & Stuart, G.J., 2000. Diversity and dynamics of dendritic signaling. *Science*, 290(5492), pp.739–744.
Hebb, D.O., 1949. *The Organization of Behavior*, Wiley.
Hering, H. & Sheng, M., 2001. Dendritic spines: structure, dynamics and regulation. *Nature reviews. Neuroscience*, 2(12), pp.880–8.
Higley, M.J. & Sabatini, B.L., 2012. Calcium Signaling in Dendritic Spines. *Cold Spring Harbor perspectives in biology*.
Holtmaat, A.J.G.D. et al., 2005. Transient and persistent dendritic spines in the neocortex in vivo. *Neuron*, 45(2), pp.279–91.
Hopfield, J.J., 1988. Artificial neural networks. *Circuits and Devices Magazine, IEEE*, 4(5), pp.3–10.
Hornik, K., Stinchcombe, M. & White, H., 1989. Multilayer feedforward networks are universal approximators. *Neural Networks*, 2(5), pp.359–366.
Hou, Q., Gilbert, J. & Man, H.-Y., 2011. Homeostatic regulation of AMPA receptor trafficking and degradation by light-controlled single-synaptic activation. *Neuron*, 72(5), pp.806–18.
Howard, M.W. & Kahana, M.J., 2002. A Distributed Representation of Temporal Context. *Journal of Mathematical Psychology*, 46(3), pp.269–299.
Huang, Y.H. et al., 2008. CREB modulates the functional output of nucleus accumbens neurons: a critical role of N-methyl-D-aspartate glutamate receptor (NMDAR) receptors. *The Journal of biological chemistry*, 283(5), pp.2751–60.
Huang, Y.-Y. & Kandel, E.R., 2007. 5-Hydroxytryptamine induces a protein kinase A/mitogen-activated protein kinase-mediated and macromolecular synthesis-dependent late phase of long-term potentiation in the amygdala. *The Journal of neuroscience*, 27(12), pp.3111–3119.
Huber, K.M., Kayser, M.S. & Bear, M.F., 2000. Role for rapid dendritic protein

synthesis in hippocampal mGluR-dependent long-term depression. *Science Signaling*, 288(5469), p.1254.

Humeau, Y. et al., 2005. Dendritic Spine Heterogeneity Determines Afferent-Specific Hebbian Plasticity in the Amygdala. , 45, pp.119–131.

Izquierdo, I. et al., 2006. Different molecular cascades in different sites of the brain control memory consolidation. *Trends in Neurosciences*, 29(9), pp.496–505.

Jadi, M. et al., 2012. Location-dependent effects of inhibition on local spiking in pyramidal neuron dendrites. *PLoS Comput Biol*, 8(6), p.e1002550.

Jadi, M.P. et al., 2014. An Augmented Two-Layer Model Captures Nonlinear Analog Spatial Integration Effects in Pyramidal Neuron Dendrites.

Jia, H. et al., 2010. Dendritic organization of sensory input to cortical neurons in vivo. *Nature*, 464(7293), pp.1307–12.

Jolivet, R. et al., 2006. Integrate-and-Fire models with adaptation are good enough: predicting spike times under random current injection. *Advances in neural information processing systems*, 18, pp.595–602.

Josselyn, S., 2010. Continuing the search for the engram: examining the mechanism of fear memories. *Journal of Psychiatry & Neuroscience*, 35(4), pp.221–228.

Kang, H. & Schuman, E.M., 1996. A requirement for local protein synthesis in neurotrophin-induced hippocampal synaptic plasticity. *Science*, 273(5280), pp.1402–1406.

Kastellakis, G. et al., 2015. Synaptic clustering within dendrites : An emerging theory of memory formation. *Progress in Neurobiology*, 126, pp.19–35.

Kastellakis, G., Silva, A.J. & Poirazi, P., 2016. Linking memories across time via neuronal and dendritic overlaps in model neurons with active dendrites. *Cell reports*, p.Accepted.

Katz, Y. et al., 2009. Synapse distribution suggests a two-stage model of dendritic integration in CA1 pyramidal neurons. *Neuron*, 63(2), pp.171–7.

Kelleher, R.J., Govindarajan, A. & Tonegawa, S., 2004. Translational regulatory mechanisms in persistent forms of synaptic plasticity. *Neuron*, 44(1), pp.59–73.

Kida, S. et al., 2002. CREB required for the stability of new and reactivated fear memories. *Nature neuroscience*, 5(4), pp.348–55.

Kim, J. et al., 2013. CREB and neuronal selection for memory trace. *Frontiers in neural circuits*, 7(March), p.44.

Kim, J. et al., 2014. Memory recall and modifications by activating neurons with elevated CREB. *Nature neuroscience*, 17(1), pp.65–72.

Kim, S. et al., 2012. Active dendrites support efficient initiation of dendritic spikes in hippocampal CA3 pyramidal neurons. *Nat Neurosci*, 15(4), pp.600–606.

Klausberger, T. et al., 2003. Brain-state-and cell-type-specific firing of hippocampal interneurons in vivo. *Nature*, 421(6925), pp.844–848.

Kleindienst, T. et al., 2011. Article Activity-Dependent Clustering of Functional Synaptic Inputs on Developing Hippocampal Dendrites. *Neuron*, 72(6), pp.1012–1024.

Kotaleski, J.H. & Blackwell, K.T., 2010. Modelling the molecular mechanisms of synaptic plasticity using systems biology approaches. *Nature reviews. Neuroscience*, 11(4), pp.239–51.

Kramár, E. a et al., 2012. Synaptic evidence for the efficacy of spaced learning. *Proceedings of the National Academy of Sciences*, 109(13), pp.5121–5126.

Kullmann, D.M. et al., 2012. Plasticity of inhibition. *Neuron*, 75(6), pp.951–62.
Labno, A. et al., 2014. Local Plasticity of Dendritic Excitability Can Be Autonomous of Synaptic Plasticity and Regulated by Activity-Based Phosphorylation of Kv4. 2. *PloS one*, 9(1), p.e84086.
Larkum, M.E. et al., 2009. Synaptic integration in tuft dendrites of layer 5 pyramidal neurons: a new unifying principle. *Science*, 325(5941), pp.756–760.
Larkum, M.E. & Nevian, T., 2008. Synaptic clustering by dendritic signalling mechanisms. *Current opinion in neurobiology*, 18(3), pp.321–31.
Lashley, K.S., 1950. In search of the engram. *Symposia of the society for experimental*.
Lavzin, M. et al., 2012. Nonlinear dendritic processing determines angular tuning of barrel cortex neurons in vivo. *Nature*, 490(7420), pp.397–401.
Legenstein, R. & Maass, W., 2011. Branch-Specific Plasticity Enables Self-Organization of Nonlinear Computation in Single Neurons. *Journal of Neuroscience*, 31(30), pp.10787–10802.
Liao, D., Hessler, N.A. & Malinow, R., 1995. Activation of postsynaptically silent synapses during pairing-induced LTP in CA1 region of hippocampal slice. *Nature*, 375(6530), pp.400–403.
Liu, X. et al., 2012. Optogenetic stimulation of a hippocampal engram activates fear memory recall. *Nature*, 484(7394), pp.381–5.
Liu, X., Ramirez, S. & Tonegawa, S., 2014. Inception of a false memory by optogenetic manipulation of a hippocampal memory engram. *Philosophical transactions of the Royal Society of London. Series B, Biological sciences*, 369(1633), p.20130142.
Longordo, F. et al., 2013. Sublinear integration underlies binocular processing in primary visual cortex. *Nature neuroscience*, 16(6), pp.714–723.
Lopez de Armentia, M. et al., 2007. cAMP response element-binding protein-mediated gene expression increases the intrinsic excitability of CA1 pyramidal neurons. *The Journal of neuroscience : the official journal of the Society for Neuroscience*, 27(50), pp.13909–18.
Losonczy, A. & Magee, J.C., 2006. Integrative properties of radial oblique dendrites in hippocampal CA1 pyramidal neurons. *Neuron*, 50(2), pp.291–307.
Losonczy, A., Makara, J.K. & Magee, J.C., 2008. Compartmentalized dendritic plasticity and input feature storage in neurons. *Nature*, 452(7186), pp.436–41.
Lovett-Barron, M. et al., 2012. Regulation of neuronal input transformations by tunable dendritic inhibition. *Nature neuroscience*, 15(3), pp.423–30, S1–3.
Lynch, G., Kramár, E.A. & Gall, C.M., 2014. Protein synthesis and consolidation of memory-related synaptic changes. *Brain research*.
Mainen, Z. & Sejnowski, T., 1996. Influence of dendritic structure on firing pattern in model neocortical neurons. *Nature*.
Major, G., Larkum, M.E. & Schiller, J., 2013. Active properties of neocortical pyramidal neuron dendrites. *Annual review of neuroscience*, 36, pp.1–24.
Makara, J.K. et al., 2009. Experience-dependent compartmentalized dendritic plasticity in rat hippocampal CA1 pyramidal neurons. *Nature neuroscience*, 12(12), pp.1485–7.
Makara, J.K. & Magee, J.C., 2013. Variable dendritic integration in hippocampal CA3 pyramidal neurons. *Neuron*, 80(6), pp.1438–50.

Makino, H. & Malinow, R., 2011. Compartmentalized versus global synaptic plasticity on dendrites controlled by experience. *Neuron*, 72(6), pp.1001–11.

Maren, S., 2005. Building and burying fear memories in the brain. *The Neuroscientist : a review journal bringing neurobiology, neurology and psychiatry*, 11(1), pp.89–99.

Maren, S. et al., 2003. Protein synthesis in the amygdala , but not the auditory thalamus , is required for consolidation of Pavlovian fear conditioning in rats. *Neuroscience*, 18, pp.3080–3088.

Maren, S. & Quirk, G.J., 2004. Neuronal signalling of fear memory. *Nature reviews. Neuroscience*, 5(11), pp.844–52.

Markram, H. et al., 2004. Interneurons of the neocortical inhibitory system. *Nature Reviews Neuroscience*, 5(10), pp.793–807.

Martin, K.C. et al., 1997. Synapse-specific, long-term facilitation of aplysia sensory to motor synapses: a function for local protein synthesis in memory storage. *Cell*, 91(7), pp.927–38.

McClelland, J.L. & Rumelhart, D.E., 1986. A distributed model of human learning and memory. *Parallel distributed processing: Explorations in the microstructure of cognition*, 2, pp.170–215.

McCulloch, W.S. & Pitts, W., 1943. A logical calculus of the ideas immanent in nervous activity. *The Bulletin of Mathematical Biophysics*, 5(4), pp.115–133.

McDonald, A.J., 1998. Cortical pathways to the mammalian amygdala. *Progress in neurobiology*, 55(3), pp.257–332.

McGaugh, J.L., 2004. The amygdala modulates the consolidation of memories of emotionally arousing experiences. *Annual review of neuroscience*, 27, pp.1–28.

McKay, B.M., Oh, M.M. & Disterhoft, J.F., 2013. Learning increases intrinsic excitability of hippocampal interneurons. *The Journal of neuroscience : the official journal of the Society for Neuroscience*, 33(13), pp.5499–506.

Mel, B.W., 1993. Synaptic integration in an excitable dendritic tree. *Journal of neurophysiology*, 70(3), pp.1086–101.

Minsky, M. & Papert, S., 1969. Perceptron: an introduction to computational geometry. *The MIT Press, Cambridge, expanded edition*, 19, p.88.

Moncada, D., Ballarini, F. & Viola, H., 2015. Behavioral Tagging: A Translation of the Synaptic Tagging and Capture Hypothesis. *Neural plasticity*, 2015, p.650780.

Moncada, D. & Viola, H., 2007. Induction of long-term memory by exposure to novelty requires protein synthesis: evidence for a behavioral tagging. *The Journal of neuroscience : the official journal of the Society for Neuroscience*, 27(28), pp.7476–81.

Morris, R.G.M., 2006. Elements of a neurobiological theory of hippocampal function: The role of synaptic plasticity, synaptic tagging and schemas. *European Journal of Neuroscience*, 23(11), pp.2829–2846.

Moyer Jr, J.R. et al., 1996. Trace eyeblink conditioning increases CA1 excitability in a transient and learning-specific manner. *The Journal of neuroscience*, 16(17), pp.5536–5546.

Müller, C. et al., 2012. Inhibitory control of linear and supralinear dendritic excitation in CA1 pyramidal neurons. *Neuron*, 75(5), pp.851–64.

Murakoshi, H., Wang, H. & Yasuda, R., 2011. Local, persistent activation of Rho

GTPases during plasticity of single dendritic spines. *Nature*, 472(7341), pp.100–104.

Murayama, M. et al., 2009. Dendritic encoding of sensory stimuli controlled by deep cortical interneurons. *Nature*, 457(7233), pp.1137–41.

Nadel, L. et al., 2012. Memory formation, consolidation and transformation. *Neuroscience and biobehavioral reviews*, 36(7), pp.1640–5.

Nevian, T. et al., 2007. Properties of basal dendrites of layer 5 pyramidal neurons: a direct patch-clamp recording study. *Nature neuroscience*, 10(2), pp.206–14.

Nguyen, P. V, Abel, T. & Kandel, E.R., 1994. Requirement of a critical period of transcription for induction of a late phase of LTP. *Science*, 265(5175), pp.1104–1107.

O'Donnell, C. & Sejnowski, T.J., 2014. Selective Memory Generalization by Spatial Patterning of Protein Synthesis. *Neuron*, 82(2), pp.398–412.

O'Donnell, C., Sejnowski, T.J. & O'Donnell, C., 2014. Selective memory generalization by spatial patterning of protein synthesis. *Neuron*, 82(2), pp.398–412.

Oh, M.M. et al., 2003. Watermaze learning enhances excitability of CA1 pyramidal neurons. *Journal of Neurophysiology*, 90(4), pp.2171–2179.

Okamoto, K., Bosch, M. & Hayashi, Y., 2009. The Roles of CaMKII and F-Actin in the Structural Plasticity of Dendritic Spines: A Potential Molecular Identity of a Synaptic Tag? *Physiology*, 24(6), pp.357–366.

Okuno, H. et al., 2012. Inverse synaptic tagging of inactive synapses via dynamic interaction of Arc/Arg3.1 with CaMKIIβ. *Cell*, 149(4), pp.886–98.

Patterson, M. & Yasuda, R., 2011. Signalling pathways underlying structural plasticity of dendritic spines. *Spine*, 1.

Penfield, W. & Rasmussen, T., 1950. The Cerebral Cortex of Man. A Clinical Study of Localization of Function.pdf. *Academic Medicine*, 25, p.375.

Peters, A., Paley, S.L. & Webster, H. de F., 1976. The Fine Structure of the Nervous System (Philadelphia: Saunders).

Pissadaki, E.K. et al., 2010. Encoding of spatio-temporal input characteristics by a CA1 pyramidal neuron model. L. J. Graham, ed. *PLoS Comput Biol*, 6(12), p.e1001038.

Poirazi, P., Brannon, T. & Mel, B.W., 2003a. Arithmetic of subthreshold synaptic summation in a model CA1 pyramidal cell. *Neuron*, 37(6), pp.977–87.

Poirazi, P., Brannon, T. & Mel, B.W., 2003b. Pyramidal neuron as two-layer neural network. *Neuron*, 37(6), pp.989–99.

Poirazi, P. & Mel, B.W., 2001. Impact of Active Dendrites and Structural Plasticity on the Memory Capacity of Neural Tissue. , 29, pp.779–796.

Polsky, A., Mel, B.W. & Schiller, J., 2004. Computational subunits in thin dendrites of pyramidal cells. *Nature neuroscience*, 7(6), pp.621–7.

Pouille, F. & Scanziani, M., 2001. Enforcement of temporal fidelity in pyramidal cells by somatic feed-forward inhibition. *Science*, 293(5532), pp.1159–1163.

Pozo, K. & Goda, Y., 2010. Unraveling mechanisms of homeostatic synaptic plasticity. *Neuron*, 66(3), pp.337–51.

Quevedo, J. et al., 2004. Protein synthesis, PKA, and MAP kinase are differentially involved in short- and long-term memory in rats. *Behavioural brain research*, 154(2), pp.339–43.

Quirk, G.J., Repa, C. & LeDoux, J.E., 1995. Fear conditioning enhances short-latency auditory responses of lateral amygdala neurons: parallel recordings in the freely behaving rat. *Neuron*, 15(5), pp.1029–39.

Rabinowitch, I. & Segev, I., 2008. Two opposing plasticity mechanisms pulling a single synapse. *Trends in neurosciences*, 31(8), pp.377–83.

Ramirez, S., Liu, X., et al., 2013. Creating a false memory in the hippocampus. *Science (New York, N.Y.)*, 341(6144), pp.387–91.

Ramirez, S., Tonegawa, S. & Liu, X., 2013. Identification and optogenetic manipulation of memory engrams in the hippocampus. *Frontiers in behavioral neuroscience*, 7, p.226.

Ramón y Cajal, S.R. y & y Cajal, S.R., 1893. *Neue Darstellung vom histologischen Bau den Centralnervensystems*,

Rashid, A.J. et al., 2016. Competition between engrams influences fear memory formation and recall. *Science*, 353(6297).

Redondo, R.L. et al., 2014. Bidirectional switch of the valence associated with a hippocampal contextual memory engram. *Nature*, 513(7518), pp.426–430.

Redondo, R.L. & Morris, R.G.M., 2011. Making memories last: the synaptic tagging and capture hypothesis. *Nat Rev Neurosci*, 12(1), pp.17–30.

Reijmers, L.G. et al., 2007. Localization of a stable neural correlate of associative memory. *Science (New York, N.Y.)*, 317(5842), pp.1230–3.

Remy, S. & Spruston, N., 2007. Dendritic spikes induce single-burst long-term potentiation. *Proceedings of the National Academy of Sciences of the United States of America*, 104(43), pp.17192–7.

Repa, J.C. et al., 2001. Two different lateral amygdala cell populations contribute to the initiation and storage of memory. *Nature Neuroscience*, 4(7), pp.724–731.

Reymann, K.G. & Frey, J.U., 2007. The late maintenance of hippocampal LTP: Requirements, phases, "synaptic tagging", "late-associativity" and implications. *Neuropharmacology*, 52(1), pp.24–40.

Robertson, E.M., 2012. New insights in human memory interference and consolidation. *Current biology : CB*, 22(2), pp.R66–71.

Rogerson, T. et al., 2014. Synaptic tagging during memory allocation. *Nature Reviews Neuroscience*, 15, pp.157–169.

van Rossum, M.C.W. & Shippi, M., 2013. Computational modelling of memory retention from synapse to behaviour. *Journal of Statistical Mechanics: Theory and Experiment*, 2013(03), p.P03007.

Rubin, J.E. et al., 2005. Calcium Time Course as a Signal for Spike-Timing – Dependent Plasticity. *Journal of Neurophysiology*, (December 2004), pp.2600–2613.

Rumelhart, D.E. & MacClelland, J.L., 1988. *Parallel distributed processing*, IEEE.

Rumpel, S. et al., 2005. Postsynaptic receptor trafficking underlying a form of associative learning. *Science (New York, N.Y.)*, 308(5718), pp.83–8.

Sah, P. et al., 2003. The amygdaloid complex: anatomy and physiology. *Physiological reviews*, 83(3), pp.803–34.

Saha, R.N. et al., 2011. Rapid activity-induced transcription of Arc and other IEGs relies on poised RNA polymerase II. *Nature neuroscience*, 14(7), pp.848–56.

Sajikumar, S. et al., 2005. Synaptic tagging and cross-tagging: the role of protein kinase Mzeta in maintaining long-term potentiation but not long-term

depression. *The Journal of neuroscience : the official journal of the Society for Neuroscience*, 25(24), pp.5750–6.

Sajikumar, S. & Frey, J.U., 2004. Late-associativity, synaptic tagging, and the role of dopamine during LTP and LTD. *Neurobiology of learning and memory*, 82(1), pp.12–25.

Schacter, D.L., 2001. *Forgotten Ideas, Neglected Pioneers: Richard Semon and the Story of Memory*, Psychology Press.

Schiller, J. et al., 1997. Calcium action potentials restricted to distal apical dendrites of rat neocortical pyramidal neurons. *The Journal of Physiology*, 505(3), pp.605–616.

Schiller, J. et al., 2000. NMDA spikes in basal dendrites. , 1261(1997), pp.285–289.

Scoville, W.B. & Milner, B., 1957. LOSS OF RECENT MEMORY AFTER BILATERAL HIPPOCAMPAL LESIONS. *Journal of Neurology, Neurosurgery & Psychiatry*, 20(1), pp.11–21.

Segev, I. & Rall, W., 1988. Computational study of an excitable dendritic spine. *Journal of neurophysiology*, 60(2), pp.499–523.

Sehgal, M., Ehlers, V.L. & Moyer, J.R., 2014. Learning enhances intrinsic excitability in a subset of lateral amygdala neurons. *Learning & Memory*, 21(3), pp.161–170.

Semon, R. (1904). D.M. als erhaltendes P. im W. des organischen G. (Leipzig: W.E., 1904. *Die Mneme als erhaltendes Prinzip im Wechsel des organischen Geschehens*, (Leipzig: Wilhelm Engelmann).

Shouval, H.Z., Bear, M.F. & Cooper, L.N., 2002. A unified model of NMDA receptor-dependent bidirectional synaptic plasticity. *Proceedings of the National Academy of Sciences*, 99(16), pp.10831–10836.

Shouval, H.Z., Wang, S.S.-H. & Wittenberg, G.M., 2010. Spike timing dependent plasticity: a consequence of more fundamental learning rules. *Frontiers in computational neuroscience*, 4(July), pp.1–13.

Sidiropoulou, K. & Poirazi, P., 2012. Predictive Features of Persistent Activity Emergence in Regular Spiking and Intrinsic Bursting Model Neurons A. Morrison, ed. *PLoS Comput Biol*, 8(4), p.e1002489.

Silva, a J. et al., 1998. CREB and memory. *Annual review of neuroscience*, 21, pp.127–48.

Silva, A.J. et al., 2009. Molecular and cellular approaches to memory allocation in neural circuits. *Science (New York, N.Y.)*, 326(5951), pp.391–5.

Silver, R.A., 2010. Neuronal arithmetic. *Nature reviews. Neuroscience*, 11(7), pp.474–89.

Sjöström, P.J. et al., 2008. Dendritic excitability and synaptic plasticity. *Physiological reviews*, 88(2), pp.769–840.

Sjöström, P.J., Turrigiano, G.G. & Nelson, S.B., 2001. Rate, timing, and cooperativity jointly determine cortical synaptic plasticity. *Neuron*, 32(6), pp.1149–64.

Smith, S.L. et al., 2013. Dendritic spikes enhance stimulus selectivity in cortical neurons in vivo. *Nature*, 503(7474), pp.115–20.

Smith, S.M. & Vela, E., 2001. Environmental context-dependent memory: a review and meta-analysis. *Psychonomic bulletin & review*, 8(2), pp.203–20.

Smolen, P., Baxter, D. a & Byrne, J.H., 2006a. A model of the roles of essential

kinases in the induction and expression of late long-term potentiation. *Biophysical journal*, 90(8), pp.2760–75.

Smolen, P., Baxter, D. a & Byrne, J.H., 2006b. A model of the roles of essential kinases in the induction and expression of late long-term potentiation. *Biophys J*, 90(8), pp.2760–2775.

Smolen, P., Baxter, D. & Byrne, J., 2012. Molecular Constraints on Synaptic Tagging and Maintenance of Long-Term Potentiation: A Predictive Model. *PLoS Computational Biology*, (832), pp.1–31.

Spruston, N., 2008. Pyramidal neurons: dendritic structure and synaptic integration. *Nature reviews. Neuroscience*, 9(3), pp.206–221.

Stanciu, M., Radulovic, J. & Spiess, J., 2001. Phosphorylated cAMP response element binding protein in the mouse brain after fear conditioning: relationship to Fos production. *Brain research. Molecular brain research*, 94(1-2), pp.15–24.

Stent, G.S., 1973. A Physiological Mechanism for Hebb's Postulate of Learning. *Proceedings of the National Academy of Sciences*, 70(4), pp.997–1001.

Steward, O. & Levy, W.B., 1982. Preferential localization of polyribosomes under the base of dendritic spines in granule cells of the dentate gyrus. *The Journal of neuroscience*, 2(3), pp.284–291.

Steward, O. & Schuman, E.M., 2007. Protein synthesis at synaptic sites on dendrites. *Handbook of Neurochemistry and Neurobiology*, 7.

Sutton, M.A. et al., 2006. Miniature neurotransmission stabilizes synaptic function via tonic suppression of local dendritic protein synthesis. *Cell*, 125(4), pp.785–99.

Sutton, M.A. & Schuman, E.M., 2006. Dendritic protein synthesis, synaptic plasticity, and memory. *Cell*, 127(1), pp.49–58.

Takahashi, N. et al., 2012. Locally synchronized synaptic inputs. *Science (New York, N.Y.)*, 335(6066), pp.353–6.

Tonegawa, S. et al., 2015. Memory Engram Cells Have Come of Age. *Neuron*, 87(5), pp.918–931.

Trachtenberg, J.T. et al., 2002. Long-term in vivo imaging of experience-dependent synaptic plasticity in adult cortex. *Nature*, 420(6917), pp.788–94.

Traub, R.D. et al., 1994. A branching dendritic model of a rodent CA3 pyramidal neurone. *J. Physiol.*, 481(Pt_1), pp.79–95.

Treves, A. & Rolls, E., 1991. What determines the capacity of autoassociative memories in the brain? *Network: Computation in Neural Systems*, 2(4), pp.371–397.

Trifilieff, P. et al., 2007. Biphasic ERK1/2 activation in both the hippocampus and amygdala may reveal a system consolidation of contextual fear memory. *Neurobiology of learning and memory*, 88(4), pp.424–34.

Trifilieff, P. et al., 2006. Foreground contextual fear memory consolidation requires two independent phases of hippocampal ERK/CREB activation. *Learning & memory (Cold Spring Harbor, N.Y.)*, 13(3), pp.349–58.

Tübing, F. et al., 2010. Dendritically localized transcripts are sorted into distinct ribonucleoprotein particles that display fast directional motility along dendrites of hippocampal neurons. *The Journal of neuroscience : the official journal of the Society for Neuroscience*, 30(11), pp.4160–70.

Turrigiano, G.G. et al., 1998. Activity-dependent scaling of quantal amplitude in neocortical neurons. *Nature*, 391(6670), pp.892–896.

Turrigiano, G.G., 2008. The self-tuning neuron: synaptic scaling of excitatory synapses. *Cell*, 135(3), pp.422–35.

Turrigiano, G.G. & Nelson, S.B., 2004. Homeostatic plasticity in the developing nervous system. *Nature reviews. Neuroscience*, 5(2), pp.97–107.

Varga, Z. et al., 2011. Dendritic coding of multiple sensory inputs in single cortical neurons in vivo. *Proceedings of the National Academy of Sciences*, 108(37), pp.15420–15425.

Vetter, P., Roth, A. & Häusser, M., 2001. Propagation of action potentials in dendrites depends on dendritic morphology. *Journal of neurophysiology*, 85(2), pp.926–37.

Viosca, J. et al., 2009. Enhanced CREB-dependent gene expression increases the excitability of neurons in the basal amygdala and primes the consolidation of contextual and cued fear memory. *Learning & memory (Cold Spring Harbor, N.Y.)*, 16(3), pp.193–7.

Wang, M. et al., 2013. NMDA Receptors Subserve Persistent Neuronal Firing during Working Memory in Dorsolateral Prefrontal Cortex. *Neuron*, 77(4), pp.736–749.

Wang, Z. et al., 2003. Bidirectional Changes in Spatial Dendritic Integration Accompanying Long-Term Synaptic Modifications. *Neuron*, 37(3), pp.463–472.

Washburn, M.S. & Moises, H.C., 1992. Electrophysiological and morphological properties of rat basolateral amygdaloid neurons in vitro. *The Journal of neuroscience : the official journal of the Society for Neuroscience*, 12(10), pp.4066–79.

Watt, A.J. et al., 2000. Activity coregulates quantal AMPA and NMDA currents at neocortical synapses. *Neuron*, 26(3), pp.659–670.

Wei, D.S. et al., 2001. Compartmentalized and binary behavior of terminal dendrites in hippocampal pyramidal neurons. *Science (New York, N.Y.)*, 293(5538), pp.2272–5.

Weinberger, N.M., 2007. Auditory associative memory and representational plasticity in the primary auditory cortex. *Hearing research*, 229(1-2), pp.54–68.

Weisskopf, M.G., Bauer, E.P. & LeDoux, J.E., 1999. L-type voltage-gated calcium channels mediate NMDA-independent associative long-term potentiation at thalamic input synapses to the amygdala. *The Journal of neuroscience : the official journal of the Society for Neuroscience*, 19(23), pp.10512–9.

Winnubst, J. et al., 2012. Synaptic clustering during development and learning: the why, when, and how. *Frontiers in molecular neuroscience*, 5(May), p.70.

Wu, G.-Y., Deisseroth, K. & Tsien, R.W., 2001. Spaced stimuli stabilize MAPK pathway activation and its effects on dendritic morphology. *Nature Neuroscience*, 4(2), pp.151–158.

Wu, X.E. & Mel, B.W., 2009. Capacity-enhancing synaptic learning rules in a medial temporal lobe online learning model. *Neuron*, 62(1), pp.31–41.

Yadav, A. et al., 2012. Morphologic evidence for spatially clustered spines in apical dendrites of monkey neocortical pyramidal cells. *The Journal of comparative neurology*, 520(13), pp.2888–902.

Yuste, R., 2011. Dendritic spines and distributed circuits. *Neuron*, 71(5), pp.772–81.
Zhang, W. & Linden, D.J., 2003. The other side of the engram: experience-driven changes in neuronal intrinsic excitability. *Nat Rev Neurosci*, 4(11), pp.885–900.
Zhang, Y. et al., 2015. Visualization of NMDA receptor–dependent AMPA receptor synaptic plasticity in vivo. *Nature Neuroscience*, 18(3), pp.402–407.
Zhou, Y. et al., 2009. CREB regulates excitability and the allocation of memory to subsets of neurons in the amygdala. *Nature neuroscience*, 12(11), pp.1438–43.